CERTIFICATE OF AUTHENTICITY

This is to certify that I am responsible for the work submitted in this thesis, that the original work is my own except as specified in acknowledgements or in footnotes, and that neither the thesis nor the original work contained therein has been submitted to this or any other institution for a higher degree.

Signed: . . . . . (Marvin G. Kelly)

Date: ……..

The Automatic Placement of Multiple Indoor Antennas using Particle Swarm Optimisation

By

Marvin G. Kelly, B. Eng(Hons), MPhil.

A Doctoral Thesis submitted in partial fulfilment of the requirements for the award of Doctor of Philosophy of Loughborough University

December 2016

© By Marvin G. Kelly 2016

To my wife Keshia and son Marvin Jr.

ABSTRACT

In this thesis, a Particle Swarm Optimization (PSO) method combined with a ray propagation method is presented as a means to optimally locate multiple antennas in an indoor environment. This novel approach uses Particle Swarm Optimisation combined with geometric partitioning. The PSO algorithm uses swarm intelligence to determine the optimal transmitter location within the building layout. It uses the Keenan-Motley indoor propagation model to determine the fitness of a location. If a transmitter placed at that optimum location, transmitting a maximum power is not enough to meet the coverage requirements of the entire indoor space, then the space is geometrically partitioned and the PSO initiated again independently in each partition. The method outputs the number of antennas, their effective isotropic radiated power (EIRP) and physical location required to meet the coverage requirements. An example scenario is presented for a real building at Loughborough University and is compared against a conventional planning technique used widely in practice.

ACKNOWLEDGEMENT

I am very thankful for all those who have said a kind word of encouragement or has in any way helped with the work presented in this thesis.

I would like to thank my primary supervisor, Dr. James Flint for his continuous support and excellent advice throughout the duration of the studies. His guidance and timely feedback have been critical to the completion of this thesis. Thanks also to Rob Seager who has given invaluable insights and has helped greatly with the formulation and path of this research.

I would like to thank also my internal examiner, Dr. Chinthana Panagamuwa for his brilliant comments and constructive feedback.

The support provided by Somara Newman of Aramos Telecommunications and Engineering Consultants (Aratel) has been timely and important in comparing this research to real life engineering problems. For this I am greatly thankful.

Finally, I would like to thank my wife Keshia and son Marvin Jr for their patience, encouragement and support for the duration of this research.

TABLE OF CONTENTS

List of Abbreviations and Symbols

Abbreviation	Meaning
BER	Bit error rate
BS	Base Station
DAS	Distributed antenna system
EiRP	Effective isotropic radiated power
GSM	Global System for Mobile Communication
GA	Genetic Algorithm
gbest	Globally best location
IEEE	Institute of Electrical and Electronics Engineers
MIMO	Multiple Input Multiple Output
MS	Mobile Station
NM	Nelder Mead
pbest	Particle local best position
PSO	Particle swarm optimisation
pwr	Power
Rx	Receiver
RxLev	Receive level
Tx	Transmitter
UWB	Ultra-wide band
WCDMA	Wideband Code Division Multiple Access

List of Figures

List of Tables

Chapter 1 : Introduction

Over the years mobile operators have had problems with providing indoor coverage. The signal propagated from based station antennas is attenuated through free space. This attenuation increases as the distance from the base station increases. The signal is also attenuated by walls with high losses some cases [1]. This means that the signal arriving in-building is greatly reduced. In some cases, this signal strength is below the receiver sensitivity of the mobile device. The building may be relatively close (less than 5km) to the base station antenna but due to the path loss and wall losses the signal strength indoors can be very poor.

Generally, a good signal quality is needed to achieve higher data rates, especially in the cases of modern mobile system technologies (2.5G, 3G and 4G systems). This will be difficult with the low signal quality inside some buildings. To improve indoor coverage, an in-building antenna system is needed.

1.1 In-building Signal Propagation

Consider the signal radiated from a transmitter as indicated in figure 1.

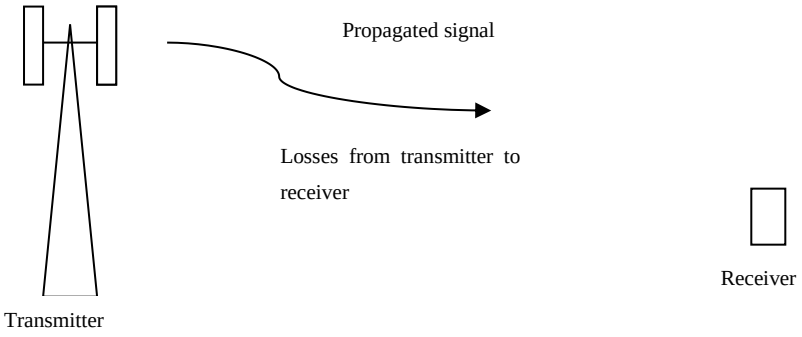

Figure 1.1 Mobile network transmitter system

The losses between transmitter and receiver can be expressed by the Okumura model [2]. The model can be expressed as follows:

$$L_{50} = L_F + A_{mu}(f,d) - G(h_{te}) - G(h_{re}) - G_{AREA} \quad \text{Equation 1.1}$$

L_{50} is the median value of the propagation path loss in decibels (dB), L_F is the free-space propagation loss in dB, A_{mu} is the median attenuation (in dB) in the medium relative to free space at frequency f in Hz, and d corresponds to the distance between the base station and the mobile station in metres. $G(h_{te})$and $G(h_{re})$ are the gain factors (in dB) for the base-station antenna and the mobile antenna respectively. h_{te} and h_{re} are the effective heights of the base-station and the mobile antennas (in metres), respectively. G_{AREA} is the gain (in dB) generated by the environment in which the system is operating.
Both $A_{mu,}$ (f d) and G_{AREA} can be found from empirical curves [3].

Equation 1.1 is usually used to express signal propagation in outdoor environments. In the basic form, it expresses loss as a function of the separation distance between transmitter and receiver and the transmission frequency. In indoor environments, the obstacles between transmitter and receiver are also considered. The Motley Keenan Model [4], as expressed in the Ericsson in-building planning manual [1] and COST 231 Model [5] both considers all walls (and wall properties) intersecting the direct ray between transmitter and receiver. Generally, the losses are expressed as:

$$L_{total} = L_0 + 20log_{10}d + \sum k_i Lw_i \quad \textit{Equation 1.2}$$

Where: L_{total} is the total path loss from the transmitter to the receiver, dB; L_0 is the spreading path loss at 1m (31.5 dB at 900 MHz); d = distance between transmitter and receiver, k_i= the number of types i separating walls; Lw_i= the penetration loss in type i walls, dB.

In-building Distributed Antenna Systems

Multiple antenna, distributed from single base transmitter stations, are used to improve the received signal levels indoors. These are usually designed to enhance the general signal transmitted from the mobile base station and improve the indoor areas where the received signals are below acceptable levels.

1.2 Problem Definition

Consider a simple indoor environment as outlined in figure 1.2. A distributed antenna system may be required to ensure that the building is covered to a minimum signal level.

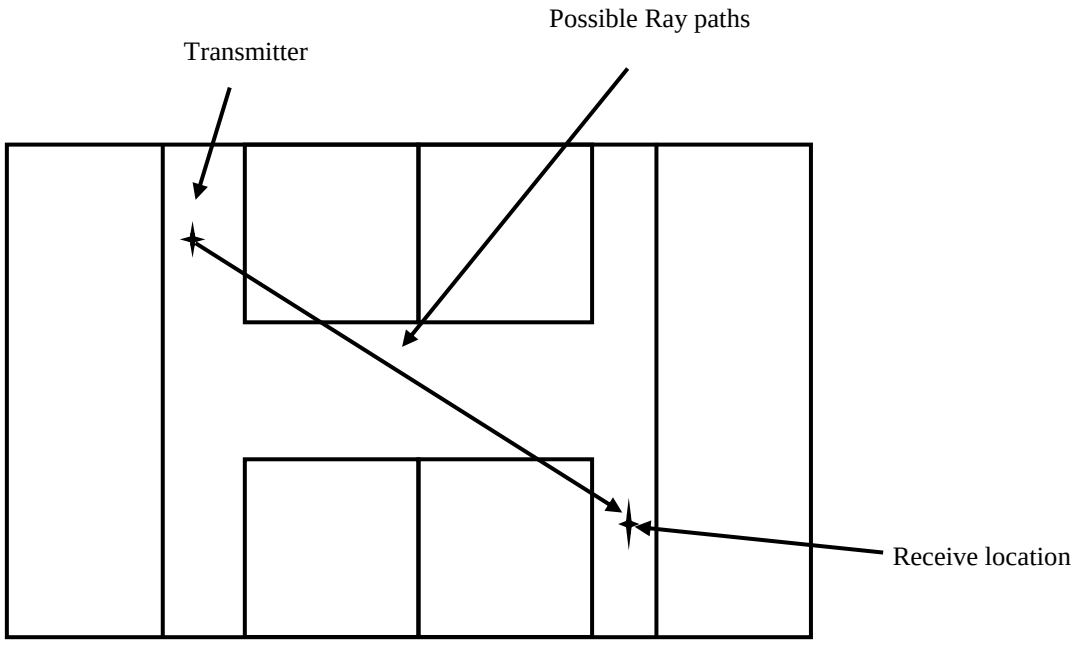

Figure 1.2. Sample building layout

With the use of a simple indoor propagation model as described in equation 1.2, the signal level at multiple receiver locations can be calculated with respect to a single antenna (transmitter) location. Given values for d, k_i and Lw_i, the path loss and hence received signal levels for a known transmitter effective isotropic radiated power (EiRP) at a given frequency. Depending on the transmitter-receiver separation distances, d, multiple transmitters may be needed to ensure that each receiver location is at least better than a desired level.

The number one aim for a wireless network system is to produce profit for the network provider. There is a cost associated with the installation of each antenna, hence the network provider will seek to provide the coverage aims while at the same time minimising the costs to build and operate the network. Hence, the placement of these transmitters in an indoor antenna system is an optimisation problem. For a given building layout, the optimal solution to this

problem is one with the minimum number of transmitters, transmitting at minimum power to achieved the minimum receiver signal levels. The parameters to optimise are:

- Number of antennas
- Location of each antenna
- The EiRP of each antenna

The number of transmitters:

The solution will provide the minimum number of transmitters to achieve the minimum received signal. This represents the lowest cost for installing the system.

The Transmitters location.

The location of each transmitter is affected by the physical characteristics (shape, layout etc) of the building and the number of transmitters. Minimizing the number of transmitters can only be achieved by determining an optimal location for these within the optimisation space. This space is the actual *x-y* position within the indoor environment.

The EiRP of each Transmitters

The effective isotropic radiated power (EiRP) of each antenna affects its optimized location and by extension, the number of required antennas. There is also a financial cost associated to the transmit power. Lower power levels will reduce the network provider running costs.

1.2.1 Manual Planning Methods

Designing in-building coverage solutions it is often a “best guess”, based on experience, as to the most optimal location to place the transmitters so that the building can be adequately covered. The method often used in practise [1] is outlined in figure 1.3 and described in the following steps.

The creation of the nominal plan is done with the aid of the building drawings. The transmitter locations are manually chosen via a suitable propagation model [4]. Basic propagation

calculations are then made to estimate the received signal strength (RxLev) at worst case locations. A typical design requirement for the Global System for Mobile Communications (GSM) at 900 MHz would be that 95% of the building have a minimum RxLev of -85 dBm [6]. The first consideration is the use of one transmitting antenna to ensure that the minimum signal (coverage) requirements are met. If the coverage is not met with one antenna then the radio planner will consider two antennas, thus treating the layout as two separate areas. This process is often repeated until an acceptable solution can be found for the number of antenna required to ensure the minimum signal levels.

The survey phase, involves a physical inspection of the building to identify unsuitable locations (no-go locations) from an implementation point of view. This may require the creation of a new nominal plan.

The walk test phase involves settings transmitters in the chosen locations, according to the nominal plan and measuring the signal levels at worst case locations throughout the building. If the coverage levels are not met the nominal plan is reviewed and the process of nominal planning, and walk testing is repeated as needed.

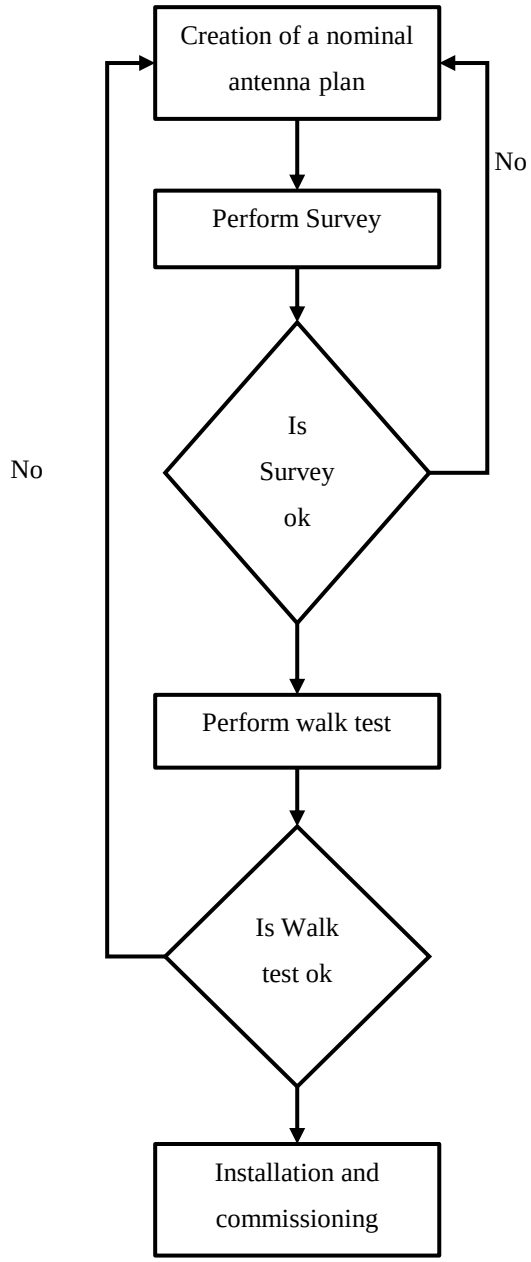

Figure 1.3. Widely use in-building planning design method.

1.2.2 Objectives of this Research

There are commercially available in-building planning software tools [7], [8]. These can automatically estimate the placement of transmitters to provide adequate coverage indoors. There have also been various approaches to solving the problem of automatic transmitter placement.

Berenguer et al. [9] show a solution using a heuristic search algorithm. The algorithm uses direct ray methods combined with a ray tracing method for determining the power received at a given location.

He et. al. [10] uses a pattern search algorithm and optimises the antenna location for power coverage and bit error rate (BER).

These and other previous work [11], [12], [13], [14] all apply a search technique where the coverage area is divided into grids of receiver locations. In each case, the algorithm will search until some optimised solution is reached. These methods all produce a workable solution. A similar optimisation process is employed in this research where, the coverage area is divided into grids of receiver locations. However, the search method used is Particle Swarm Optimisation (PSO).

This thesis presents a novel method to optimally locate multiple antennas within a distributed antenna system. This method combines Particle Swarm Optimisation (PSO) with a process of geometrically partitioning the optimisation space. This produces an optimal solution for the number of antennas, the location and the EiRP of each antenna.

This thesis shows the development of this method, making specific references to the factors affecting the effectiveness of this method. It outlines the propagation model considerations, the optimisation method and the development of a MATLAB simulation to show the effectiveness of the solution. It compares the output from the manual[1] distributed antenna system design methods, as presented in the Ericsson In-building Design Manual [1] to those obtained by this novel approached.

1.3 Thesis Overview

Chapter 2 presents the general aspects of signal propagation and how this is applied in mobile phone technology. The propagation model consideration with respect to an indoor environment is also outlined here.

[1] This is the output one would expect from the design by an experienced engineer using the methods outlined in a typical design manual.

Chapter 3. The different optimisation techniques used to solve the base station placement problem is considered in chapter 3. Here the focus is on Particle Swarm Optimisation and how it can be applied in a distributed antenna system.

Chapter 4 outlines the general method developed with the combination of PSO and the geometric division of the optimisation space. Presented in this chapter also is the development of a MATLAB simulation to show the effectiveness of this solution.

Chapter 5 shows the evaluation and implementation of the proposed method within real buildings. Firstly, the method is validated in smaller layouts with known logical solutions. Then the top floor (W2) of the Sir David Davies building at Loughborough University was planned using the method. Transmitters were set up at the locations indicated by the optimisation method. The measurement setup and results are presented in the chapter. Additionally, the proposed is method is used to plan the antenna configuration for the Xerox building in Montego Bay, Jamaica. The output is compared to the existing plan as done by a local in-building design company [15].

Chapter 6 concludes with general findings and proposes areas for further examination.

Chapter 2 : Signal Propagation

The growth of mobile communications systems has demanded a better understanding of propagation in complex environments. Iskander et al. [16], (for example) has indicated the need for accurately knowing the propagation characteristics of the environment before implementing designs and confirming planning of wireless communication systems.

This chapter introduces the general properties of a radio signal at frequencies used in mobile networks. The propagation models for both outdoor and indoor propagation are described in detail with specific reference made to the model chosen for this research.

2.1 General propagation properties

A radio propagation model is a mathematical formulation to describe how radio waves propagate within a particular environment. Propagation models are widely used by mobile network planners to help determine the best locations to place base transmitter stations to obtain the best radio coverage. Propagation models predict the path loss between transmitter and receiver at different frequencies. Usually, propagation models fall into one of three categories, empirical, site specific and theoretical [16].

An **empirical model** is one in which a set of radio measurements is made and a formulation is used to describe the signal propagation within that environment. This function describes the general signal spreading at particular frequencies with respect to the transmitter to receiver separation distances for different environment classifications.

A **site-specific model** requires very detailed and accurate input parameters. It uses detailed maps to trace ray paths between transmitter and receiver.

A **theoretical model** is derived physically assuming some ideal conditions, like uniform spacing between buildings within an urban environment.

The simplest approach to formulating a propagation model is to estimate the power ratio, *L* between transmitter and receiver as a function of the separation distance *d*. This ratio is referred to as the path loss. The Friis' power transmission formula in free space [17] is indicated in equation 2.1.

$$P_R = P_T \frac{G_t G_r \lambda^2}{(4\pi d)^2} \quad (2.1)$$

Where: P_R is received power, in Watts, P_T is the transmitted power in Watts, G_t and G_r are the transmitter and receiver antenna gain, λ is the wavelength of the signal in metres, and *d* is the transmitter to receiver separation distance in meters.

From equation 2.1, the ratio of transmitted power to received power can be deduced. If transmitter and receiver gains are considered to be unity, this ratio (loss) can be expressed in decibels as follows:

$$L = 20[\log_{10}(4\pi d) - \log_{10}(\lambda)] \quad (2.2)$$

Now $\lambda = \frac{c}{f}$, where *c* is the velocity of light in vacuum, ≈3x10^8 m/s, equation (2.2) becomes:

$$L = 32.44 + 20\log_{10} f + 20\log_{10} d \quad (2.3)$$

Where *L*= path loss in decibels, *f* is the transmit frequency in MHz and *d* is the transmitter to receiver separation distance in km.

2.2 Outdoor Propagation Models

Consider the mobile system propagation environment [18] depicted in figure 2.1. This is different from the free space transmission environment described in section 2.1 and hence, equation (2.3) is not adequate to describe how a signal is propagated in such an environment.

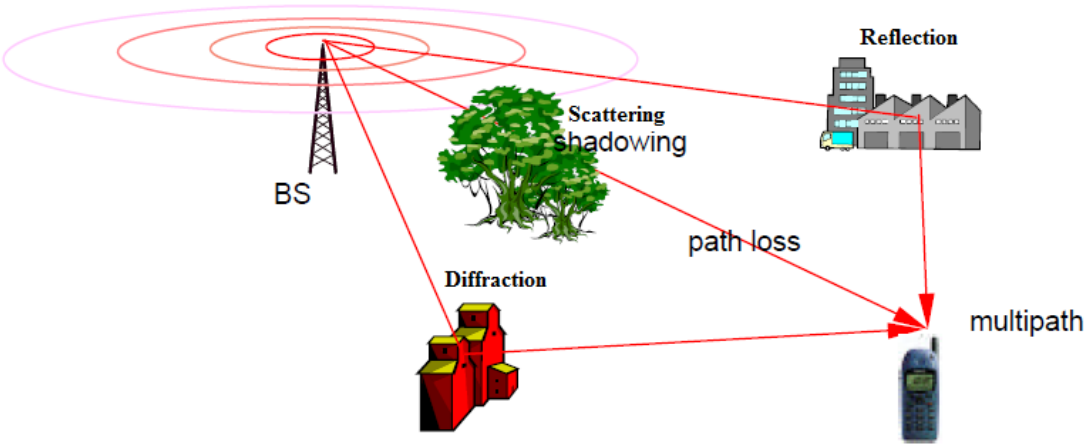

Figure 2.1. Mobile propagation environment from Mahmood [18].

In an outdoor environment, there are additional loss mechanisms to consider. Equation 2.3 can be modified to describe these conditions. The propagation environment is very complex and cannot be fully described by only one model. Hence, there are many different models and approaches to characterising an outdoor radio propagation environment. As an example, work by Walfish et al. [19] shows the development of propagation models at UHF in Urban environments. Andrade et. al. [20] show the comparison between different models for indoor propagation at frequencies described by IEEE (Institute of Electrical and Electronics Engineering) 802.11. Tahat et. al. [21] shows the analysis of outdoor macro models at 2.1 GHz for 3G mobile networks. Iskander et al. [22] outlines general characteristics of different models for general wireless systems. Walh et. al. [23] describe a model that can be used in urban (outdoors) and indoor situations. All these models make reference to the following parameters, described as follow:

$d_{m.}$ The distance between mobile and nearest building, (m).

$f.$ The carrier frequency, (Hz).

$h_{b.}$ The height of the base station (transmitter) above the ground, (m).

$h_{m.}$ The height of the mobile station (receiver) above the ground, (m).

$h_{o.}$ The mean height of a building above local terrain, (m).

$r.$ The distance between transmitter and receiver, (m).

$\lambda.$ Free space wavelength.

A few of these models that are most relevant to the subject matter of the present thesis are described below.

2.2.1 Okumura - Hata Model

The Okumura – Hata model may be the most widely used model in mobile communications. This model is valid for frequency ranges from 150 MHz – 1.5 GHz. This is a fully empirical model where there is a classification of different environment types and the path loss component considers the plane earth model of direct ray or the ground reflection point. Using measurements collected within the city of Tokyo, Okumura developed a set of curves to illustrate the signal propagation in the environment of urban, suburban and open (rural) areas [24].

Area	Formulation
Urban	$L_P = 69.55 + 26.16\log_{10} f_c - 13.82\log_{10} h_b - a(h_m) + (44.9 - 6.55\log_{10} h_b)\log_{10} R\ (dB)$ $a(h_m)$ is the correction factor for vehicular station antenna height Medium-small city $a(h_m) = (1.1\log_{10} f_c - 0.7)\, h_m - (1.56\log_{10} f_c - 0.8)$ Large city $a(h_m) = 8.29(\log_{10} 1.54h_m)^2 - 1.1 : f_c \leq 200\ MHz$ $= 3.2(\log_{10} 11.75h_m)^2 - 14.97 : f_c \geq 400\ MHz$
Suburban	$L_{ps} = L_p\{Urban\ area\} - 2\{\log_{10}(\frac{f_c}{28})\}^2 - 5.4\ (dB)$
Open Area	$L_{po} = L_p\{Urban\ area\} - 4.78\{\log_{10} f_c\}^2 + 18.33\log_{10} f_c - 40.94\ (dB)$
Where: f_c= frequency (MHz) ---------- 150-1500 (MHz) h_b=base station effective antenna height(m)---------- 30-200(m) h_m=vehicular station antenna height(m) ---------- 1-10(m) R=distance (km)---------- 1-20km	

Table 2.1 Hata [25] propagation formulation for different environments.

From the measurements done by Okumura, Hata later produced an empirical formulation for the propagation losses [25]. Table 2.1 shows the formulation [25] for the different environments.

2.2.2 Walfisch-Ikegami Model

The Ikegami Model [26, 27] considers diffractions in addition to the direct ray. These signals may be due to buildings and other path obstacles within a radio environment. Consider the radio environment depicted in figure 2.2. Figure 2.3 show a cross-sectional representation of the path of both rays [28]. From this physical approximation, Ikegami proposed a summation of both reflected and diffracted ray given in [26, 28] as:

$$L_E = 10\log f_c + 10\log(\sin\phi) + 20\log(H - h_r) - 10\log W - 10\log\left(1 + \frac{3}{L_r^2}\right) - 5.8 \quad (2.4)$$

Where L_E is the signal losses in dB, f_c is the frequency in Hz, ϕ is the angle between the street and the direct line from base to mobile, H and h_r are the building and mobile heights respectively, W is the width of the street and L_r=0.25 is the reflection loss.

This model assumes that the height of the base station does not affect the propagation of the radio signal [26]. Hence, losses at large distances are underestimated.

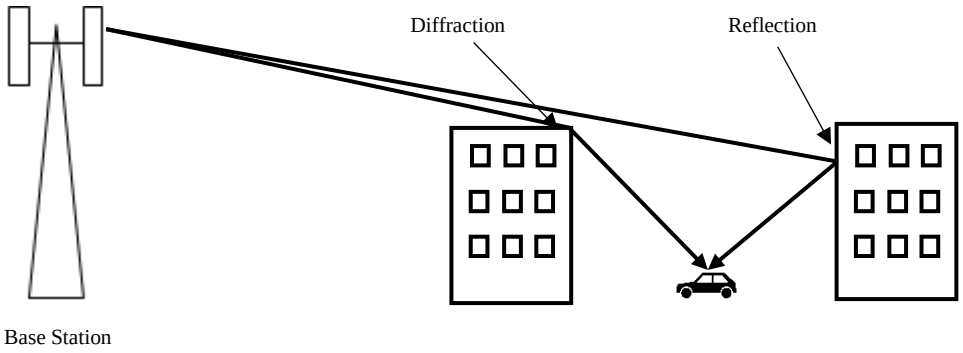

Figure 2.2. Multipath environment with diffraction and reflection

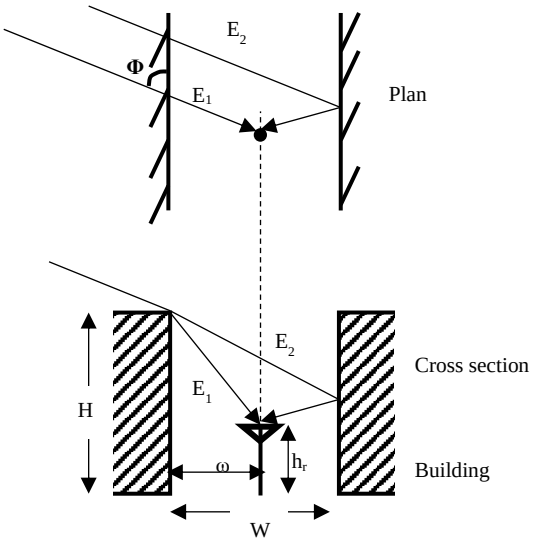

Figure 2.3. Cross-sectional representation of ray paths after Ikegami et al. [28]

Walfisch and Bertoni [19] developed a theoretical model to show the effects that buildings have on signal propagation within an urban environment. The Walfisch-Ikegami model combines the approaches of Walfisch-Bertoni and Ikegami and is applicable for frequencies between 800 MHz and 2 GHz. This model is comprised of three components as outlined in [29]. These are losses in the free space (L_0), losses by diffraction to the level of the streets and by scattering (L_{rts}) and losses due the Multi-paths (L_{ms}). The model is used in urban environments where buildings have a fairly uniform height and fairly equally separated. The total Losses [19] is given by:

$$L_T = L_0 + L_P \tag{2.5}$$

And

$$L_0 = 32.44 + 20\log_{10} f + 20\log_{10} R \tag{2.6}$$

$$L_P = 57.1 + A + \log_{10} f_c + 18\log_{10} R - 18\log_{10} H - 18\log_{10}\left[1 - \frac{R^2}{17H}\right] \tag{2.7}$$

And

$$A = 5\log_{10}\left[\left(\frac{d}{2}\right)^2 + (h - h_m)^2\right] - 9\log_{10} d + 20\ \log_{10}\{\tan^{-1}[2(h - h_m)/d]\} \tag{2.8}$$

Where: *R* is transmitter-receiver separation distance, *m* and *d* is the spacing between buildings. The last term of equation 2.7 accounts for the curvature of the earth and *H* is in metres, *h* is the height of the buildings and h_m is the height of the mobile station.

2.2.3 Ericsson Model (Algorithm 9999)

This model was developed by Ericsson Radio Systems for use GSM mobile systems and is valid for transmitter-receiver separation distances of 0.2km to 100km [6]. Algorithm 9999 is a modification of the Okumura-Hata Model [21] and it takes into account land usage as well as knife-edge diffraction and effects of the curvature of the earth. It allows for the adjustment of certain parameters based on the given environment. This is given as:

$$L = a_0 + a_1 \log_{10}(d) + a_2 \log_{10}(h_b) + a_3 \log_{10}(h_b) . \log_{10}(d) - 3.2[\log_{10}(11.75h_r)^2] + g(f) \quad (2.9)$$

And

$$g(f) = 44.49 \log_{10}(f) - 4.78[\log_{10}(f)^2] \quad (2.10)$$

Where *d* is the transmitter to receiver separation distance, h_b is the base station height, *f* is the frequency, and the constants a_0, a_1, a_2 and a_3 are chosen based on the terrain. Table 2.2 show these values for different terrains.

Parameter	Urban	Suburban	Rural
a_0	36.2	43.2	45.95
a_1	30.2	68.93	100.6
a_2	12	12	12
a_3	0.1	0.1	0.1

Table 2.2 Ericsson model 9999 parameters for different terrains after Tahat et al. [21]

This model is often employed in traditional network planning tools used in the planning of mobile networks. The user has the ability to tune these parameters based on the local environment.

2.3 Indoor Propagation models

There are two possible sources that may present a radio signal inside a building. These are external and internal. In a mobile network, the external source is usually from one or more macro base stations while the internal source would normally consist of a distributed antenna system of a single or multiple transmitter sources. For this research, a distributed antenna system with one or more transmitter sources is considered.

The indoor environment is very different from the outdoor one, consequently, the outdoor propagation models cannot normally be used indoors. The propagation of radio signals inside a building will be affected by the layout, and by different types of building materials. Consider the building layout depicted in figure 2.4. There are open spaces and dividing walls between transmitter and receiver. Additionally, there are normally other indoor obstacles such as tables and chairs and other building furniture. The transmitted signal will reach the receiver via more than one path via the methods of reflection, refraction and diffraction. In figure 2.4 only a two-dimensional signal path is shown, but the signal propagation is also three-dimensional. For this research, the mobile height is considered at 1.5 metres and the transmitter height is at about 2.5 metres. Due to the small difference in transmitter and mobile heights, only the two-dimensional analysis is considered.

An indoor propagation model will seek to characterise how a radio signal will travel between transmitter and receiver within this environment. Consequently, there are many different models that have been used to characterise the propagation of radio signals inside buildings. A few of these are outlined below.

Generally, the transmitted signal arriving at the receiver can be expressed as:

$$Rx_{lev} = P_{Tx} - \sum(L_D + L_{Df} + L_{Rfl} + L_{Rfr} + LNF) \tag{2.11}$$

Where Rx_{lev} is the signal arriving at the receiver in dBm, P_{Tx} is the power of the transmitted signal in dBm, L_D is the signal loss along the direct path in dB, L_{Df} is the signal loss due to diffraction in dB, L_{Rfl} is the signal loss due to reflection in dB and L_{Rfr} is the signal loss due to refraction in dB, LNF is the in-building log normal fading.

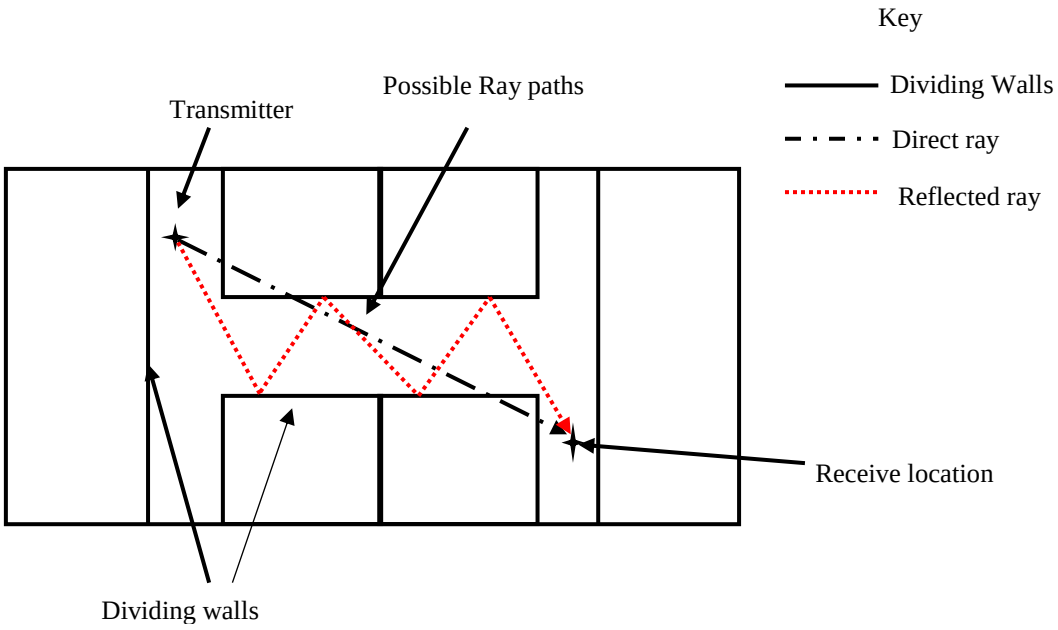

Figure 2.4. Indoor propagation environment

There are generally four main types of rays within an indoor environment [30] as indicated in figure 2.5.

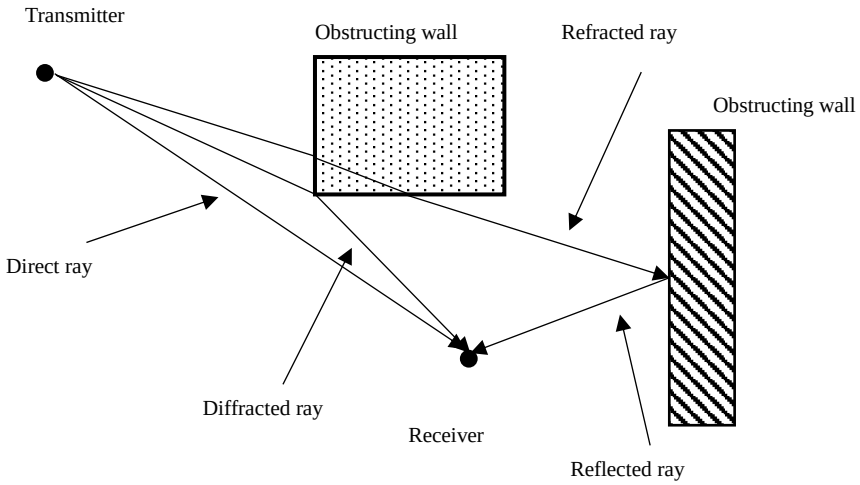

Figure 2.5. Different types of rays

2.3.1 Ray tracing models

A ray tracing algorithm [31] predicts the received strength of a multi-ray system based on the building floor plan. The ray tracing techniques in indoor propagation models are based on Geometric Optics. This assumes that energy can be radiated through infinitesimally small tubes called rays [2]. The rays emanate from the transmitter and travel to the receiver via means of reflection and refraction. The diffraction of the waves is analysed via the Geometrical Theory of Diffraction (GTD). Constantinou [32] describes two general ray-tracing methods, the imaging method and the point and shoot method. Figure 2.6 outlines these.

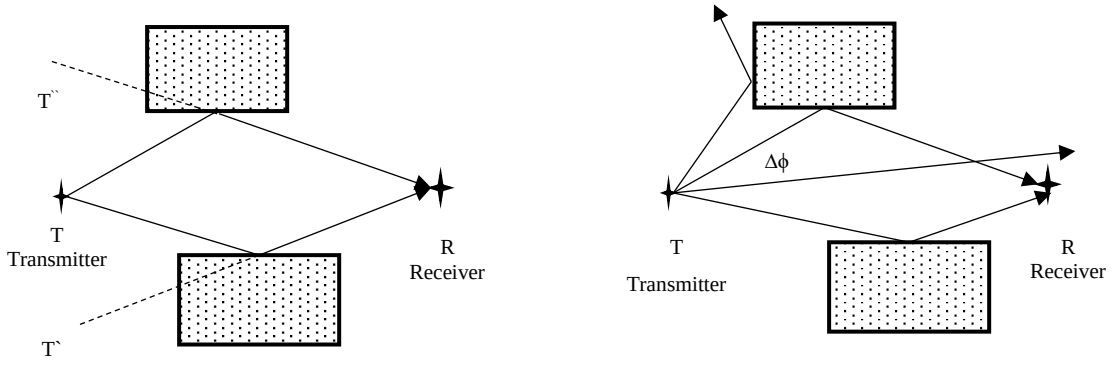

a. Imaging method *b. Point and shoot method*

Figure 2.6. Ray-tracing Methods after Constantinou [32]

In the imaging method, all images of the transmitter are located in order to model single and multiple reflections and to model diffractions all the illuminated edges are located.

The point and shoot method involve launching of rays spaced apart with small angular increment at the transmitter [33]. Not all of these rays may reach the receiver.

Given a mixed path with *n* reflection and *m* diffractions, the field strength associated with each path can be computed as indicated in equation 2.12 below [32] [34].

$$E(R_x) = E_{ref} . \prod_{v=1}^{n} R(\theta_i) . \prod_{\mu=1}^{m} D(\varphi\varphi') A(\{r_i\}) e^{-jk\sum_i |r_i|} \qquad (2.12)$$

Where, E_{ref} is the E-field at a reference point, R and D, the reflection and diffraction coefficients are dyads along the whole ray path. A is an appropriate amplitude spreading factor to account for astigmatism in the ray and $\{r_i\}$ are the lengths of the segments comprising of this path. $e^{-jk\sum_i |r_i|}$ is the propagation phase factor due to the path length r_i, $k = 2\pi/\lambda$, with λ representing the wavelength.

2.3.2 Log Distance Path Loss Model

The log-distance path loss model, also known as the **one slope** model characterises the loss between transmitter and receiver as a function distance and environment. This is the general propagation formulation derived from the Friis power transmission formula and expressed in equation 2.3. This can also be written as:

$$L = L_0 + 10n \log_{10} d \tag{2.13}$$

Where L is the path loss in dB, L_0 is the path loss at distance 1m from the transmitter in dB, d is the transmitter to receiver separation distance in metres and n is path loss exponent.

The path loss exponent n, is used to indicate the propagation characteristics of the environment. In free-space, this is taken to be 2 as represented in equation 2.3 but it can take values up to 5. In particular environments such as tunnels and aisles in buildings, n can take values smaller than 2 [21]. Table 2.3 shows typical values for n in indoor areas at 900 MHz [2], [35].

Building	**Value for *n***
Grocery store	1.8
Retail store	2.2
Open plan factory	1.4-3.3
Open plan office	2.4
Office with soft partitions	2.8

Table 2.3 Typical wall for path loss exponent

The one slope method only considers the direct ray excluding losses due to walls, reflection, refraction etc.

2.3.3 Dual Slope Model

The dual slope model, also known as the **two-ray model** offers an improvement on the one slope model. It considers losses due to the direct ray plus losses due to one reflected ray. Figure 2.7 shows a graphical representation for the consideration of the ray paths for the two-ray method.

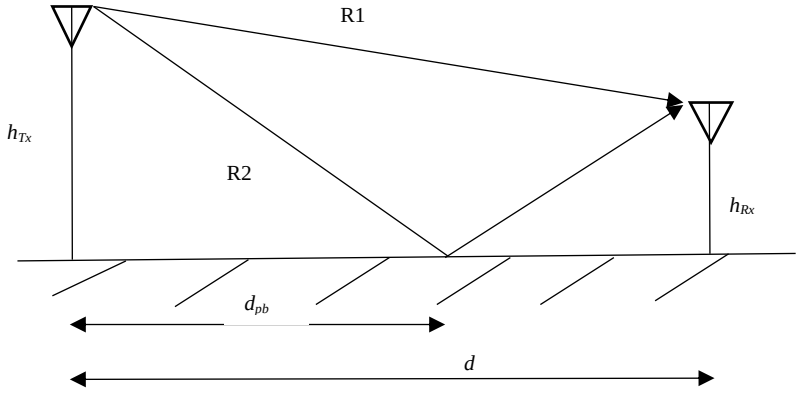

Figure 2.7. Two ray depiction

The two-ray model can be written as described in [20] and [36] :

$$L = L_0 + \begin{cases} 10n_1 \log_{10} d, & 1m < d \leq d_{bp} \\ 10n_1 \log_{10} d_{bp} + 10n_2 \log_{10}\left(\frac{d}{d_{bp}}\right), & d > d_{bp} \end{cases} \quad (2.14)$$

Where L is the path loss in dB, L_0 is the path loss at distance 1m from the transmitter in dB, n_1 and n_2 the path loss exponents are determined experimentally, d is the transmitter to receiver separation distance in metres d_{bp} is the break point distance in metres.

In an in indoor environments the break point is given as described in [20].

$$d_{bp} = \frac{4h_{Tx}h_{Rx}}{\lambda} \quad (2.15)$$

Where, h_{Tx} is the transmitter height in metres and h_{Rx} is the height of the receiver in metres.

2.3.4 The Motley Keenan Model

The Motley-Keenan model improves upon the dual slope model by considering also walls and ceiling along the path of the direct ray. In this model only the direct ray considered. All intersecting walls and ceiling are given an attenuation value. This can be written as:

$$L = L_0 + 10n \log_{10} d + N_w W + N_f F \tag{2.16}$$

Where L is the path loss in dB, L_0 is the path loss at distance 1m from the transmitter in dB, d is the transmitter to receiver separation distance in metres, n is path loss exponent, N_w is the number of walls, W is the average wall attenuation, N_f is the number of floors (or ceilings) and F is the floor attenuation.

This model is also referred to as the average wall model because it uses average values for intersecting walls and ceilings/floor respectively. Table 2.4 indicates the wall losses for different types of walls as indicated in [37].

Material	**Attenuation at 900 MHz, dB**
Glass 6 mm (thickness)	0.8
Glass 13 mm	2
Lumber 76 mm	2.8
Brick 89 mm	3.5
Brick 178 mm	5
Concrete 102 mm	12
Masonry Block 203 mm	12
Concrete 203 mm	23
Reinforced Concrete 203 mm	27
Concrete 305 mm	35

Table 2.4 Typical wall losses for different walls after [37].

2.3.5 The COST 231-Multiwall Model

Instead of using an average value for all the intersecting wall the COST 231 Model add individual losses depending on the wall types [5]. This can be expressed as:

$$L = L_0 + 10n\log_{10} d + k_f^{\left[\frac{k_f+2}{k_f+1}-b\right]} L_f + \sum_{i=1}^{k_w} k_{wi} L_{wi} \qquad (2.17)$$

Where L is the path loss in dB, L_0 is the path loss at distance 1m from the transmitter in dB, d is the transmitter to receiver separation distance in metres, n is path loss exponent, k_f *is* number of penetrated floors, b *is* empirical parameter used to fit the non-linear effects of the number of floor along the path, L_f *is* loss between adjacent floors, k_{wi} is number of penetrated walls of type i and L_{wi} is loss of wall type i.

The wall types are divided into two categories [20], [5]. Table 2.5 shows these categories and the typical values for these categories.

Wall Type	**Description**	**Loss Value(dB)**
Light wall (L_{w1})	A wall that is not bearing load: e.g. plasterboard, particle board or thin (<10 cm), light concrete wall.	3.4
Heavy wall (L_{w2})	A load-bearing wall or other thick (>10 cm) wall, made of e.g. concrete or brick.	6.9

Table 2.5 Typical wall losses for different for the multi-wall model after [5].

2.4 Coverage Vs Interference

In a mobile network system, it is important to differentiate between coverage and interference. Consider an internal source as indicated in section 2.3, then the assumption is that the building has no mobile signal and the problem becomes a coverage issue. The solution is to produce a transmitter source or sources that will present all part of the building with a minimum receive signal of say -85 dBm for example. This is not an interference problem as there are no external interfering sources.

In this research, the aim is to improve the signal coverage in no-coverage areas. The test building is treated as one with no present signals and hence there is no need to consider interference. All external sources are ignored and signal leakage from the building is also not considered. Additionally, each transmitter location is considered to be transmitting at a different frequency so the effects of multi-path and other internal/own interference are not considered.

2.5 Discussion

In this research, a multiple antenna in-building system is required to ensure that a single floor of a building is covered to a required signal level. The Keenan-Motley propagation model is used in the research. It has been shown to be more accurate than the multiwall model [20]. When used at 900 MHz on a single floor it can be expressed as:

$$L_{total} = L_0 + 20log_{10}d + \sum k_i Lw_i \tag{2.18}$$

Where: L_{total} is the total path loss from transmitter to receiver, dB; L_0 is the loss at 1m given as 31.5 dB at 900 MHz; d = transmitter-receiver distance, m; n, the path loss exponent is taken to be 2; k_i= the number of type i separating walls; Lw_i= the penetration loss in type i walls, dB; Chapter 4 outlines the wall attenuation value used in this research and chapter 5 outlines how these were estimated.

Combined with equation 2.11 the received signal level can be expressed as a function of transmit power as:

$$Rx_{lev} = P_{Tx} - 31.5 + 20\log_{10} d + \sum k_i Lw_i \tag{2.19}$$

Where Rx_{lev} is the received signal level at a distance d from the transmitter in dBm and P_{Tx} is the transmitter power level in dBm.

The reasons for the choice of this model are due to its simplicity and ease of comparison with normal planning methods.

Simple calculations

The optimisation methods proposed as described in chapter 3 requires substantial computational resources. For this reason, the calculations for propagation model needs to be relatively simple. The Keenan-Motley does not consider multipath, or multiple rays and hence this reduce the computational requirements for this model. However, it has been shown to have acceptable performance in similar situations [20].

Ease of comparison to normal planning methods

One of the usual methods of planning an in-building distributed antenna system is indicated in the Ericsson in-building planning manual [1]. Here the recommended propagation model is Keenan-Motley. In this research, the aim is to compare any planning method to the method used day to day by Engineers in the practical situations. For this purpose, this model is also chosen.

2.6 Conclusion

Signal propagation in an outdoor environment differs from that in an indoor environment. The inbuilding propagation model chosen in this research is Motley-Keenan model. This has been shown [1] to be effective when used in the planning of inbuilding systems.

Chapter 3 : Optimisation Methods

Within concext of this research, optimisation means the process of finding the optimal solution to the problem defined in chapter 1. The optimal solution to this problem is one with a **minimum** number of transmitters, transmitting at **minimum** power to achieved the **minimum** receiver signal levels. The antenna is moved through the optimisation space (building layout) until the a location is found where all the measured receiver location are above a requied threshold.

The manual design and planning for the placement of antennas in a distributed antenna system is described in [1]. This is often a 'best guess,' based on experience, as to the most optimal location to place the transmitters so that the building's design requirements are met. The conventional method will see the engineer with the aid of the building drawings, manually choose the antenna locations and perform simple calculations to estimate the received signal strength (*RxLev*) at worst case locations. This process is often repeated several times until a solution can be found. The antennas are usually arbitrarily placed with little regard to optimising these locations to reduce the number of antennas and improve receive levels (*RxLev*). The process is often ended once the desired covered levels are achieved, and solutions for an optimum number of antennas are not often pursued.

There are commercially available in-building planning software tools [8]. These require the user to select the various antenna locations and then calculations are made to determine how effective the selected locations are. So far, this does not provide a method to automatically select the most optimal antenna locations.

There have also been various approaches to solving the problem of automatic transmitter placement. Berenguer et al. [9] show a solution using a heuristic search algorithm. He et al. [10] uses a pattern search algorithm and optimises the antenna location for power coverage and bit error rate (BER). Other previous work [11], [13], [12] and [14] all apply a search technique where the coverage area is divided into grids of receiver locations. In each case, the algorithm will search until an optimal solution is reached.

In this chapter, a review of various optimisation search techniques is presented. Presented also is a review of how to geometrically partition a two-dimensional space. Finally, this chapter concludes with the **novel** approach of combining particle swarm optimisation with geometric partitioning of the optimisation approach for solving the automatic placement of **multiple** antennas within an in-building system. This approach is very logical in that the optimisation space can be easily visualized as a two-dimensional field and this approach builds on the recommended method for the design of in-building planning systems as described in the Ericsson GSM In-building Solution Manual [1].

3.1 General Optimisation Methods

The problem of automatic antenna placement within a building is a global one. Its solution requires optimisation of the number of antennas, their individual EIRP and their physical location (*x, y* coordinates) within the building. In this research, the objective function for this problem is the percentage coverage. A typical design requirement for the Global System for Mobile Communications (GSM) at 900 MHz would be that 95% of the building have a minimum *RxLev* of -85 dBm [6]. The percentage coverage would be obtained by noting the number of receiver location better than the minimum *RxLev* compared to the total number of receiver locations.

Due to the building layout (obstructing walls, etc.), the coverage at receiver location can change dramatically with small change in antenna locations. This means that objective function can be described as nondifferentiable and obtaining a gradient of the objective function is not practical [12]. Hence, an appropriate search method is needed. A few possible approaches to solving this problem are discussed below.

3.1.1 Direct search methods.

Direct search methods are best known as unconstrained optimization techniques that do not explicitly use derivatives [38]. With this method, one parameter is varied at a time in small steps. The steps are halved when there is no change in outcome.

The Nelder-Mead Simplex Method (NM) [39] and [40] is a direct search method that has been suggested as a possible solution to the indoor transmitter location problem [12]. A simplex is

defined [41] as a geometrical figure of *n* dimensions consisting of *n+1* points. *n=2* describes a triangle for example. The vertices of each simplex are sorted according to functions given as:

$$f(x_1) \leq f(x_2) \ldots\ldots \leq f(x_{n+1}) \tag{3.1}$$

Where x_1, $x_2 \ldots x_{n+1}$ represent the each of the *n+1* simplex vertices.

This method simply compares the objective function at a set of point. The result of each iteration is either a single new vertex or a set of *n* new points that, together with the previous best vertex, forms the simplex at the next iteration [12]. The aim is to replace the worst vertex with a new point in the steps of reflection, expansion, contraction and shrinkage. For example, with reflection, the worst point is replaced by a point reflected through the centroid of the remaining points. The algorithm has been explained in further details in [41]. It has been shown [12], over four years of extensive testing to be an effective method for dealing with one of the variables in the problem indoor antenna location placement problem.

3.1.2 Bundle methods.

A bundle algorithm collects information about the previous iteration in a set, the bundle. This information is then used to compute a tentative descent direction along which the next points are generated [42].

A Bundle method for optimal transmitter location in indoor wireless systems has been suggested by Aguado Agelet et al. [41] and [43]. First, a cost function *f(x,y)* is introduced which consists of two objective functions f_1 and f_2 given as:

$$f_1(x,y) = \sum_{i=1}^{m} \frac{\omega_i}{m} [g_i(x,y) + \mu_i \max\{0, g_i(x,y) - S_i\}] \tag{3.2}$$

And

$$f_2(x,y) = \max_{i=1,\ldots,m} (\omega_i [g_i(x,y) + \mu_i \max\{0, g_i(x,y) - S_i\}]) \tag{3.3}$$

Where f_1 is the mean of all the weighted path loss predictions, along with a penalty term representing the violation of a maximum tolerated path loss threshold, S_i at each receiver

location and f_2 is the maximum of the weighted path loss predictions, $g_i(x, y)$ represent the path loss at the *i*th receiver location from a given transmitter location *(x,y)*.

The aim is to minimize the measurement of the weighted path loss. In this bundle method, the generalized gradient in each iteration is approximated by the information collected from previous iterations. After *k* iterations, the cutting plane model of *f* is built:

$$p_k(x) = \max\{f^j + \left(x - x^j\right)^t S^j, j = 1, \dots\dots, k\} \tag{3.4}$$

Where the bundle is formed by:

$$\{x^j, f^j = f\left(x^j\right), S^j = S\left(x^j\right) \in \partial f\left(x^j\right), j = 1, \dots., k\} \tag{3.5}$$

The mechanism involves generating two sequences: a sequence of sampling point $\{x^j\}$ to construct the model and a subsequence of serious points $\{\underline{x}^s\}$ to warrant a sufficient decrease in the original function *f*:

$$\underline{x}^{s+1} = x^k \text{when} f(x^k) \leq f\left(\underline{x}^s\right) - \alpha\delta_k \tag{3.6}$$

Where δ_k is the nominal decrease in the model and $\alpha \in (0,1)$ is an Armijo-like [44] tolerance. This limits the optimisation movements and is needed to ensure that the function converges.

The bundle method usually provides a good solution with few iterations but the cost functions can be very complicated and difficult to formulate. This is in contrast to the simplistic approach taken in the manual planning methods described in [1] that is widely used in day to day network planning.

3.1.3 Genetic Algorithms.

Genetic Algorithm (GA) is an optimisation method inspired by evolution in nature. This is a heuristic search procedure based on the ideas of natural selection and genetics [45]. These algorithms encode a potential solution on a simple chromosome-like data structure and apply recombination operators to these structures so as to preserve critical information [41].

The first step in the GA process is the formulation of the population. After this, the algorithm progresses through steps known as selection, cross-over, and mutation.

Selection is where preference is given to the better individuals within the population
Cross-over is the combination of two individuals selected from the population using the selection criteria.
Mutation is used to maintain diversity within the population and prevent premature convergence.

The GA can be implemented in the following procedures [45]:

1. randomly initialize population at time *t*
2. determine the fitness of the population at time *t*
3. repeat
    a. select parents from population at time *t*
    b. perform crossover on parents creating population at time *t +1*
    c. perform mutation of population at time *t +1*
    d. determine fitness of population at time *t +1*
4. until the best individual is good enough

One of the approaches to using GA to solving the base station problem is shown in [46]. Here the genome is denoted as a vector

$$g = (c_1, \ldots., c_K), \tag{3.7}$$

Where $c_k=(x_k,y_k)$ is the chromosome for the *k*th base station position. K is the maximum number of base stations and all of them are located in the *X*-range [$-X_{max}$, X_{max}] and *Y*-range [$-Y_{max}$, Y_{max}] as indicated in figure 3.1

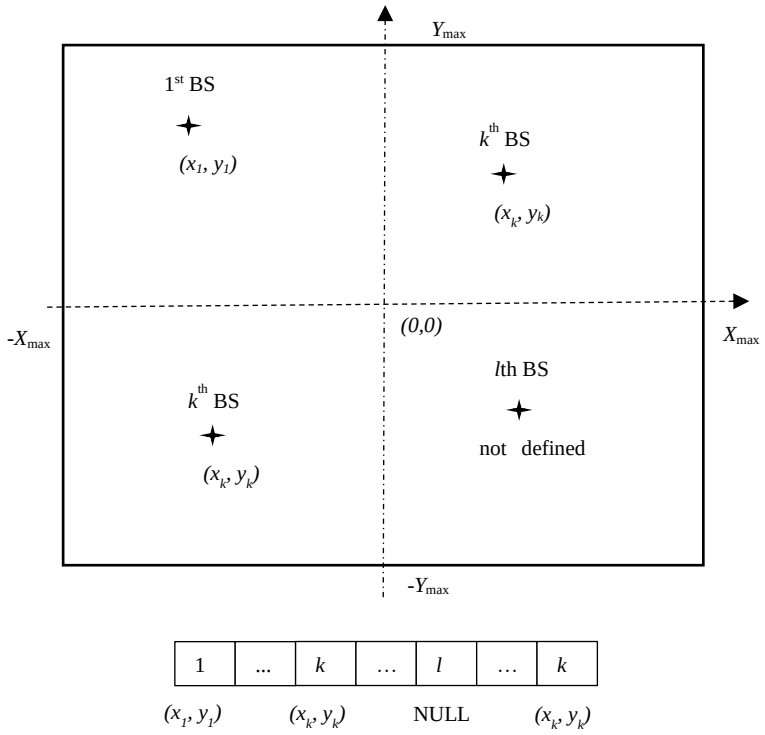

Figure 3.1. Representation of genome for base station placement adapted from Byoung-Seong et al. [46].

The fitness function is given as:

$$f(g) = w_t * f_t(g) + w_e * f_e(g) \tag{3.8}$$

Where f_t and f_e are the objective functions for coverage and economy fitness, respectively. w_t and w_e are weight used to determine the number of base stations. $w_t + w_e = 1$.

f_t and f_e are defined as:

$$f_t(g) = \frac{covered\ traffic}{total\ offered\ traffic} \tag{3.9}$$

and,

$$f_e(g) = \frac{K - n(g)}{K} \tag{3.10}$$

Where *n(g)* is number of existence in *g*.

The algorithm goes through the process as described above to find the optimum location of each base station and the least number of base stations to provide the best coverage. This was employed in an outdoor environment with the assumption that each transmitter (cell) is a hexagon with a radius of 2.5 km.

Another application of GA is explored by Mangoud [47]. Here, a method of optimization of channel capacity for indoor multiple input multiple output (MIMO) systems is outlined. This optimizes the number of array elements at the base station *(Mr)*, and the mobile station *(Mt)* and the configuration of the element. The fitness function is given by:

$$Fitness = c = \log_2 \left[\det \left(I_{Mr} + \frac{SNR}{Mt} TT^H \right) \right] \quad (3.11)$$

Where I_{Mr} is the identity matrix with dimensions *Mr* x *Mr*. *SNR* is the average signal to noise ratio and *T* is the complex matrix obtained as indicated in [48].

3.2 Other Optimisation Methods

There are other optimisation methods which also provides effective solutions to the base station placement problem in an indoor system. Two of these are described in details below. These are Particle Swarm Optimisation and Simulated Annealing.

3.2.1 Simulated Annealing

Simulated annealing is another considered optimisation method. It is likened to metal working where the temperature of the metal is heated and cooled to alter its physical properties. If the metal is allowed to cool quickly it will become brittle, however if it cools slowly, its atoms will have enough time to settle in a strong configuration. In simulated annealing a temperature variable is kept to simulate this heating process [49]. As indicated in [49] and [50] the algorithm works as described in the following steps:

1. The initial temperature is set and a random initial solution is created
2. The system is looped until the exit conditions are met. Usually either the system has sufficiently cooled, or a good-enough solution has been found.
3. Then a neighbour is selected by making a small change to the current solution.

4. This new candidate solution is evaluated and if it is better than the previous, it is accepted as the current solution. If it is not better than the previous, there will be a probability of this new worst solution to be accepted based on the cost of each solution and the present temperature in the system.
5. Then the temperature is decreased and continue looping

The process indicated in step 4 can be described by the following equation [51]

$$A = e^{-\frac{c(N)-c(P)}{t}} \tag{3.12}$$

Where *A* is the probability of accepting the worst solution, *c(N)* is the cost of the new solution, *c(P)* is the cost of the present solution and *t* is the temperature.
The temperature is the basic driving mechanism of the algorithm. At high temperatures, the system is more likely accept solutions that are worse. It is the manipulation of the temperature that leads to a solution. This procedure is done in a loop and after an arbitrary number of iterations occurs the temperature is multiplied by a reduction factor. This will make the temperature decrease and consequently more difficult to accept worst solutions. This technique uses only one solution and tries to guide it to the best place in the design space [51].

Simulated annealing is often compared to the hill climber algorithm [49] to demonstrate its advantages. Figure 3.2 below show the logic behind the hill climber algorithm [49], [52] and [53].

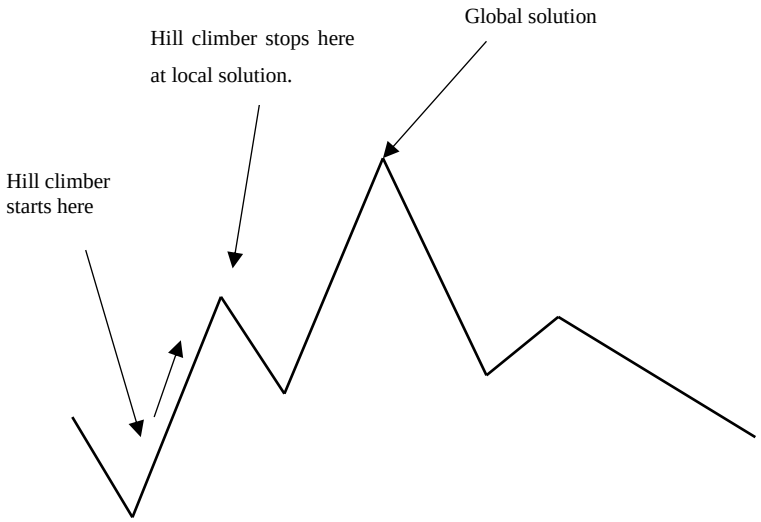

Figure 3.2. Hill climber algorithm

The hill climber algorithm works by accepting a neighbour that is better than the current one. So the hill climber will climb until it reaches a point where it will have to first decent before it can climber any higher. This point will be considered the solution. As in the case depicted in figure 3.2, this is not a global solution. Hence, the hill climber has the tendency to get stuck in local optimums [50]. This problem is avoided in simulated annealing. It will accept local solutions occasionally but over time, it will move to the global solution.

One of the implementations of Simulated Annealing can be seen in [54]. It is employed as a proposed method to solving the base station placement problem in a distributed antenna system (DAS). In this case, all the antennas share the same base station. It uses a neighbour discovery approach that increases the probability to drive the solution towards the optimal configuration. Firstly, four objective functions were formulated. These are

$$Min\left\{F_1 = \sum_{i \in B} b_i C_i\right\} \tag{3.13}$$

Where F_1 is the cost to install all the antennas. It is to be minimized depending on the number of antennas b_i and the financial cost of each c_i, B is the set of all possible locations of antennas

$$Max\left\{F_2 = \frac{1}{|M|}\sum_{j\in M}\sum_{i\in B} b_i P_i^{(r)}\right\} \tag{3.14}$$

Where F_2 is maximized the received power in all the receiving location. M is the set of all users receiving points and $P_i^{(r)}$ is the received power at a point j from antenna i.

$$Max\left\{F_3 = P_{min,j}^{(r)}\right\} \qquad \forall j \in M$$

Where:

$$P_{min,j}^{(r)} = Min\sum_{i\in B} b_i P_i^{(r)} \quad \forall j \in M \tag{3.15}$$

Where F_3 varies the power of each antenna output such that the minimum value of the received powers is minimized.

$$Min\left\{F_4 = \frac{1}{|W_E|}\sum_{j\in W_E}\sum_{i\in B} b_i P_i^{(r)}\right\} \tag{3.16}$$

Where F_4 minimized the power leakage outside the building by decreasing the power received on the external walls of the building. W_E is the set of external walls.

These objective functions are further subjected to two particular constraints. The first indicates the minimum value of received power that has to be satisfied at all the receiving locations in order to provide the users with the required bit rate.

Constraint 1. (C1)

$$\sum_{i\in B} b_i P_{i,j}^{(r)} > \hat{P}^{(r)} \tag{3.17}$$

Where $\hat{P}^{(r)}$ is the minimum received power threshold.

The second constraint indicates the summation of all the transmitting powers of the antennas must be equal to the radio cabinet maximum power (ignoring the cable losses).

Constraint 2. (C2)

$$\sum_{i \in B} b_i P_i^{(t)} > P_{max}^{(t)} \tag{3.18}$$

Where $P_i^{(t)}$ is the transmitting power of antenna *i*, and $P_{max}^{(t)}$ is the maximum transmitted power from the base station.

Simulated Annealing is now used to find the solution to these formulations.
The first step is to find an initial location. This location is such that both constraints (C1 and C2) are satisfied. The general process as indicated in [54] is explained as follows:

> "three different functions were introduced: *dropMove*, *addMove*, and *randMove*, to explore neighbourhood solutions of the initial solution in addition to the power optimization function *optimizePower* that is applied after each of these three functions. The *dropMove* is used to optimize the objective function by removing deployed antennas that are not the best to optimize F2, F3 and F4 and redistribute their power among the other antennas. While *addMove* aims to optimize F2, F3 and F4 and satisfy the coverage constraint (C1) while keeping the value of F1 constant by changing the power and locations of the deployed antennas. If C1 remains violated, a new antenna must be deployed. The *randMove* is used to randomly explore neighbourhood solutions. The *optimizePower* is used to optimize the transmitting power of deployed antennas. The above three functions are executed successively until a feasible neighbour solution is obtained and compared with the best-found solution so far which is accepted if it is better or according to the simulated annealing probability"

This Simulated Annealing probability is indicated in equation 3.16.

Another implementation of Simulated Annealing is indicated in [55]. Here it has been employed as means to position base stations in network planning for Wideband Code Division Multiple Access (WCDMA).

3.2.2 Particle Swarm Optimisation

Particle Swarm Optimisation (PSO) is a population-based optimization method originally proposed by Kenney and Eberhart [56] and it has been used to solve numerous optimisation problems [57]. The basic description of the elements of a PSO algorithm is explained in [58] where the PSO is likened to a swarm of bees searching a field for the location of the most flowers. The algorithm seeks to move all the bees/particles to the best location by changing the velocities and hence positions of each particle. It does this by combining the best position of each particle and the best position reported by the entire swarm. PSO has many advantages when compared to other search method, such as fewer parameters needed to be adjusted and the rapid convergence speeds [59]. The parameters of a PSO systems as explained in [58] are:
Particle or *Agent:* Each individual in the swarm is referred to as a particle or agent. All the particles in the swarm will individually accelerate toward a vector summation of the best personal (*pbest*) location and best overall (*gbest*) location.
Position: In the analogy above *position* referred to a bee's place in the field. This is represented by coordinates on the *x*-*y* plane. In general, however, this idea can be extended into any N-dimensional space according to the problem at hand. This N-dimensional space is the solution space for the problem being optimized, where any set of coordinates represents a solution to the problem. In the analogy above the solution is a physical location on the *x*-*y* plane, but this could just as easily represent amplitude and phase of element excitation in a phased array. In general, these can be any values needed to be optimized. Reducing the optimization problem to a set of values that could represent a position in solution space is an essential step in utilizing the PSO.
Fitness: The fitness is used to rank the suitability of each position. In the analogy above the fitness function would simply be the density of flowers: the higher the density, the better the location. In general, this could be antenna location within a building, weight, peak cross-polarization, or some kind of weighted sum of all these factors. The fitness function provides the interface between the physical problem and the optimization algorithm.
pbest: In the analogy above each bee remembers the location where it personally encountered the most flowers. This location with the highest fitness value personally discovered by a bee is known as the personal best or *pbest*. Each bee has its own *pbest* determined by the path that it has flown. At each point along its path, the bee compares the fitness value of its current location to that of *pbest*. If the current location has a higher fitness value, *pbest* is replaced with its current location.

gbest: Each bee also has some way of knowing the highest concentration of flowers discovered by the entire swarm. This location of highest fitness encountered is known as the global best or *gbest*. For the entire swarm, there is one *gbest* to which each bee is attracted. At each point along their path, every bee compares the fitness of their current location to that of *gbest*. If any bee is at a location of higher fitness, *gbest* is replaced by that bee's current position.
The general PSO algorithm is given as:

$$V(n) = \omega V(n) + C_1\alpha_1[\text{pbest}(n) - X_1(n)] + C_2\alpha_2[\text{gbest}(n) - \text{X}_1(n) \quad (3\text{-}19)$$

And:

$$X(n) = X_1(n) + V(n)t \quad (3\text{-}20)$$

Where *V(n)* is the velocity of the nth particle, $\text{X}_1(\text{n})$ is the initial position of the nth particle, gbest is the globally best position for all the particles and pbest is the best position for the nth particle. ω applies weighting to initial velocity, C_1 and C_2 determines the pull of the particle to pbest and gbest respectively, α_1 and α_2, are random numbers between 0 and 1, $X(n)$ is the new position of the nth particle, and *t* denotes the time for which this velocity is applied.

The advantages of PSO are is its simplicity, speed and robustness in overcoming the local minima problem [60]. The effectiveness of PSO can be improved via the selection of the parameters namely ω, C_1 and C_2. A few of the suggestions for values for these constants are given in [58], [61], [62] and [63]. The effect of these constants are described as follows:
ω- This is the initial weight. This scales the old velocity and controls the speed at which the particle/bee flies over the solution. Typical values [58] can be between 0.9-0.4.
C_1 and C_2 – These determine the relative pull towards *pbest* and *gbest*. C_1 describes the pull towards *pbest* (the local solution) and C_2 describes the pull towards *gbest* (the global solution). Typical values [58] for both is 2. The size of the swarm is also very important for the PSO algorithm to converge, suggested values for this is shown in [64].

Vilovic et al. [60] describe PSO combined with a neural network for the placement of a single antenna in an indoor system. In this implementation, the fitness function is described to represent the quality of coverage over a given space as a function of transmitter location.
This is given as:

$$f_i = \sum_{i=1}^{N}\sum_{j=1}^{M} S_i(x_j, y_j) w\left(S_i(x_j, y_j)\right) \tag{3.21}$$

Where *N* and *M* are the numbers of possible locations of the base station and receiving points respectively. S_i is the relative signal level (dBm) received from base station *i* at the location with coordinates (x_j, y_j) while w_j is the relevant priority weight ascribed to the *jth* receiver location and it makes constraint in the cost function. This constraint indicates the quality of signal coverage at each receiver location. At different receiver thresholds, w_j can be obtained as:

$$w_j = \begin{cases} S_i(x_j, y_j) > -60\ dBm & w = 1 \\ -60 \geq S_i(x_j, y_j) \geq -72\ dBm & w = 10 \\ S_i(x_i, y_i) < -72\ dBm & w = 100 \end{cases} \tag{3.22}$$

This method is limited by the number of transmitters being a single transmitter.

Another application of PSO is shown in [65] where it is used to allocate the location of receiver antenna in ultra-wideband (UWB) wireless communication systems in an indoor environment. The bit error rate (BER) is calculated and PSO is used to find the best optimum receiver locations that would minimize the outage probability relative to transmitter location.

Additional applications of PSO to the indoor antenna placement problem can be seen in [66], [67] and [68]. In these cases, the PSO is used to optimize the best locations for a given number of transmitters.

3.3 Discussion

As stated in section 3.1, the objective function for the indoor antenna placement problem can be described as nondifferentiable and obtaining a gradient of this objective function is not practical [12]. A few of the approaches to solving this base station problems have been shown in section 3.1 and section 3.2 above. In section 3.1, the direct search method, the Bundle methods and genetic algorithms have been presented. In section 3.2 particle swarm

optimisation and simulated annealing have been presented. The methods all have advantages and disadvantages in solving the base station placement problem within an indoor environment.

The Nelder-Mead Simplex Method is not guaranteed to converge [41] and can be inefficient as described by Olsson and Nelson [40];
"Given an extremely sharp ridge, produced by high inter-dependency among the variables, the method can become inefficient to the point of failure"

The bundle method shown in [41] provides a very useful solution but the formulation of the cost functions and the programming can be very difficult.

Genetic Algorithms are similar to PSO in that both are population based search methods. These both move from a set of points (population) to another set of points in a single iteration with likely improvement using a combination of deterministic and probabilistic rules [69]. Table 3.1 shows a general comparison of between both these methods.

Genetic Algorithm	**PSO**
* High computational time to converge. *Several implementation selection options (tournament or proportionate selection) *Can get stuck in local solutions	*Quick convergence *Ability to explore the entire optimisation space (global search) and avoid local solutions *More computationally efficient *Better quality of solution *Easy to implement

Table 3.1. Comparison of Genetic Algorithm and Particle Swarm Optimisation

The solution proposed in [54] using Simulated annealing provides a workable one but generally, PSO performs better than Simulated Annealing with substantially improved execution times because of the smaller number of function evaluations needed for convergence. It has been shown [70] that as a randomized search algorithm, the PSO algorithm is better suited to detect a developing induction motor winding fault. It achieved a success rate of about 99% compared with 60% for the SA algorithm.

For this research PSO have been chosen, PSO offers a very simple and potentially very efficient solution. Many different research [41], [69], [71], have shown PSO to be more computational efficient than GA. Aguado et al. [43] have shown that the computational time for a simple GA is very high and the convergence is not assured. Via a set of bench mark test problems Hassan et al. [69] have shown that the computational efficiency superiority of PSO over the GA is statically proven with a 99% confidence level.

With PSO, the problem can be easily formulated with a simple fitness function and the optimisation space is directly translated to the building coordinates. In PSO there are fewer parameters that need to be adjusted and hence it rapidly convergences in comparison to other algorithms such as SA. PSO is very robust in overcoming local minima problem [60] and it is faster and more accurate in comparison with other optimisation methods [58]. The PSO applications seen so far, usually involves the case of a single antenna [60], [59] or it is applied in an outdoor situation [66].

The problem as indicated in the introduction to this chapter requires a solution that incorporates multiple antennas in an indoor scenario. The solution proposed in this research is presented in section 3.5, it combines PSO with a means of geometrically dividing the optimisation space.

3.4 Geometric Partitioning

A few applications of PSO to the solution of the indoor antenna location problem can be seen in [66], [60], [67] and [68]. These cases all demonstrate the effectiveness of PSO in solving the indoor antenna placement problem. In these cases, the PSO is used to optimize the best locations for a given number of transmitters but there is no method to automatically select the number of antenna. Compared to one transmitter in two-dimensional Cartesian space, each new transmitter introduces two additional variables to the problem as indicated in [68]. This introduces additional constraints that can be easily incorporated in the original PSO equations. However, the problem is how to determine how many antennas are needed for a complete solution of the base station placement problem.

In section 1.2.1, the manual inbuilding planning process is described. In this method, if the received signal levels are not met with one antenna then the radio planner will consider two antennas, thus treating the layout as two separate areas. This planning method is widely used

by mobile network operators as it provides practical workable results. For this research, a similar consideration is used to determine if additional transmitters are needed.

For the problem presented in this thesis, the optimisation space is the physical floor layout. With the aim of providing a simple geometric description of the entire space including areas where antennas are not allowed to be placed (no-go areas), this space is assumed to be rectangular. Subsequently, the partition of this space will also result in rectangles.

Consider a two-dimensional space with dimensions *(a,b)* as indicated in figure 3.3. They are numerous was this space can be divided.

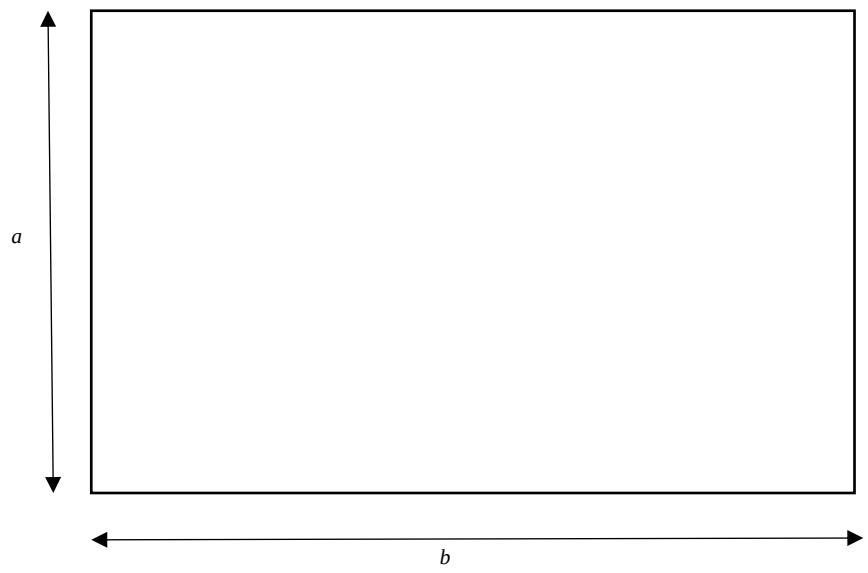

Figure 3.3. Two-dimensional space

A few of these possible divisions are indicated by the broken lines in figure 3.4. In the present thesis, this rectangular shape is to be divided into two parts. This is a similar problem described by Kong [72] and Kleitman [73]. The following conditions must be met for the new shapes.

1. The new shapes must be rectangles.
2. The area of the two new shapes must be equal.
3. The difference between the length and the height of each of the new shapes should be minimised.

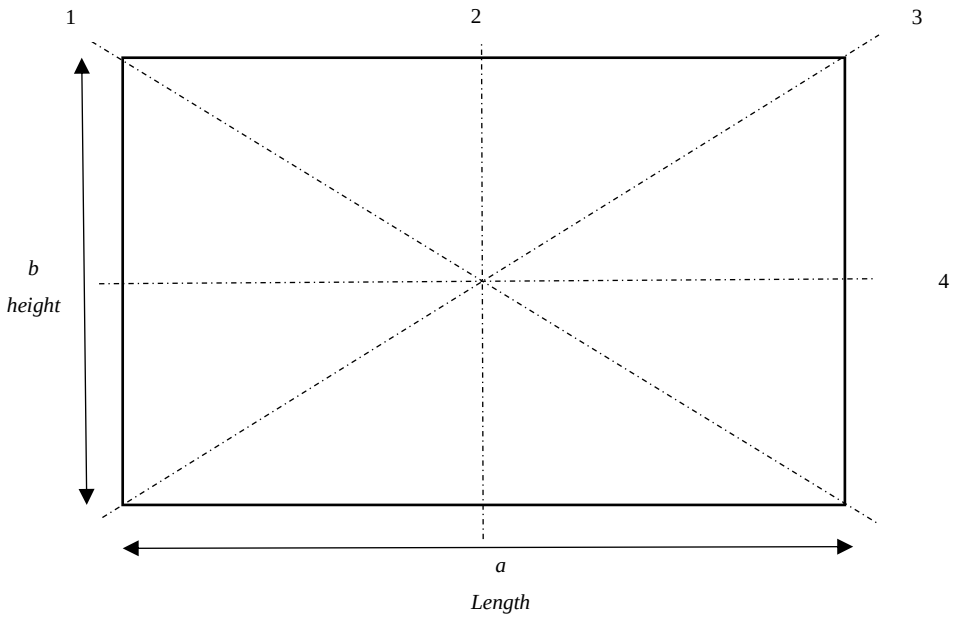

Figure 3.4. Dividing a two-dimensional space

To meet these conditions, the diagonals (lines 1 and 3) would be excluded as these would produce triangles. This means that the line will either be horizontal and parallel to the length face (line 4) or vertical and parallel to the height face (line 2).

If we consider this rectangle within the Cartesian system and it vertices at *(x,y)= (0,0), (0,b), (a,0)* and *(a,b)*, then the equation describing line 2 can be written as;

$$x = \frac{a}{2} \tag{3.23}$$

Similarly, the equation describing line 4 can be written as:

$$y = \frac{b}{2} \tag{3.24}$$

Figure 3.5 shows the rectangles produced when the divisions are done along line 2 (case 1) and line 4 respectively (case 2).

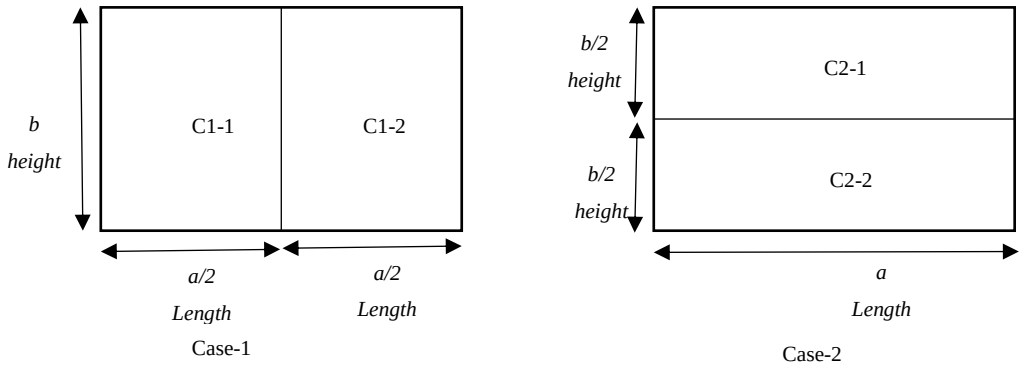

Figure 3.5. Possible ways of dividing a rectangle

Both case-1 and case-2 have fulfilled the first conditions. That is the areas must be rectangles.

The second condition requires both rectangles to be the same area. Again, both cases fulfil this condition. In case-1, the area of the rectangles can be calculated as:

$$Area\ of\ C1-1 = Area\ of\ C1-2 = \frac{a \times b}{2} \tag{3.25}$$

In case-2, the area is the same. Generally, the area of the new rectangles must be half the size of the original rectangle.

The third condition requires the difference between the length and the height of each of the new shapes must be as close to zero as possible. This means that the perimeter of the rectangle must be the minimum possible.
For case-1, the perimeter of each rectangle is given as:

$$Perimeter\ of\ C1-1 = perimeter\ of\ C1-2 = 2b + a \tag{3.26}$$

For case-2, the perimeter of each rectangle is given as:

$$Perimeter\ of\ C2-1 = perimeter\ of\ C2-2 = 2a + b \tag{3.27}$$

From equations 3.26 and 3.27 it can be seen that the perimeter for the rectangles of case-1 and case-2 depended on the values of *a* and *b*. If the size of *a* is greater than *b*, then only case-1 fulfils the third condition. Similarly, when *b* is greater than *a* case-2 will have the smallest perimeter.

Generally, as applied in this research, the rectangle is partitioned by dividing along the length of the longest sides. For the Cartesian system described above, if the length *a* is greater than the height *b*, the dividing line is line 2 and if height *b* is greater than length *a*, this line is line 4.

3.5 Proposed Optimisation Procedure

The goal of the in-building design process is to achieve a minimum signal level for a percentage of the area of the building. Achieving this goal involves placing antennas (transmitters) throughout the design space. The design space or the optimisation is defined by the building layout drawings. Within this building drawing the transmitters will have an *x, y* location with reference to a defined point. The final solution will seek to have optimum conditions for the following parameters:

- The total number of transmitters,
- The location of each transmitter
- The power of each transmitter, P_{Tx},

The novel optimisation process used in this research combines the methods of Particle Swarm Optimisation and geometric partitioning. First, PSO is used to find the best transmitter location within the entire building layout. If this transmitter transmitting at maximum power does not adequately meet the required coverage percentage of the building, then, the space is divided into two and PSO is again independently implemented within each space. Again, the percentage coverage is measured in each new partition and the process is continued until a solution is reached. The complete process is described in detail in below.

3.5.1 Optimisation Parameters

The total number of transmitters

For economic reasons, it is assumed that the best solution is the one that requires the fewest number of transmitters transmitting with minimum output power while meeting the coverage requirements.

The location of each transmitter

Within the optimisation space, there are forbidden or no-go areas for antenna locations. The optimum location will be bound by these forbidden locations while at the same time considering the number of transmitters and the output power of each transmitter.

The power of each transmitter

The final value for each individual transmitter P_{Tx} will be the range from P_{Tmin} to P_{Tmax}, where: P_{Tmin} = 0 dBm and P_{Tmax} = 21 dBm. These represent actual power ranges used by telecoms equipment manufacturers [1]. To reduce the number of steps required to get to an optimal solution P_{Tx} may vary between P_{Tmin} and P_{Tmax} in steps of 3 dB.

3.5.2 Optimisation Phases

There are three main phases to the optimisation/search procedure, these are swarming, power optimisation and geometric partitioning. All three phases are interlinked to optimize the parameters described in section 3.5.1 above.

The **swarming** phase is implemented via the particle swarm optimisation process. It involves moving the transmitter around the optimisation space to find the best location. All the transmitters will move to this best/optimum location. It is the optimum location that will give the maximum coverage to most parts of the building/optimisation space. In the swarming phase, we seek the transmitter location that gives the highest number of receiver locations above the defined received threshold. The process of swarming is described by equation 3.28 and 3.29.

$$V(n) = \omega V(n) + C_1\alpha_1[\text{pbest}(n) - \text{X}_1(n)] + C_2\alpha_2[\text{gbest}(n) - \text{X}_1(n)] \quad (3.28)$$

And

$$X(n) = X_1(n) + V(n)t \tag{3.29}$$

The particles/transmitters will change velocity within the optimisation space. This space is the (*x, y*) coordinates described by the building layout drawing with reference to some fixed point. Therefore, within this two-dimensional space, the velocity and resulting positions are made up of two components. Thus, for each transmitter within the swarm, equations 3.28 and 3.29 can be re-written to indicate the *x*- components and the *y*-components as:

$$V_x(n) = \omega V_x(n) + C_1\alpha_1[pbest_x(n) - \mathrm{X}_1(n)] + C_2\alpha_2[gbest_x(n) - \mathrm{X}_1(n)] \tag{3.30}$$

$$V_y(n) = \omega V_y(n) + C_1\alpha_1\left[pbest_y(n) - \mathrm{Y}_1(n)\right] + C_2\alpha_2[gbest_y(n) - \mathrm{Y}_1(n)] \tag{3.31}$$

And

$$X(n) = X_1(n) + V_x(n)t \tag{3.32}$$

$$Y(n) = Y_1(n) + V_y(n)t \tag{3.33}$$

Where V_x and V_y are the components of the velocity, X and Y are the components of the positions and similarly *pbest* and *gbest* are indicated with components with the (*x, y)* coordinate space and *n= 1,2, …… m*, where *m* is the size of the swarm. The PSO algorithm will optimise the best position for each transmitter composing of an *x* and a *y* component.

Figure 3.6 below shows a block diagram representation of this process. This can be explained in the following steps.

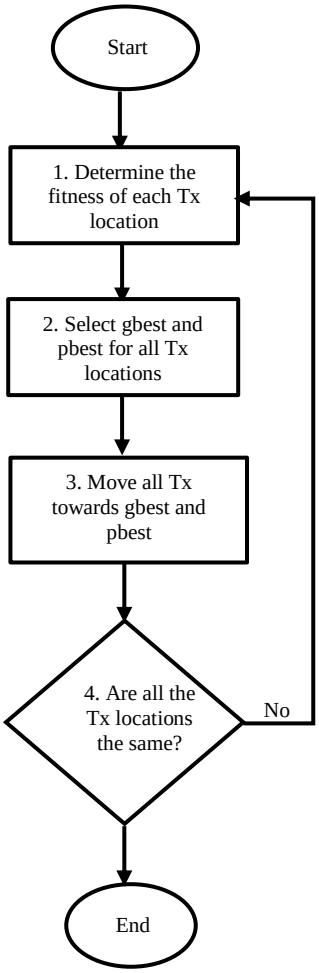

Figure 3.6. Block diagram of swarming process

Step 1. The process starts with the transmitter within the swarm having random locations. The aim is to now move all the transmitters to best location within the optimisation space. From each transmitter location, the Rx_{lev} at each receiver location is calculated as described in equations 2.18 and 2.19. From this, the fitness of each *Tx* location is calculated.

Step 2. The best is defined by the fitness function described in section 3.5.3. The best location (*gbest*) of all the transmitter within the swarm is noted, also the best location of each transmitter *(pbest)* is noted. At initial point, since each transmitter would have had only one location that will be its *pbest* location. The *gbest* will be the best of all the *pbest* locations.

Step 3. Each transmitter will have an *x, y* coordinate within the optimisation space. The PSO process will seek to move each particle by considering the position of the *pbest* and *gbest*. This is indicated in figure 3.7

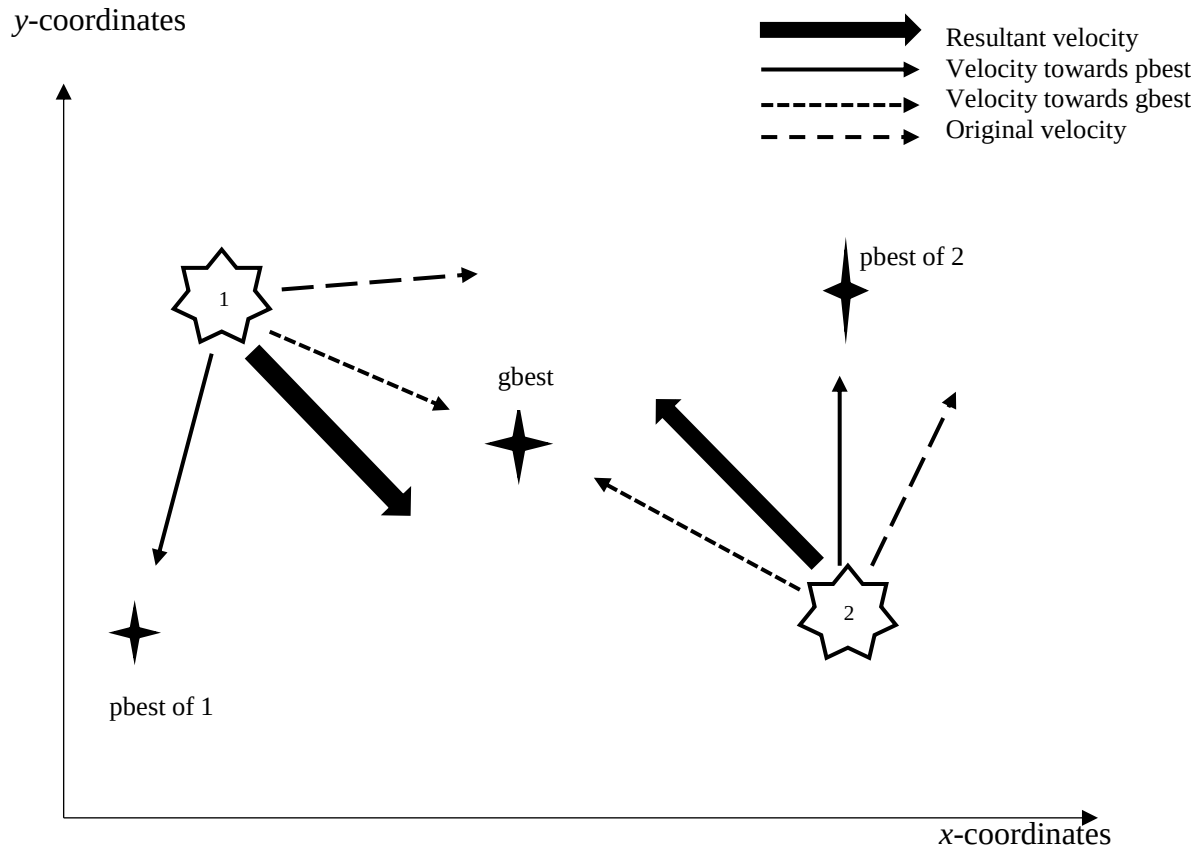

Figure 3.7. PSO particle movement adapted from Robinson et al. [58].

Step 4. This indicates the exit from the swarming process. All the transmitters in the swarm will move towards the *gbest* location over time. If *t* (in equation 3.32) is assumed to be unity, then a stepwise optimisation will be indicated with all the transmitters converging after a finite number of steps. This can mean many iterations which can have an impact on computation power and resources. For practical purposes, the exit maybe taken at a defined standard deviation for all the particles of the swarm/transmitters or after a set number of iterations.

In the **power optimisation** phase, the transmitter effective isotropic radiated power (EiRP) is optimised for the transmitter at the swarmed location

The **geometric partitioning** phase is only initiated if there is no solution after the power optimisation phase. Here the optimisation space is portrayed to be contained in a rectangle. This rectangle is now divided/partitioned into two equal parts as indicated in section 3.4. The swarming phase is initiated again independently in each new partition. If no solution is found

in either partition, then that partition is again divided into equal parts. The number of partitions represents the solutions for the number of transmitters.

3.5.3 Exit conditions

The search procedure will end when the exit conditions are met. The main parameter that is monitored is the received signal threshold. From this, the percentage coverage can be obtained. The received signal threshold is monitored via the fitness function for PSO and percentage coverage is evaluated in the power ramping stage indicated in section 3.5.2 above.

The fitness function evaluates the received signal at each receiver location and calculates the percentage of locations having received signal levels above a defined threshold. This is defined as:

$$F = \frac{T}{k} \tag{3.34}$$

Where: F = fitness at each transmitter location, k = total number of received locations within the optimisation space and T is the number of received locations in the problem space that exceed a minimum defined receive threshold.

In this research, a receive threshold of -85 dBm is used. This is based on a typical value widely used in practise [1]. The fitness function also describes the percentage coverage. The Motley-Keenen propagation model described in equation 2.18 is used to calculate the received signal levels. For this research, a minimum percentage coverage of 95% [6] is considered as the overall exit condition. The power optimisation phase will optimise this value for the best transmitter location and the entire optimisation process will end when the percentage coverage is greater than a specified value.

3.5.4 Boundary Conditions

There are walls (boundaries) and forbidden (no-go) spaces within the building layout. The optimisation procedure also describes how the transmitters will react when they are moved towards a boundary or a forbidden space. The general ways that standard PSO considers boundaries or obstructions are described in [58] where a boundary or obstruction can be absorbing, reflective or invisible. Lu et. al [74], have developed an augmented particle swarm

optimisation algorithm (AugPSO) using a particle position resetting strategy. If the new location of the particle will be outside the boundary or within the no-go location, a new random location is chosen for the particle. This method has been shown to be improve the quality of the solution (when compared to standard PSO) by introducing diversity and preventing the convergence into some local minima. In the present thesis, we consider this particle resetting strategy. This is outlined further in section 4.5.4.

3.5.5 Complete Optimisation Steps

The complete optimisation steps are indicated in the flow chart in figure 3.8. In chapter four all the specific input parameters are discussed. Here, the general optimisation procedure is discussed. The steps are outlined as follows:

Step 1. The initial number of particles (transmitters) are chosen. This determines the size of the swarm. Also, the optimisation space is divided into a number of equally spaced receiver locations, *m*.

Step 2. A random position and velocity are assigned to each particle throughout the optimisation space. Each initial position is a possible transmitter location. The first phase is to find the best location of all these initial locations and to swarm the particles towards these.

Step 3. The PSO algorithm as described in equation 3 and 4, is now used to find the best location for all the particles (swarming described in section 3.5.2).

Step 4. The swarmed location achieved in step 3 is the transmitter location that will ensure optimal received signal levels at all the receiver locations. The required percentage coverage is checked against the fitness function. If this is greater than the fitness function a solution is achieved with one transmitter at the swarmed location. If this is less than the fitness function the transmit power (P_{Tx}) is increased in 3dB steps from 0 to a maximum 21 dBm. This maximum represents a typical indoor base station output power found in [1].

Step 5. If the percentage coverage has still not been met the defined space (layout) is geometrically partitioned into two and the PSO algorithm is independently initiated again in each of the new spaces. This process is continued until the percentage coverage is met for the

entire layout. One transmitter will be required for each partition so the total number of transmitters will be dependent on the number of partitions created.

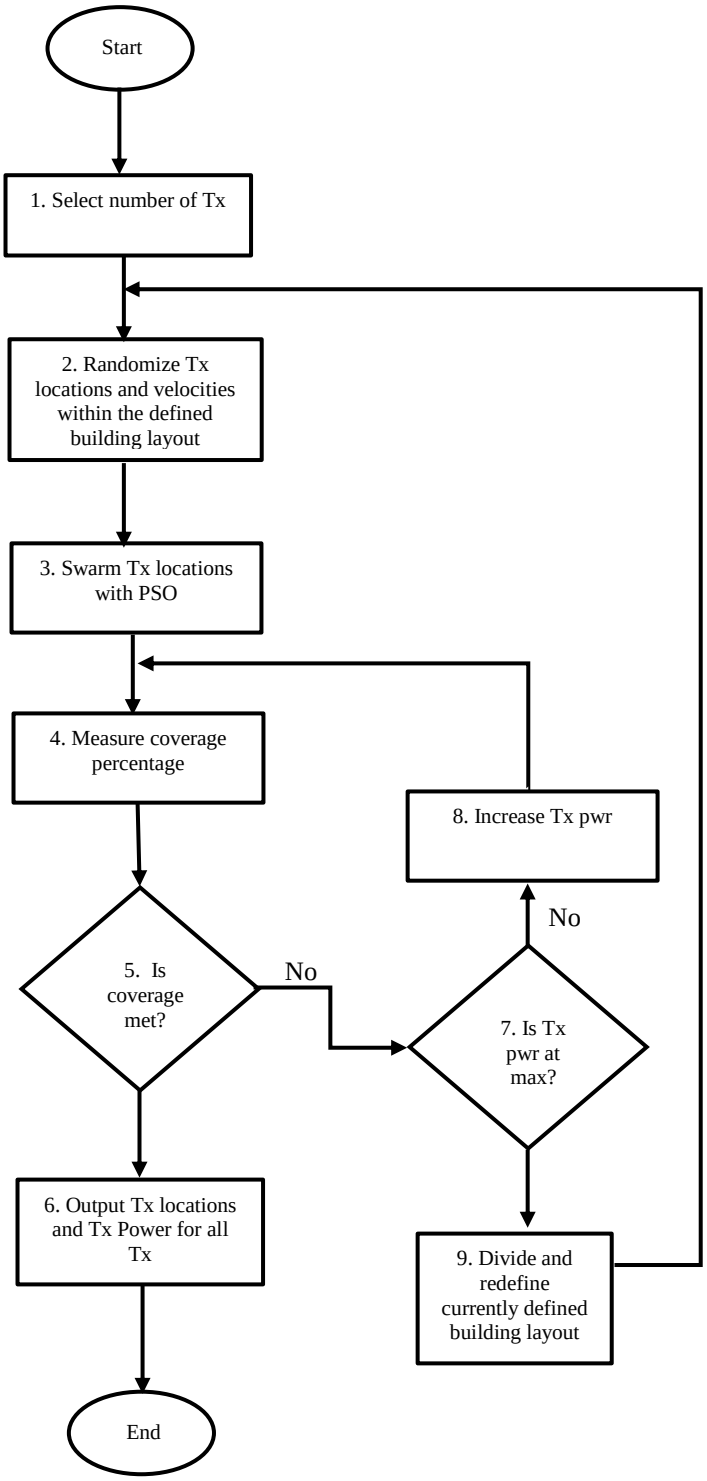

Figure 3.8. Search Procedure

3.6 Conclusion

The proposed solution is a combination of Particle Swarm Optimisation and Geometric Partitioning. This method allows the adaptation of PSO to produce a solution with multiple antenna locations.

With PSO there are fewer parameters needed to be adjusted and it has a rapid convergence speed. PSO is very robust in overcoming local minima problem [60] and has been shown to be faster and more accurate in comparison with other optimisation methods [58].

PSO shows great potential when used in solving the problem of multiple antenna placements in an indoor environment. This is because the problem can be easily formulated as there is a good analogy between the general optimisation space described by PSO and the transmitters/bees within the building layout.

Chapter 4 : Algorithm Development

The solution to the indoor base station placement problem is implemented in two parts, namely the signal propagation stage and the optimisation stage. In this research, a MATLAB simulation is used to show how the proposed solution is implemented in a real building.

The optimisation method is outlined in section 3.5. The algorithm describing these steps along with samples of the MATLAB code will be discussed in this chapter. Here the formulations and the steps taken towards developing this algorithm and program is presented. The input and output parameters are shown along with the methods of calibrating the system.

Although the choice of compiler is MATLAB, the general algorithm is presented so that the program can be written in any other programming language.

4.1 Test Building

The top floor (W2) of the Sir David Davies building at Loughborough University was chosen as the test location as it was readily accessible. This is considered a complex building layout as described in chapter 5. This building layout is shown in figure 4.1. The minimum signal strength at any point in the building must be so planned that the coverage requirements are met. In this research, the coverage requirements are taken to be a minimum received level ($RxLev_{min)}$ of -85 dBm through 95% of all measured received locations.

As stated in chapter 3, to meet this coverage requirement this research seeks to find the following:

- the number of antennas
- the location of these antenna throughout the building
- the EIRP of these antennas

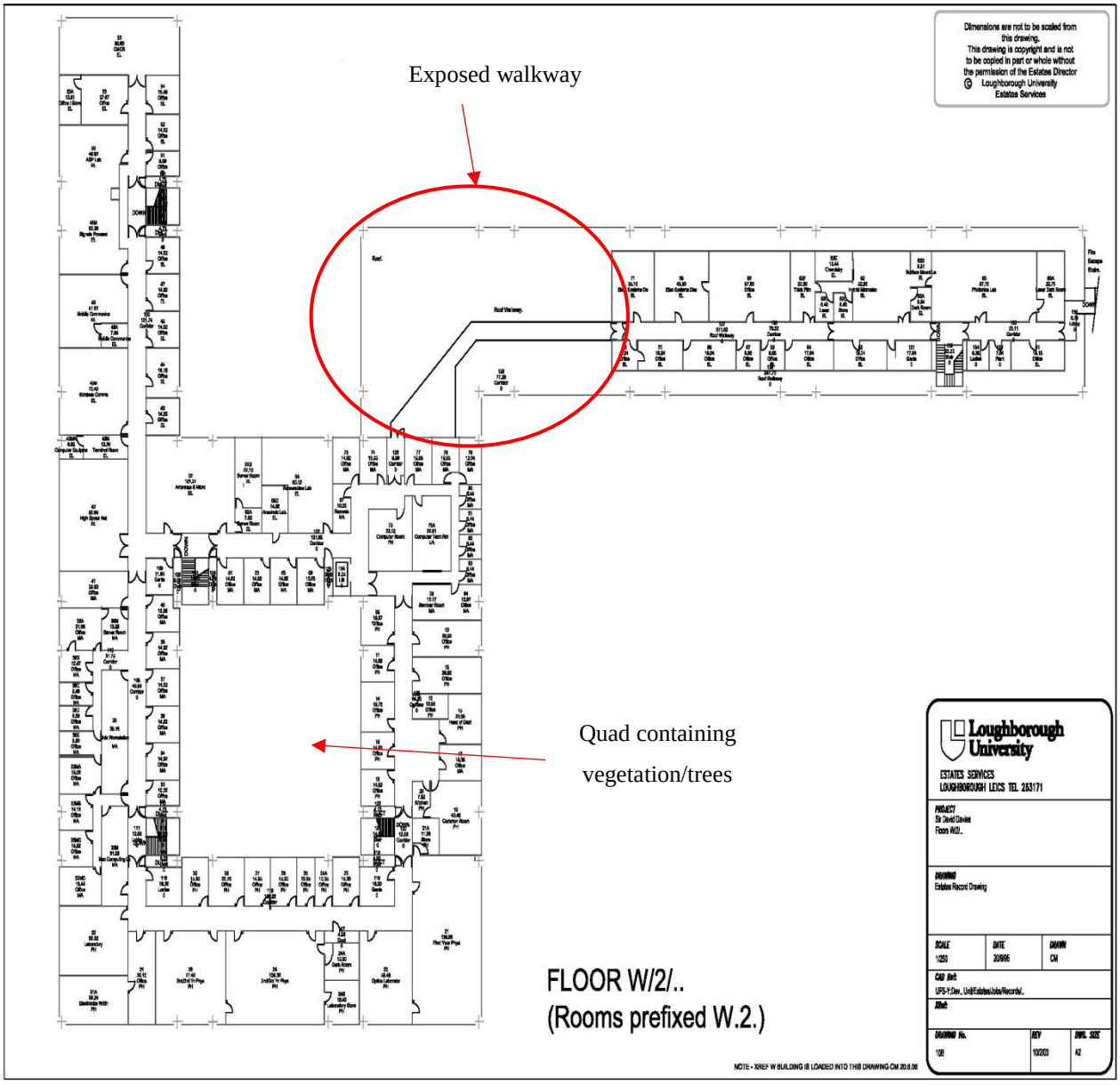

Figure 4.1. Test building layout.

4.2 The Optimisation Space

The main input required to develop the MATLAB program is the optimisation space. This is the test building, described in figure 4.1. The program will search the optimisation space for the best locations to place the antennas so that the coverage requirements are met. Hence, it is required to define the optimisation space. This definition requires the location all walls and partitions, wall thickness and locations of corridors.

To meet these requirements a digital representation of the test building is needed. The layout could be represented in actual latitude and longitude values with respect to a geographical coordinate system or by *x*, *y* locations within a Cartesian system. In this research, the Cartesian system is used as there is no need to reference the actual location of the test building.

The building layout with the noted dimensions in metres, is first saved in as an image in a Jpeg file. With the use of the "GetData" software [75], the vertices/corners of the walls in the drawing were noted with reference to the Cartesian coordinate system. Figure 4.2 shows an example of the points taken from a wall.

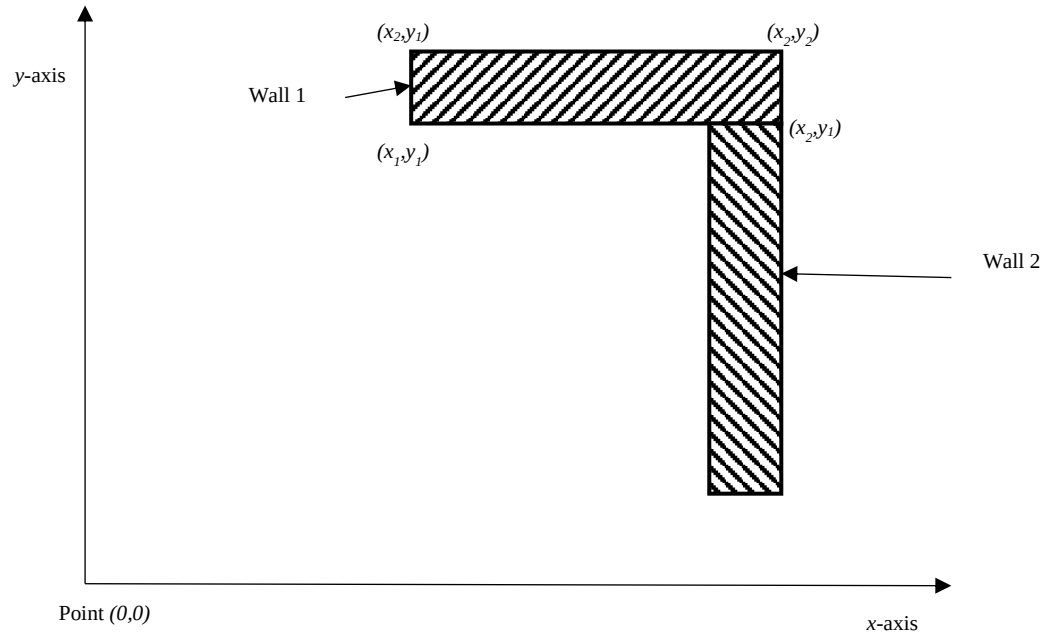

Figure 4.2. Encoding the building layout.

Each wall can be described as a rectangle with four vertices. The "GetPoint" software is used get the *x*-*y* coordinates of each of these four points.

Additionally, the type of wall is required to add to the description of the wall. As described in section 2.3.5, different walls will have different effects on the radio signal propagation. For this test building, interior walls are described as type 1 walls with a loss of 2dB while exterior walls are type 2 with a loss of 5dB. This is shown in table 4.1.

Now there are two input files for the MATLAB program. One shows the positions of all the elements/walls describing the optimisation space and the other shows the different types of walls and losses. Table 4.2 shows examples of the wall positions.

Wall Types	Losses (dB)
Type 1	2
Type 2	5

Table 4.1. Wall losses for Sir David Davies building at Loughborough University.

x_1	y_1	x_2	y_2
8.066565	142.3017	8.00909	86.78072
95.79948	142.3017	8.066565	142.3017
8.00909	86.78072	59.25133	86.78072
59.25133	86.78072	59.44766	126.4386
59.44766	126.4386	95.93834	126.4386
95.93834	126.4386	95.79948	142.3017
90.9764	133.2037	90.98582	142.3017
90.9764	133.2037	40.66584	133.2037
40.66584	133.2037	40.67526	142.3017
44.40197	142.3017	44.39255	133.2037

Table 4.2. Example of an input file

Figure 4.3 show the optimisations space as deployed within the Cartesian system. It shows all the wall locations as described in the sample files indicated in Table 4.2.

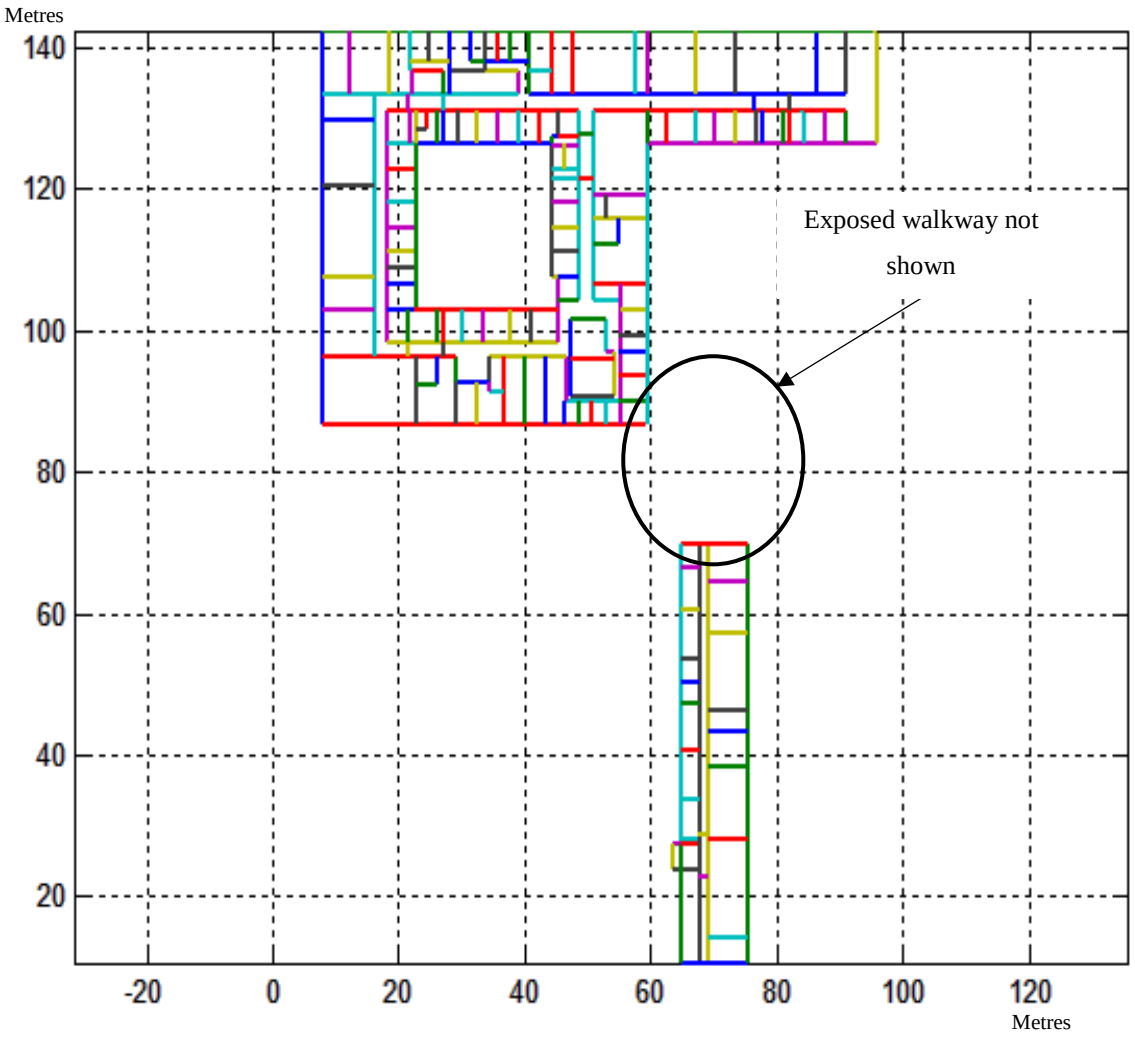

Figure 4.3. The test building defined within the Cartesian space.

4.3 Program Initialisations

With the optimisation space now defined, the development of the MATLAB program can now progress as described in optimisation methods section 3.5. The goal is to produce a MATLAB simulation that will find a solution for the problem of planning the optimum location for antennas within the test building.

There two distinct processes contained within the optimisation methods described in section 3.5. These are the propagation process and the search process. These processes indicate the parameters sets and their initial values for the program.

4.3.1 Propagation Parameters

The parameters needed for the propagation process can be derived from equation 2.19. These are obtained from the following categories:

- The receive signal threshold.
- The transmit power
- The path loss parameters
- The wall losses

The received signal threshold.

The set of parameters involved here is used to determine when the coverage levels are met. The optimisation space is divided into a number individual receiver grids. Figure 4.4 shows an example with 4 grids. In the real problem 200 grids are used. The number of grids is the square of the number of points. In figure 4.4 the number of points is chosen to be 4. This produces 16 receiver grids located at the interception of the vertical and horizontal grid lines. The spacing between these grid lines for the *x* and *y* domains are given as:

$$dx = \frac{x\_max - x\_min}{number\ of\ points - 1} \tag{4.1}$$

and

$$dy = \frac{y\_max - y\_min}{number\ of\ points - 1} \tag{4.2}$$

Where *dx* and *dy* are the spacing between grid lines for the *x* and the *y* domains respectively, *x_max, x_min, y_max* and *y_min* are the maximum and minimum boundary walls defining the optimisation for the *x* and *y* domains, the number of points must be greater than 1.

The received signal level is calculated at the intersection of each grid line. The received signal level at each point is compared to the received signal threshold. From this, the percentage coverage is calculated.

Parameters: Number of points, Received signal threshold, percentage coverage, *x*-minimum, *x*-maximum, *y*-minimum, *y*-maximum, *RXpoint (x,y)*

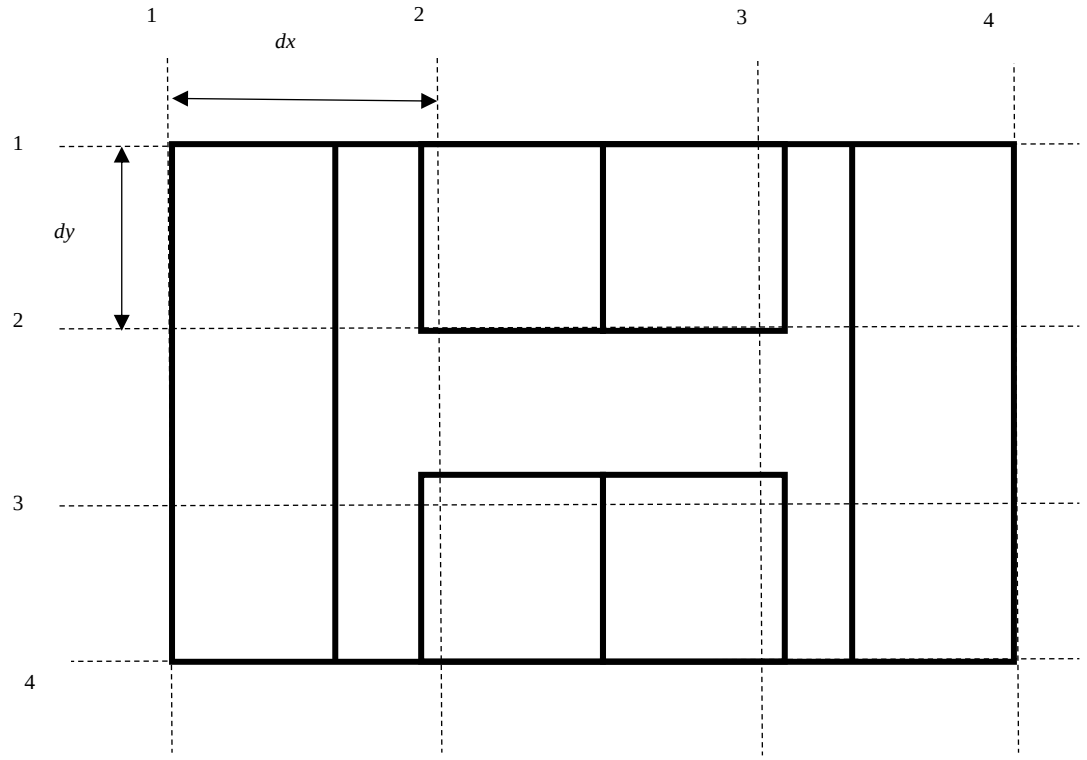

Figure 4.4. Example of how receiver locations are calculated in a sample building layout

The transmit power.

The transmit power is used to determine the receiver signal levels at the centre of each grid throughout the building. The typical base station [1] will have a range of values which will determine the EiRP of the transmitter. In this research, the power will be cycled through the range of values to find the optimum transmitter EiRP to meet the receiver signal threshold. The transmitter power will be between 0 and 21dBm and changes in 3dB steps. This will create a set of values of 0,3,6,9,12,15,18 and 21 (all in dBm).

The path loss parameters

The path loss parameters are derived from the propagation model. The propagation model used in this research is the Motley-Keenan. The reasons for the choice of this model are due to its simplicity and ease of comparison with normal planning methods. This model is given as:

$$L = L_0 + 10n \log_{10} d \tag{4.3}$$

In this research, a frequency of 900 MHz is chosen, in this case, L_0 becomes equal to 31.5. The path loss exponent, *n* is chosen to be 2 and *d* is the receiver to transmitter separation distance. The process of calculating *d* is explained in section 4.
Parameters: L_0. Path loss exponent, *n*. Total path loss

The wall losses
The wall losses are obtained from the input file describing the optimisation space as described in section 4.2. The position of each and the type of wall are used in the calculations for received signal levels.
Parameters: Average wall attenuation, *W*

4.3.2 Search Parameters

The search parameters are obtained from the PSO equations. These are described in chapter 3 and are given as:

$$V_x(Nt) = \omega V_x(Nt) + C_1\alpha_1[pbest_x(Nt) - \mathrm{X}_1(Nt)] + C_2\alpha_2[gbest_x(Nt) - \mathrm{X}_1(Nt)] \quad (4.4)$$

$$V_y(Nt) = \omega V_y(Nt) + C_1\alpha_1\left[pbest_y(Nt) - \mathrm{Y}_1(Nt)\right] + C_2\alpha_2[gbest_y(Nt) - \mathrm{Y}_1(Nt)] \quad (4.5)$$

And

$$X(Nt) = X_1(Nt) + V_x(Nt)t \quad (4.6)$$

$$Y(Nt) = Y_1(Nt) + V_y(Nt)t \quad (4.7)$$

Size of the swarm
The values for *Nt* are integers from 1 to *bees* where *bees* is the size of the swarm. The size of the swarm is very important in determining how efficiently PSO converges to a solution [57] and [64]. A large swarm will provide more accurate results but will require more processing resources. It has been shown [64] that a swarm size greater that 30 does not provide a better quality of solution compared with the proportionate increased in processing resource demands. In this research, the suggested value of 30 bees [64] is used.
Parameter: Size of the swarm.

Constants

The effectiveness of PSO can be improved via the selection of the parameters namely ω, C_1, C_2, α_1, and α_2. Typical values for these parameters are described in [58], [61] [62], [63]. ***ω-*** This is the initial weight. This scale the old velocity and controls the speed at which the transmitter flies over the solution. ***C_1 and C_2*** – These determine the relative pull towards *pbest* and *gbest*. *C_1* describes the pull towards *pbest* (the local solution) and *C_2* describes the pull towards *gbest* (the global solution).

Parameters: ω, C_1, C_2, α_1, and α_2.

Main Search Parameters

The main search parameters are the *fitness, pbest, gbest, velocity, position* and *time*. These are described as; **Fitness:** The fitness is used to rank the suitability of each transmitter location. The fitness is calculated from the received signal strength at indicated in section 3.5.

***pbest*:** The best location of each transmitter. Required for both *x* and *y* locations

***gbest*:** The best location of all the all transmitters in the swarm. Required for both *x* and *y* locations

Velocity: The velocity of the transmitter, comprising of *x* and *y* components

Position: The position of the transmitters, comprising of *x* and *y* components

Time, *t*: taken to be 1

Table 4.3 list all the parameters and their initial values.

Parameter	Symbol	Initial value
Average wall attenuation	*W*	Based on building layout
Fitness	*Fv*	0
Global best, *x*-*y* component	*gbest_x, gbest_y*	Randomly selected
Local best, *x*-*y* component	*pbest_x, pbest_y*	Randomly selected
Number of points	*nb_pts*	200
Path loss at 1m and 900 MHz	L_0	31.5
Path loss exponent	*p*	2
Percentage coverage	*Percent_coverage*	95%
Position (*x* and *y* components), TXpoints(*x*,*y*)	*pos_x, pos_y*	Randomly selected
PSO constant	ω	0.01
PSO constant	C_1	2
PSO constant	C_2	2
PSO constant	α_1	1
PSO constant	α_2	1
Received signal level	*Tot_Rx_pwr*	0 dBm
Received signal threshold	*rxthreshold*	-85 dBm
Receiver locations	*RXpoint (x,y)*	Based on number of point on optimisation space
Size of the swarm, each transmitter in the swarm	*bees, Nt*	30,
Time	*t*	1 sec
Total path loss	*rs_amp*	0 dB
Transmitter power	*txpower*	0 dBm
Velocity (*x* and *y* components)	*vel_x, vel_y*	Randomly selected
x-maximum	*x_max*	Based on building layout
x-minimum	*x_min*	Based on building layout
y-maximum	*y_max*	Based on building layout
y-minimum	*y_min*	Based on building layout

Table 4.3. List of parameters used in MATLAB program, alphabetically ordered

4.4 Initial Placement of Transmitters

In this step, the initial locations of the transmitters are randomly chosen. The program gives the transmitters and initial position within the optimisation space while being constrained by the no-go locations.

4.4.1 No-Go Locations

There are areas within the building where it may not be possible to install transmitters. Also, because the building layout is defined within a rectangle there may be areas within the rectangle that are not a part of the layout. These are no-go areas and should be ignored during the optimisation process. The PSO algorithm must be able to recognise these areas and avoid moving the transmitter within these areas during the swarming phase and also avoid placing in this location during the initial random placements of the transmitters. The no-go areas in the test building are indicated in figure 4.5.

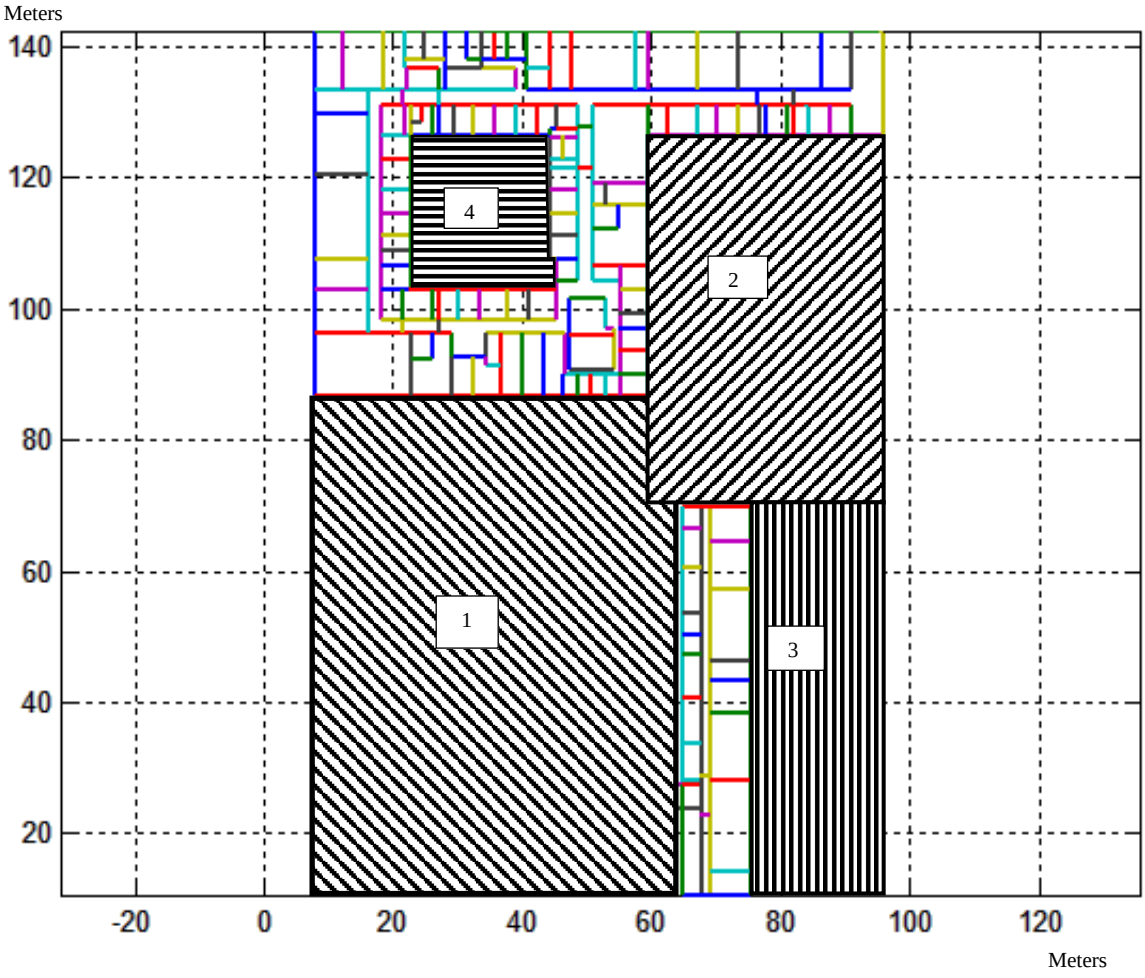

Figure 4.5. No-go locations.

In this building layout (figure 4.5) the no-go areas are bounded by four rectangles defined as described in table 4.4.

Rectangle	Vertices			
	x_1 (m)	x_2 (m)	y_1 (m)	y_2 (m)
Rect- 1	*x-min*	64.90	*y-min*	86.78
Rect- 2	59.4	*x-max*	69.75	126.44
Rect- 3	75.32	*x-max*	*y-min*	69.75
Rect- 4	22.50	45.45	102.87	126.44

Table 4.4. Rectangles defining No-Go areas of building layout

The following pseudocode is used to choose the initial random position and velocity of all the transmitters within the swarm while avoiding these no-go locations.

Begin

For (Nt =1 to the number of bees)

Choose a random *x*-location for each transmitter between *x-max* and *x-min*

Choose a random *y*-location for each transmitter between *y-max* and *y-min*

While (the transmitter location is in rect-1 or rect-2 or rect-3 or rect-4)

Choose a random *x*-location for each transmitter between *x-max* and *x-min*

Choose a random *y*-location for each transmitter between *y-max* and *y-min*

End

Choose a random velocity in the *x*-direction

Choose a random velocity in the *y*-direction

End

End

A simple flow chart of the process is shown in figure 4.6.

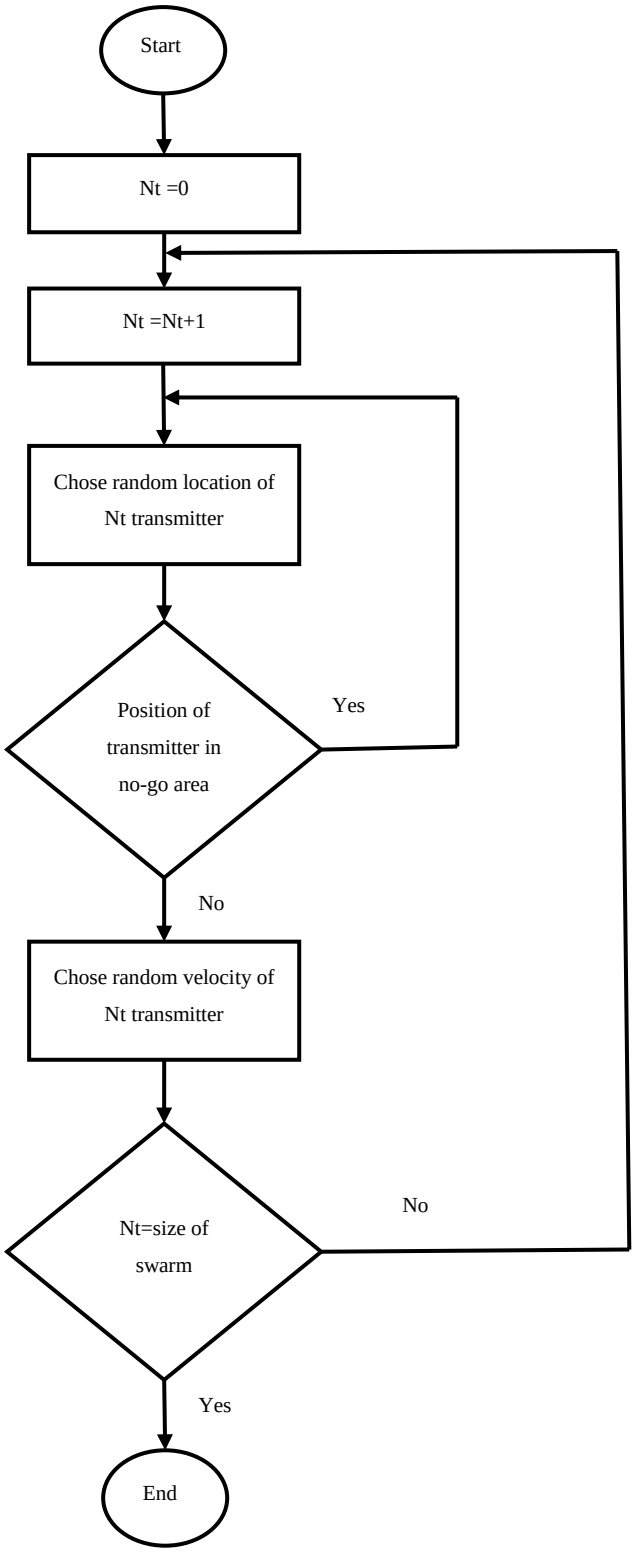

Figure 4.6. Flow chart showing the initial placement of transmitter while avoiding no-go locations.

Figure 4.7 show the initial transmitter locations while avoiding the no-go areas. For visualisation porposes, the size of the swarm is chosen to be 500 transmitters.

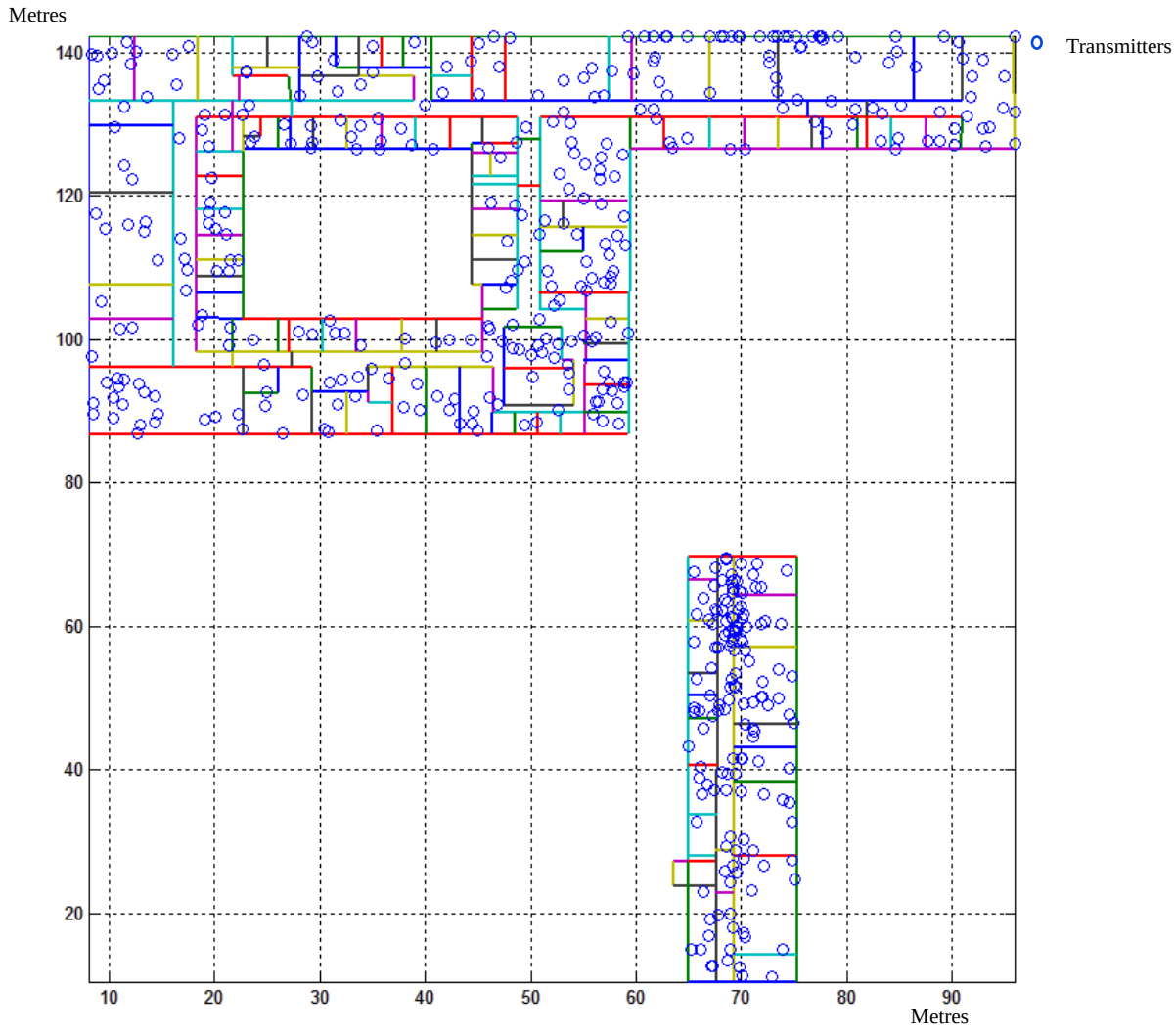

Figure 4.7. Initial placement of transmitter within the test building while avoiding no-go locations. Each circle represents a transmitter location

4.5 Swarming

Now that each particle has a position and velocity as obtained in section 4.4 the next step is to start the swarming process. This is predicated on the values of *pbest* and g*best*. To calculate *pbest* and *gbest*, the received signal level at each receiver location (grid) position with respect to each transmitter is to be first calculated. The receiver signal level is calculated based on the

path loss between transmitter and receiver. This path loss is dependent on distance and the number of intercepting walls between transmitter and receiver.

4.5.1 Path Loss Calculation.

De Luca et al. [76] have shown how radiated power indoors can be used to improve localization techniques. A MATLAB program showing this had been implemented by Paris [77]. This research uses elements of this program to develop the required MATLAB simulation.

At each receiver point, described in section 4.3.1, the received signal level (*RxLev*) is needed for each transmitter location. The pseudo code expressed in its simplest form can be given as below.

Begin
Input
TXpoint, RXpoint, walls, materials, L0, n.
Output
rs-amp
For (each receiver point)
    Calculate the distance to each transmitter
    Calculate the number of intersecting walls
    Calculate the path loss to each transmitter ($L_{total} = L_0 + 20log_{10}d + \sum k_i Lw_i$)
End
End

The parameters of this code can be described as:
TXpoint is a matrix containing *Nt* rows and two columns. The columns are *x-y* positions initially randomly selected for each transmitter (bees) within the optimisation space.
RXpoint is two by *nb_pts* squared matrix containing all the receiver points denoted in *x-y* components. *Walls* and *material* are the input files defining the number of walls and wall types described in section 4.2. L_0 is the path loss at 1m transmitter-receiver separation distance at 900 MHz. *n* is the path loss exponent taken to be 2. *rs_amp* is a Nt by *nb_pts* squared matrix containing the path loss for each transmitter at each receiver point.

Distance Calculations

The separation distance is a simple calculation between the receiver coordinates and the transmitter coordinates within the Cartesian space. For example if the transmitter is at position denoted (x_t,y_t) and the receiver is at point (x_r,y_r) as indicated in figure 4.8, then the distance from transmitter to receiver, *d* can be calculated as:

$$d = \sqrt{(x_r - x_t)^2 + (y_r - y_t)^2} \tag{4.8}$$

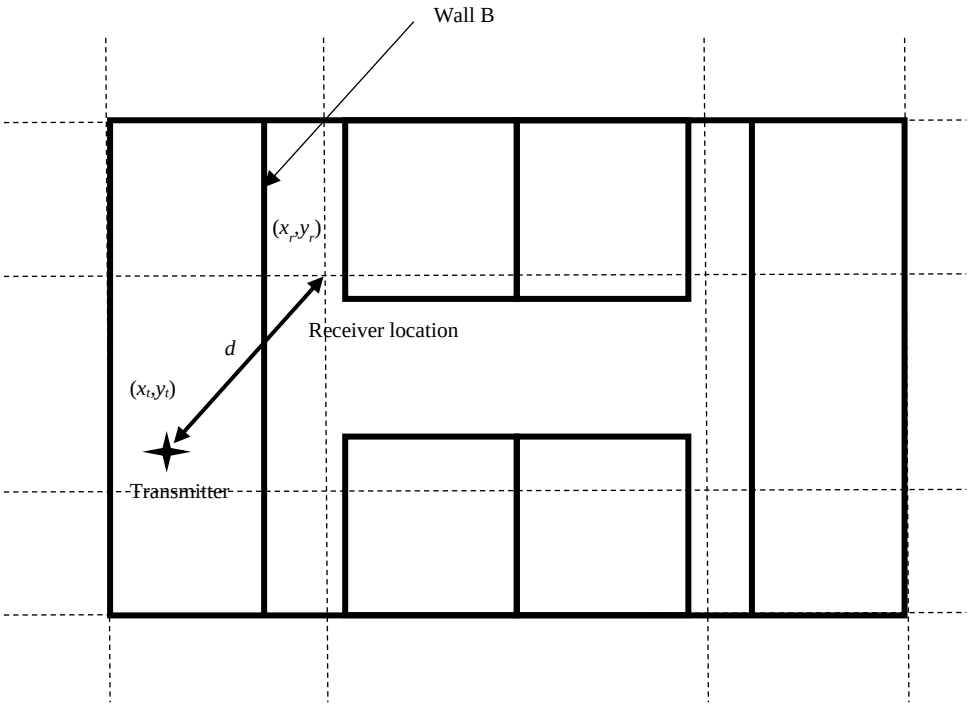

Figure 4.8. Distance calculation.

Intersecting walls

Figure 4.8 also shows that wall B is intersecting the transmitter to receiver direct ray path. The general test to indicate whether two line segments intersect is described in [78], [79] and [80]. Consider the wall and the direct ray as line segments within the Cartesian coordinate space with end points as indicated in figure 4.9. The end points of the direct ray can be described as p_T and p_R and the end points of the wall can be described as p_{w1} (x_{w1}, y_{w1}) and p_{w2} (x_{w2}, y_{w2}). The wall and the direct ray will intercept if the following two conditions are met:

1. The end points of the wall are on opposite sides of the direct ray path

2. The end points of the direct ray are on opposite sides of the wall.

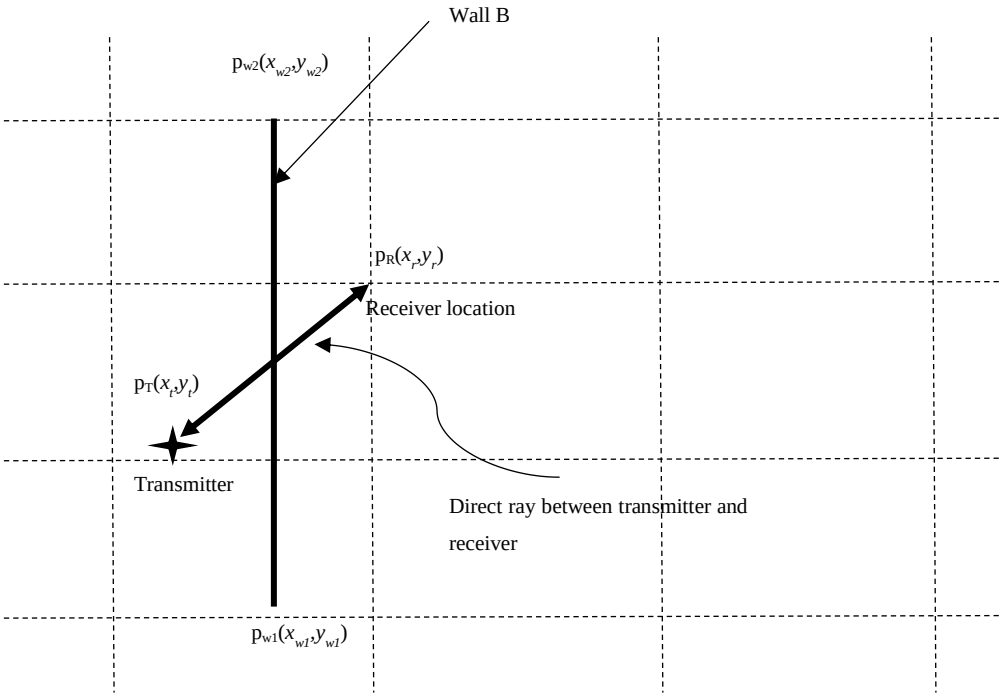

Figure 4.9. Testing for the intersection of a direct ray and walls.

The expression of the line segment representing the direct ray can be written as:

$$p_T + t(p_R - p_t) \tag{4.9}$$

And the expression for the wall segment is:

$$p_{w1} + u(p_{w2} - p_{w1}) \tag{4.10}$$

Where $0 \leq t \leq 1$ and $0 \leq u \leq 1$ defines a point along the line. For example, the point t=0 is p_T.

At the point where these two line segments intersect the expressions will be equal. Therefore:

$$p_T + t(p_R - p_t) = p_{w1} + u(p_{w2} - p_{w1}) \tag{4.11}$$

Substituting the *x* and *y* coordinates:

$$x_t + t(x_r - x_t) = x_{w1} + u(x_{w2} - x_{w1}) \tag{4.12}$$

$$y_t + t(y_r - y_t) = y_{w1} + u(y_{w2} - y_{w1}) \tag{4.13}$$

Solving for *t* and *u* gives:

$$t = \frac{(y_{w1} - y_{w2})(x_t - x_{w1}) + (x_{w2} - x_{w1})(y_t - y_{w1})}{(x_{w2} - x_{w1})(y_t - y_r) - (x_t - x_r)(y_{w2} - y_{w1})} \tag{4.14}$$

$$u = \frac{(y_t - y_r)(x_t - x_{w1}) + (x_r - x_t)(y_t - y_{w1})}{(x_{w2} - x_{w1})(y_t - y_r) - (x_t - x_r)(y_{w2} - y_{w1})} \tag{4.15}$$

For any point of intersection along these segments, $0 \leq t \leq 1$ and $0 \leq u \leq 1$. If values for *t* and *u* falls outside [0, 1], then the intersection is outside these line segments. If the denominator in equation 4.14 and 4.15 is zero then there is no solution and the lines either has no intersections or infinitely many intersection points.

In the program, each wall is checked against each direct ray between each transmitter and each receiver location during the swarming process. If a wall is intercepting the path, then its wall losses are considered in the path loss calculations.

4.5.2 Receiver Level and Fitness Calculations

The matrix with path loss values is now used to calculate the receive signal level *(Tot_Rx_pwr)* at each receiver location and then the fitness of each location. The location with the best fitness will be *gbest* value. The fitness of each transmitter location is calculated by comparing the receiver level at each receiver location (for each transmitter location) to the receive threshold.

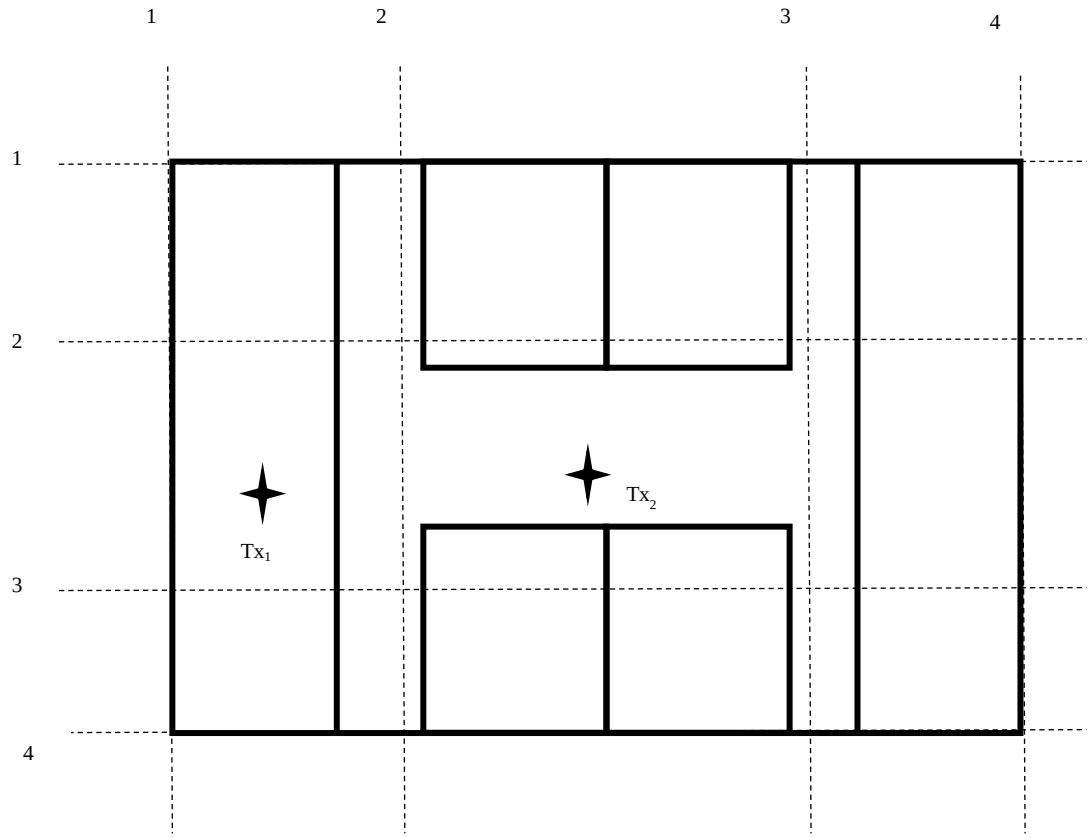

Figure 4.10. Fitness calculation for each transmitter.

Figure 4.10 shows a sample building layout to illustrate how the fitness of each transmitter is calculated. For this example, only the receiver levels at locations (2,2), (2,3), (3,2) and (3,3) are considered. Given that the levels from each transmitter is assumed as indicated in table 4.5 and the *rxthreshold* is -85dBm, then fitness of each transmitter is calculated as:

$$Fitness = \frac{number\ of\ receiver\ locations\ above\ threshold}{number\ of\ receiver\ locations} \tag{4.16}$$

Then it can be seen that Tx_2 has a better fitness than Tx_1 and the location of Tx_2 will, therefore, be taken as *gbest*.

Transmitter	Receiver levels at different locations(dBm)				Fitness
	Location (2,2)	Location (2,3)	Location (3,2)	Location (3,3)	
Tx_1	-84	-86	-95	-100	¼=0.25
Tx_2	-84	-80	-82	-81	¾=0.75

Table 4.5. Sample fitness calculations

To calculate *pbest* for Tx_2 for example, the fitness of all the previous locations of Tx_2 will be considered. Of all these locations, the one with the highest fitness value will be used as the *pbest* of Tx_2. Clearly this set of fitness values will be updated each time Tx_2 is moved to a new location. The pseudo code for the overall process can be given as:

Begin
Tot_Rx_pwr = txpower-rs_amp
For (Each transmitter)
    Calculate the fitness at each receiver point
    Calculate *pbest* by comparing each transmitter location to previous transmitter locations
End
Calculate gbest
END

4.5.3 Moving the transmitters

With the *pbest* and *gbest* values, the transmitters can now be moved based on PSO algorithm. With each new location, the PSO swarming process is initiated again until the exit conditions are met. The *x*-component of the velocity is calculated using equation 4.4.

$$V_x(Nt) = \omega V_x(Nt) + C_1\alpha_1[pbest_x(Nt) - \mathrm{X}_1(Nt)] + C_2\alpha_2[gbest_x(Nt) - \mathrm{X}_1(Nt)]$$

The *y*-component is obtained from equation 4.5.

$$V_y(Nt) = \omega V_y(Nt) + C_1\alpha_1\left[pbest_y(Nt) - \mathrm{Y}_1(Nt)\right] + C_2\alpha_2[gbest_y(Nt) - \mathrm{Y}_1(Nt)]$$

4.5.4 Boundaries and No-go Swarming Locations

The transmitters must only move within the defined optimisation space while avoiding the no-go locations. Therefore, there must be a process of describing how the transmitters will react at these boundaries and when moved within these no-go locations. The PSO algorithm will consider a boundary or a wall to be either absorbing, reflective or invisible [58]. When a particle/transmitter collides with an absorbing boundary the velocity of the particle becomes zero. Collisions with a reflective boundary will make the velocity of the particle negative while an invisible boundary will have no effects on the velocity of the particle.

The optimisation space contains interior walls and is bounded by the exterior walls defined by the *x_min, x_max, y_min,* and *y_max* values. In this research, the interior walls are considered to be invisible as far as the PSO algorithm is concerned, so the transmitters can pass freely through these walls.

In section 4.4.1, the process of avoiding no-go location during the initial placement phase is shown. A similar method is used to re-position the transmitters if their new position is outside a boundary or within the no-go areas. The flow chart of the swarming process is represented in figure 3.6. The pseudo code describing the swarming while avoiding no-go locations and negotiating the boundaries given as:

For (each transmitter)

Calculate new velocity

$$V_x(Nt) = \omega V_x(Nt) + C_1\alpha_1[pbest_x(Nt) - \mathrm{X}_1(Nt)] + C_2\alpha_2[gbest_x(Nt - \mathrm{X}_1(Nt)]$$

$$V_y(Nt) = \omega V_y(Nt) + C_1\alpha_1\left[pbest_y(Nt) - \mathrm{Y}_1(Nt)\right] + C_2\alpha_2[gbest_y(Nt) - \mathrm{Y}_1(Nt)]$$

Calculate new position

$$X(Nt) = X_1(Nt) + V_x(Nt)t$$

$$Y(Nt) = Y_1(Nt) + V_y(Nt)t$$

While (New position is greater than *x_max* and *y_max*, respectively)

Choose a random *x*-location for transmitter between *x-max* and *x-min*

Choose a random *y*-location for transmitter between *y-max* and *y-min*

End

While (New position is less than *x_max* and *y_max*, respectively)

Choose a random *x*-location for transmitter between *x-max* and *x-min*

Choose a random *y*-location for transmitter between *y-max* and *y-min*

End

While (New transmitter position is in rect-1 or rect-2 or rect-3 or rect-4)

Choose a random *x*-location for transmitter between *x-max* and *x-min*

Choose a random *y*-location for transmitter between *y-max* and *y-min*

END

End

In the last section of the above pseudo code, if the new transmitter location is within the no-go location, a new random position is selected. The implementation of this part of the solution is similar to the "particle position re-setting strategy" used in [74] and can be very effective in allowing the particle/transmitters to further explore the optimisation space and improve the solution.

Figure 4.11 to figure 4.14 illustrates elements of the swarming process with 200 transmitters. Snapshots of the motion of the transmitters are shown after a number of position changes. It can be seen that the transmitters are swarming towards an optimum location after about 10 position changes. After about 60 position changes most of the transmitters are at the optimal location, this is further illustrated in chapter 5.

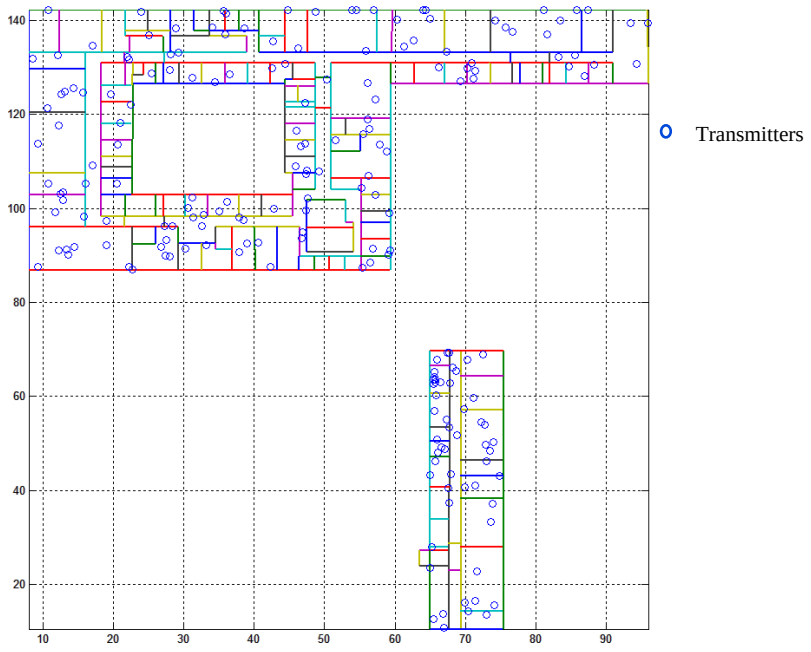

Figure 4.11. Initial placement of transmitters

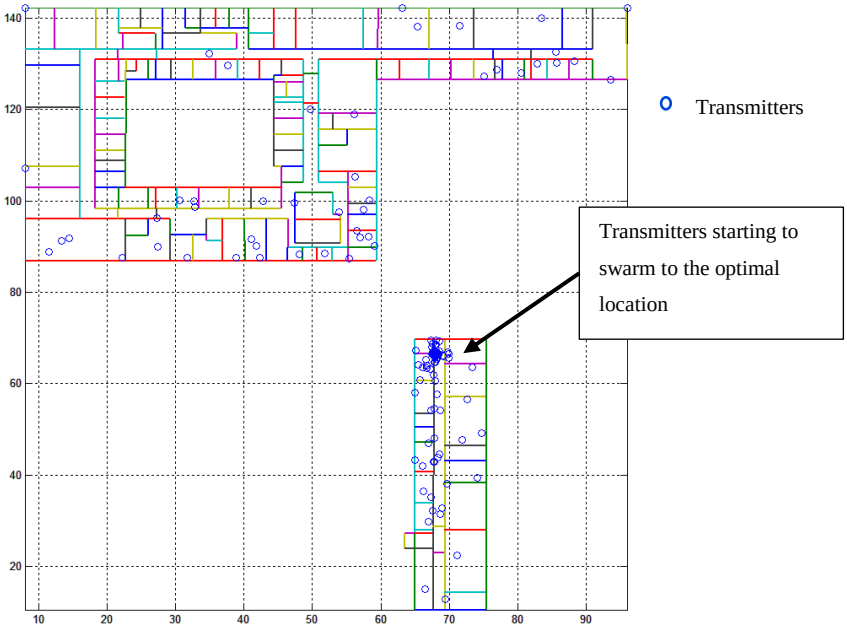

Figure 4.12. Transmitters swarming after 10 position changes.

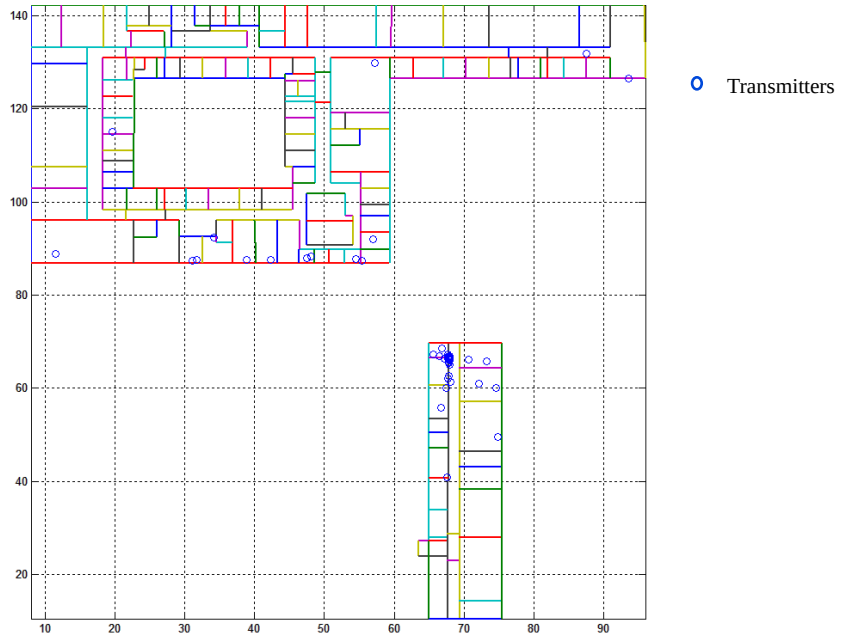

Figure 4.13. Transmitters swarming after 20 position changes.

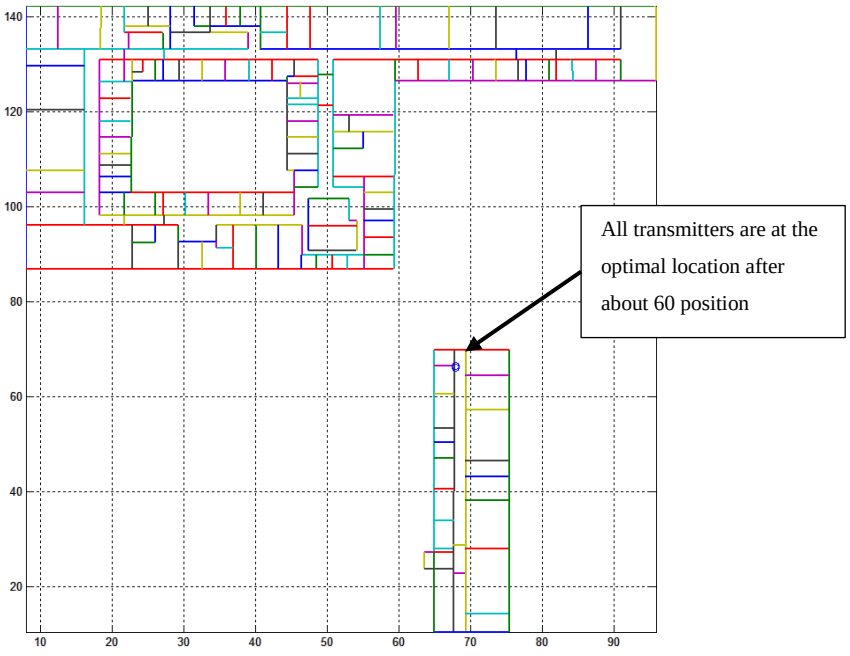

Figure 4.14. Transmitters swarming after 60 position changes

4.5.5 Swarming Exit Conditions

The goal of the PSO algorithm is the find the optimal location for the transmitters. All the transmitters will move around until they all have the same *pbest* values. Depending on the size of the optimisation space and the number of transmitters this can mean many iterations which can have an impact on computation power and resources. For practical purposes, the exit maybe taken at a defined standard deviation for all the particles of the swarm/transmitters or after a set number of iterations.

In normal inbuilding planning situations [1], [6], there is not a great difference in the propagations characteristics of transmitters placed less than 1 metre apart. Therefore, a logical value for the standard deviation is 1 metre. For this specific test building, after several simulations (discussed in chapter 5), it was found that the transmitters will converge after about 60 iterations. The processing is with an Intel Core i7-5600U (speed 2.6 GHz) processer with Windows 10 64-bit operating systems with 12GB RAM.
The pseudo code for the exits condition can be written as:

Begin
While (The standard deviation of all the transmitters is greater than 1 meter and the number of irritation are less than 60)
    Perform swarming
End
End

4.6 Power Optimisation

The power optimisation phase starts after exit from the swarming phase. Here the best location for the transmitter will have been found. The best location for the transmitter will be denoted by *gbest_x* and *gbest_y* for the *x* and *y* components respectively. All the transmitters will have the same location meaning that *pbest_x* of any transmitter will be equal to *gbest_x*. This is the same for the *y*-components of the location. Additionally, all the transmitters will have the same fitness. Now the aim is to test if this best location will meet the required percentage coverage.

The fitness would have been calculated as indicated in section 4.5.2. If the fitness is less than the percentage coverage, then the aim is to increase is to increase the transmitter power and in

effect increase the receiver signal strength at each receiver point. The transmitter power will be increased in steps of 3 dB from 0 dBm to 21 dBm. Figure 4.15 is a flow chart representation of the power ramping process the pseudo code is given as:

Begin

Input

fitness, Percentage_coverage, txpower, rs_amp

While (fitness is less than or equal Percentage_coverage and txpower is less than 21dBm)

Increase txpower

Calculate new receiver levels (Tot_Rx_pwr = txpower-(-rs_amp)
Calculate the fitness for any transmitter

End

End

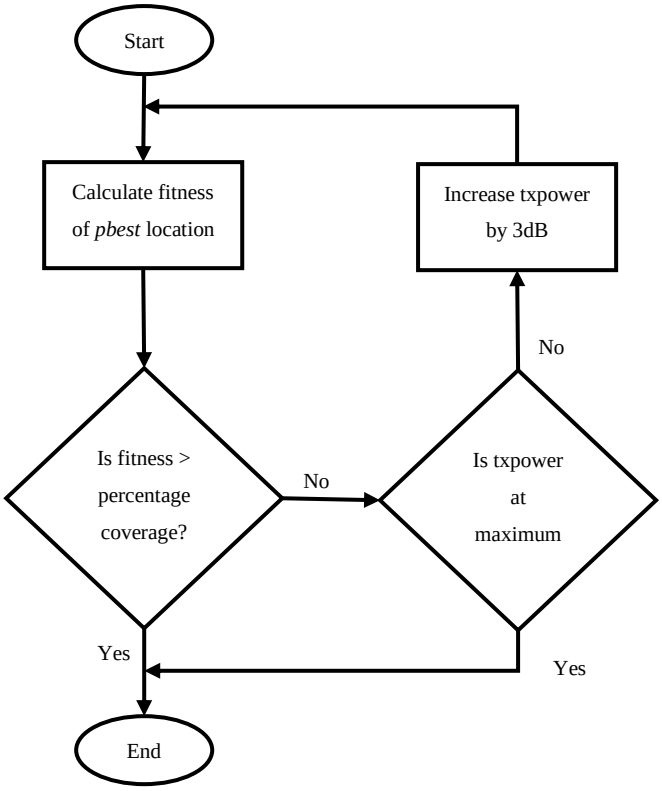

Figure 4.15. Flow chart indicating power ramping

4.7 Geometric partitioning

If after the power ramping phase, as described in section 4.6, the percentage coverage has still not been met the next step in the optimisation process is to perform geometric partitioning. In

this phase, the optimisation space is divided into two and PSO is initiated independently in each phase. The process of dividing has been explained in section 3.4. The pseudo code can be given as:

Begin
Input
txpower, percentage coverage, fitness
If (txpower is at maximum and fitness is less than percentage coverage)
    Divide optimisation space
    Re-define *x-min, x-max, y-min* and *y-max* for new optimisation spaces
    Re-start the swarming process independently in each of the new optimisation spaces
End
End

The optimisation process will be re-started in each of the new optimisation spaces. Separate swarms will be established in each partition and each swarm will follow the steps of swarming, power ramping and if needed further geometric partitioning independently of each other. The process will end when each of the partitioned optimisation spaces has met the coverage threshold. Figure 4.16 and Figure 4.17 show the test building before and after geometric partitioning. The size of the swarm and the no-go areas remain the same, but the *x-min, x-max, y-min* and *y-max* are redefined to indicate two separate optimisation spaces.

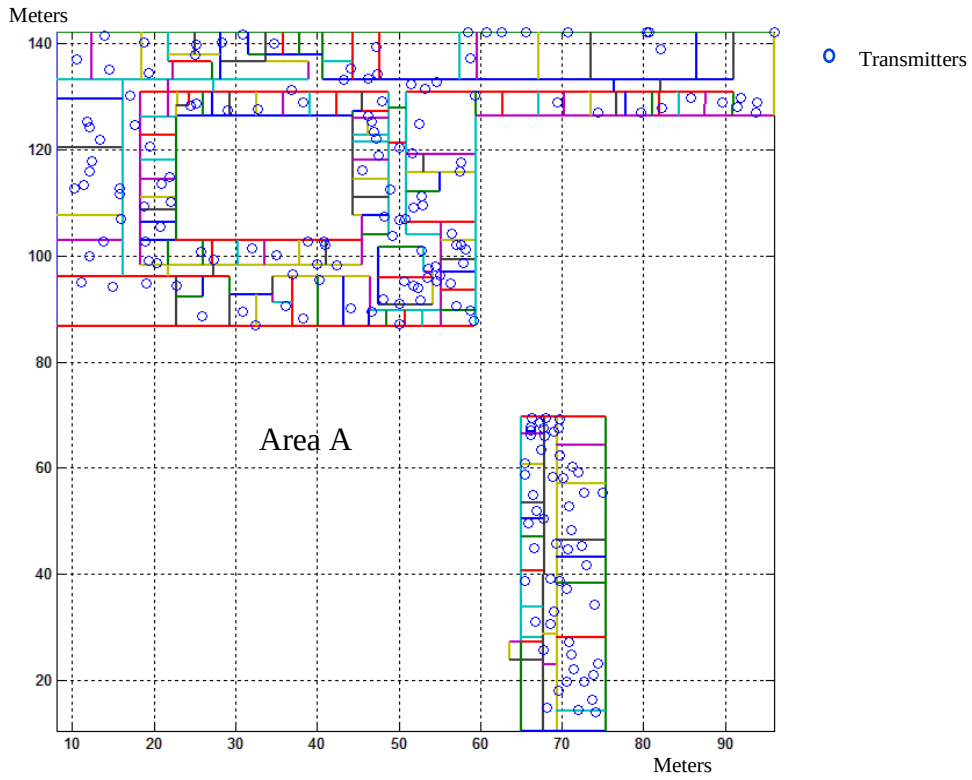

Figure 4.16. Before geometric partitioning.

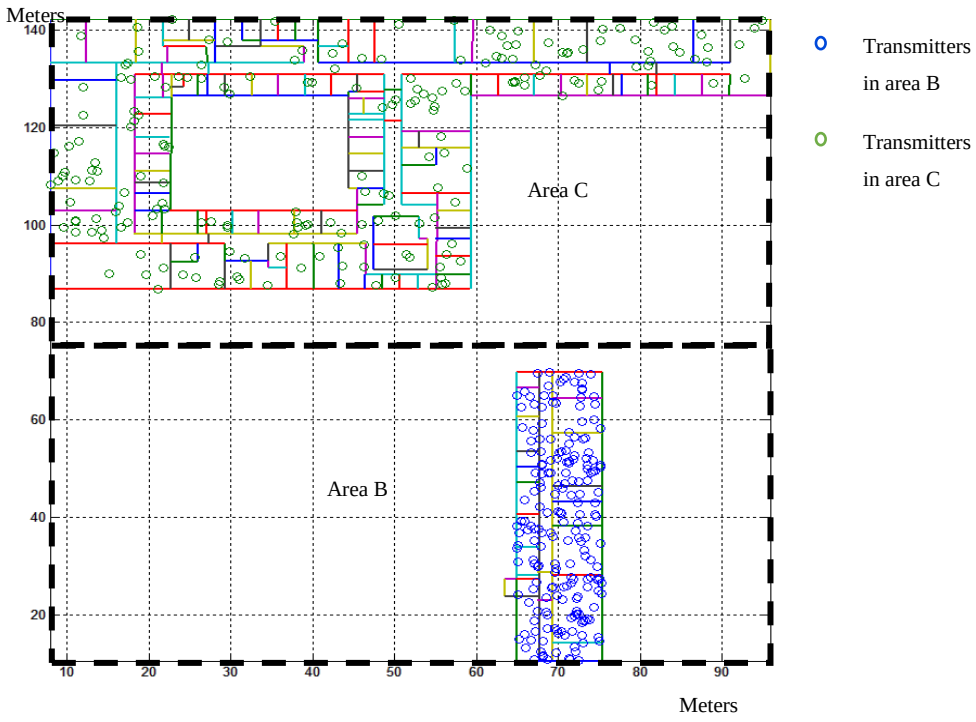

Figure 4.17. After geometric partitioning.

The longest sides of the rectangle are divided in two. For the test building, this is along the y-dimensions. This introduces *y-mid* to re-define the boundaries so that optimisation spaces A and B are defined as indicated in table 4.6.

Optimisation Spaces	**Boundaries (metres)**			
	x-min	*x-max*	*y-min*	*y-max*
Before Partition, Area A	8.01	95.94	10.50	142.30
After Partition, Area B	8.01	95.94	10.50	76.40
After Partition, Area C	8.01	95.94	76.40	142.30

Table 4.6. Boundaries before and after geometric partitioning.

It can now be seen in figure 4.17 that there are two different set of transmitters (swarms), one set in each of the new partitions. Each will independently start the swarming process. After the optimal location is chosen each of these newly portioned spaces, the optimisation process will proceed to the power ramping stage separately in each partition. If after the power ramping (described in section 4.6) the percentage coverage has not been met, then a new process of partitioning will be initiated in that area. In the end, each new partition may be further divided in two until the percentage coverage is met. Finally, the number of partitions will be equal to the number of transmitters required for the final solution.

4.8 Conclusions

There are two aspects to solving the indoor base station placement problem, namely the propagation consideration and the optimisations considerations. The major considerations for the development of a computer program to show the solution described in chapter three have been presented.

The general programming considerations have been presented so that the program can be written in whatever programming language required. In this research, the optimisation process was formulated using MATLAB.

The basis pseudo code and have been presented and where necessary there are additional flow charts to show the how the program has been constructed.

Chapter 5 : Implementation and Evaluation of Proposed System

The purpose of this chapter is to evaluate the proposed method in simple canonical situations where it is likely to be possible to deduce the solution. The chapter then goes on to apply the method on more and more complex situations. Finally, the chapter considers real buildings and validation evidence is presented based on a measurement campaign.

5.1 Test Scenarios

The aim of the validation is to ensure that the program is performing as required. This validation includes testing the proposed method in a series of building layouts with known logical outcomes. These range from a rectangular shaped building to a series of more complex layouts with multiple dividing walls and corridors. The different phases of the proposed algorithm are validated against different building layouts of varying complexities. There are three different cases to consider, namely the low, medium and high complexity problems.

The low complexity layouts provide the simplest demonstrations of the swarming phases described in section 3.5. This is illustrated in section 5.2 with the following specific geometries;

i. Rectangular box (10 m x 15 m)
ii. Rectangular box (10 m x 15 m) with 1 dividing wall

The medium complexity layouts are a better representation of actual buildings. In addition to the swarming phase, this helps validate the power ramping and avoidance of no-go areas. Section 5.3 show the validation for the following cases;

i. Long corridor with *n* offices either side.
ii. Long corridor with *n* offices either side and one no-go area

The high complexity layouts are fully representative of known structures. The floors WU and W2 of the Sir David Davies building at the Loughborough University are specific examples. The WU floor has less rooms and dividing walls but the geometric shape is somewhat similar to the W2 floor as described in section 4.1.

After the validation is completed, the system can be evaluated to provide an estimation as to when to exit the swarming process and to select the PSO parameters.

The test building (floor W2 of the Sir David Davies building at the Loughborough University) provides a good case to be able to test the effectiveness of the algorithm versus the manual in-building planning methods outlined in [1]. The wall loss is estimated as indicated in table 4.1. The planned coverage (*rxthreshold*) for the building is taken as -85dBm at 900 MHz with 95% percentage coverage. This means that 95% of the building must have a minimum receiver signal level of -85 dBm. The antenna layout for the building is planned via the methods described in [1] and then with the developed program. Both methods are compared to show the effectiveness and the number of antennas used.

This method is also used to plan the antenna configuration for the Xerox building Montego Bay, Jamaica. The output is compared to a plan produced by an in-building company [15]. Here, the number of antennas and their location are compared.

Finally, a test transmitter is set up at one of the locations chosen by the MATLAB program within the test building. Receiver level measurements are then taken at different locations throughout the building. This is then compared with the simulated results to test the effectiveness of the propagation model and to improve the estimation of the wall losses.

5.2 System Validation in Low Complexity Layouts

In this research, a low complexity layout is defined as one with an area less than 500 m^2 with less than three dividing walls. This area would normally require one transmitter transmitting at less than the full power (21 dBm) to meet the standard coverage requirements [6] of -85dBm at 900 MHz and 95% of the area covered. In the low complexity validation, there are two cases to consider, a rectangular box with and without a dividing wall. The accuracy of the swarming process, the choice of PSO parameters and the exit conditions can be evaluated in the simple layouts.

A rectangular building layout with length 10 m and width 15 m is used as the low complexity validation test layout. This is indicated in figure 5.1 initially with no dividing walls. In figure 5.8 one partition wall is added.

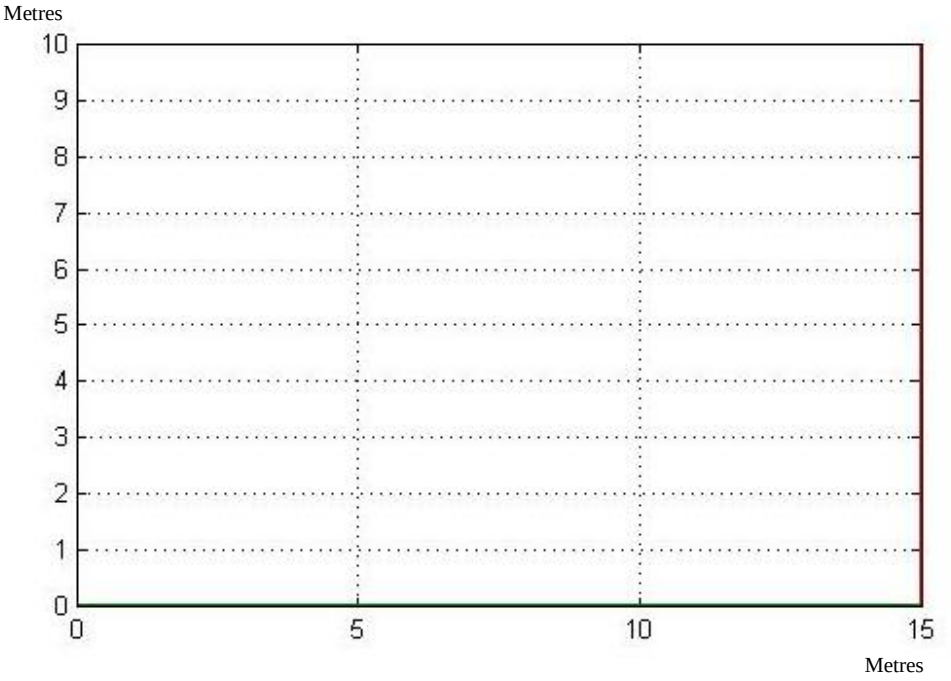

Figure 5.1. Low complexity layout

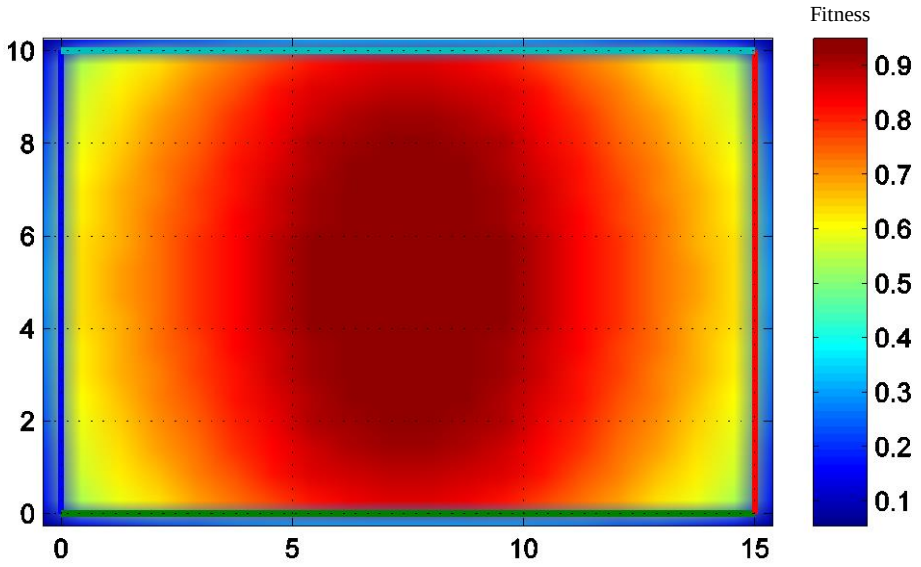

Figure 5.2. Fitness of transmitter locations

Figure 5.2 shows the fitness of possible transmitter locations within this layout. The signal spreading from a transmitter to receiver location is calculated using the propagation model described in chapter 2 as:

$$Rx_{lev} = P_{Tx} - 31.5 + 20\log_{10} d + \sum k_i Lw_i \quad (5.1)$$

Where Rx_{lev} is the received signal level at a distance d from the transmitter in dBm and P_{Tx} is the transmitter power level in dBm, k_i is the type of wall and Lw_i is the loss for each type of wall.

Given that P_{Tx} = 0 dBm and the layout is evenly divided into 625 (25 x 25) transmitter grids and 2500 (50 x 50) receiver grids. From each transmitter grid location, the signal level at each receiver grid location is calculated. Then with a receiver signal threshold of -50 dBm, the fitness of each receiver location is calculated as discussed in section 3.5.3. The fitness function is given as:

$$F = \frac{T}{k} \quad (5.2)$$

Where: F = fitness at each transmitter location, k = total number of received locations and T is the number of received locations that exceed the receive threshold.

The transmitter location of greatest fitness as indicated in figure 5.2. With the grid resolution used, the point of greatest fitness (7.5, 5).

The first test is to evaluate how accurately the transmitters swarms to the optimum location. With the validation parameters indicated in table 5.1, the transmitters should swarm to the centre of the validation space. The swarm size is chosen to be larger than that which is strictly necessary to allow the swarming process to be visualized. Extreme values are also chosen for the percentage coverage and the *rxthreshold* to force the swarm to the centre of the room. Figure 5.3 shows the initial random position of all the particles and Figure 5.4 shows the transmitters moving towards *gbest* (swarmed location) after three iterations.

Parameters	Validation Values
Swarm size	400
ω	0.01
C_1	2
C_2	1
α_1	1
α_2	1
Percentage coverage	95%
L_0	31.5
rxthreshold	-50 dBm
nb_points	100

Table 5.1. Validation parameters.

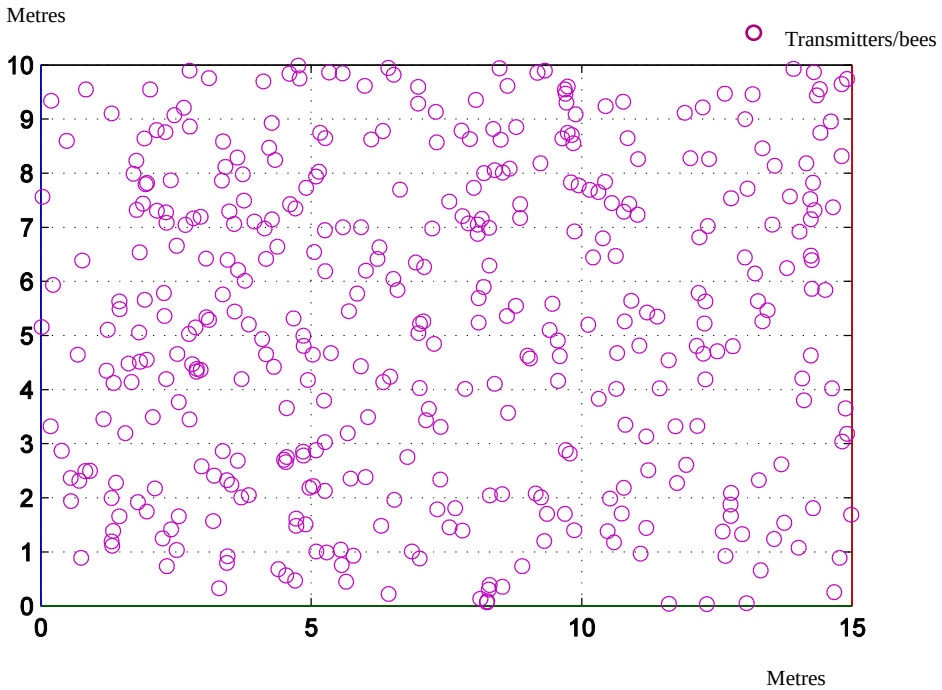

Figure 5.3. Initial random positions of the particles within the low complexity layout

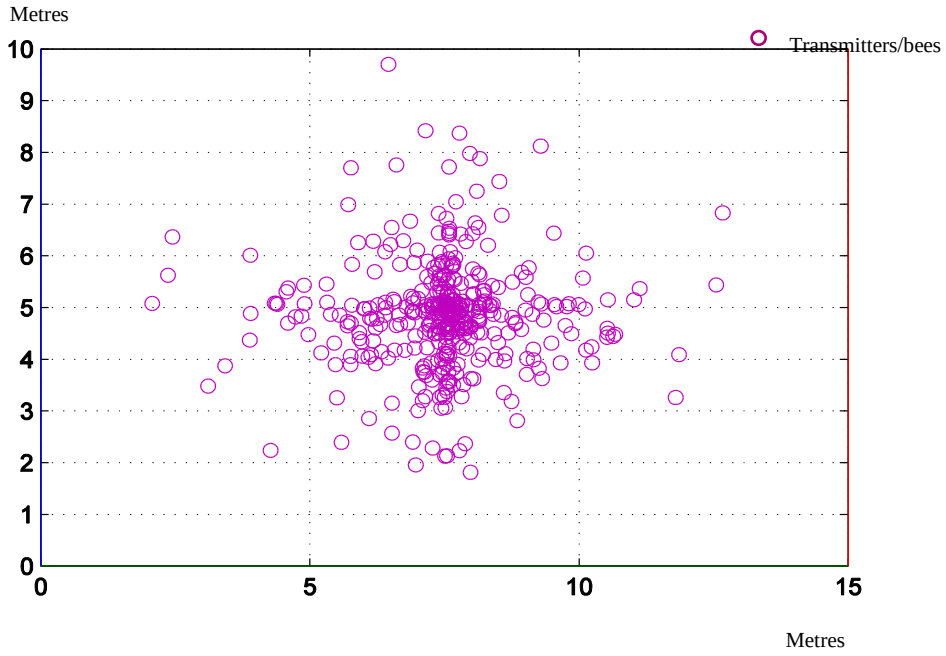

Figure 5.4. Swarming after 3 iterations (low complexity layout)

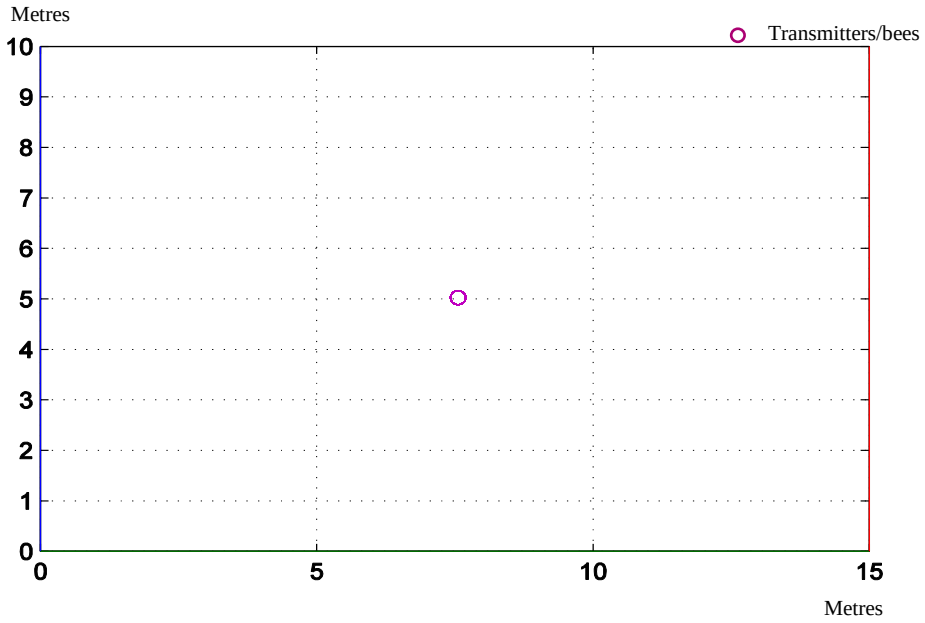

Figure 5.5. Final location after convergence after 30 iterations.

The MATLAB program performed as expected converging to the area of greatest fitness. Figure 5.5 show the final swarmed location and figure 5.6 show the receiver signal levels from this location with transmitter power of 0 dBm. A scatter plot (table available in appendix A) of the final positions (*x-y* positions) over 25 runs (executions of the program) is shown in figure

5.7. The mean value for *gbest(x,y)*=(7.5073, 5.0051) and the standard deviation for *gbest(x,y)*=(0.1587, 0.0254).

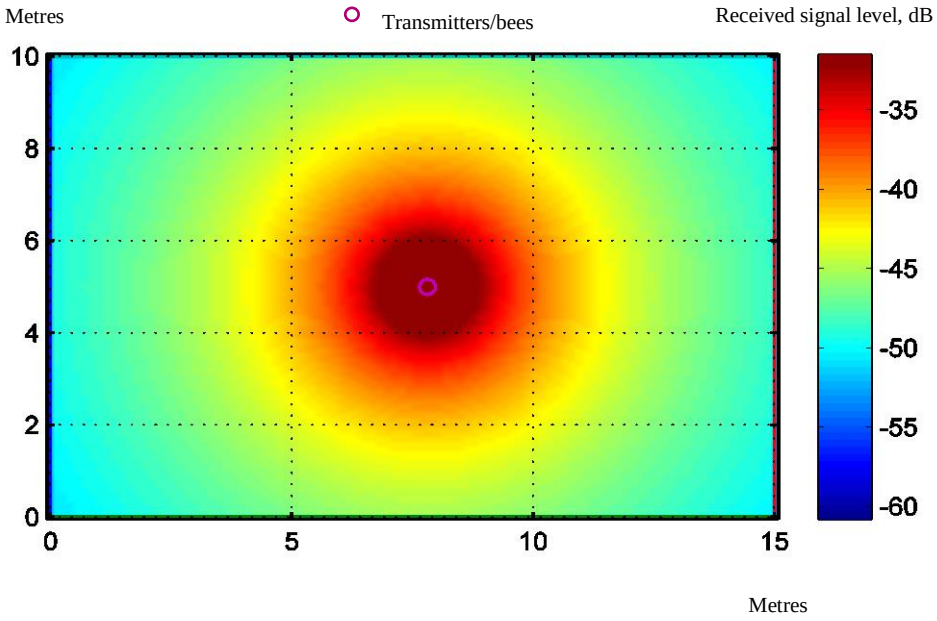

Figure 5.6. Received signal levels with the transmitter at the final location.

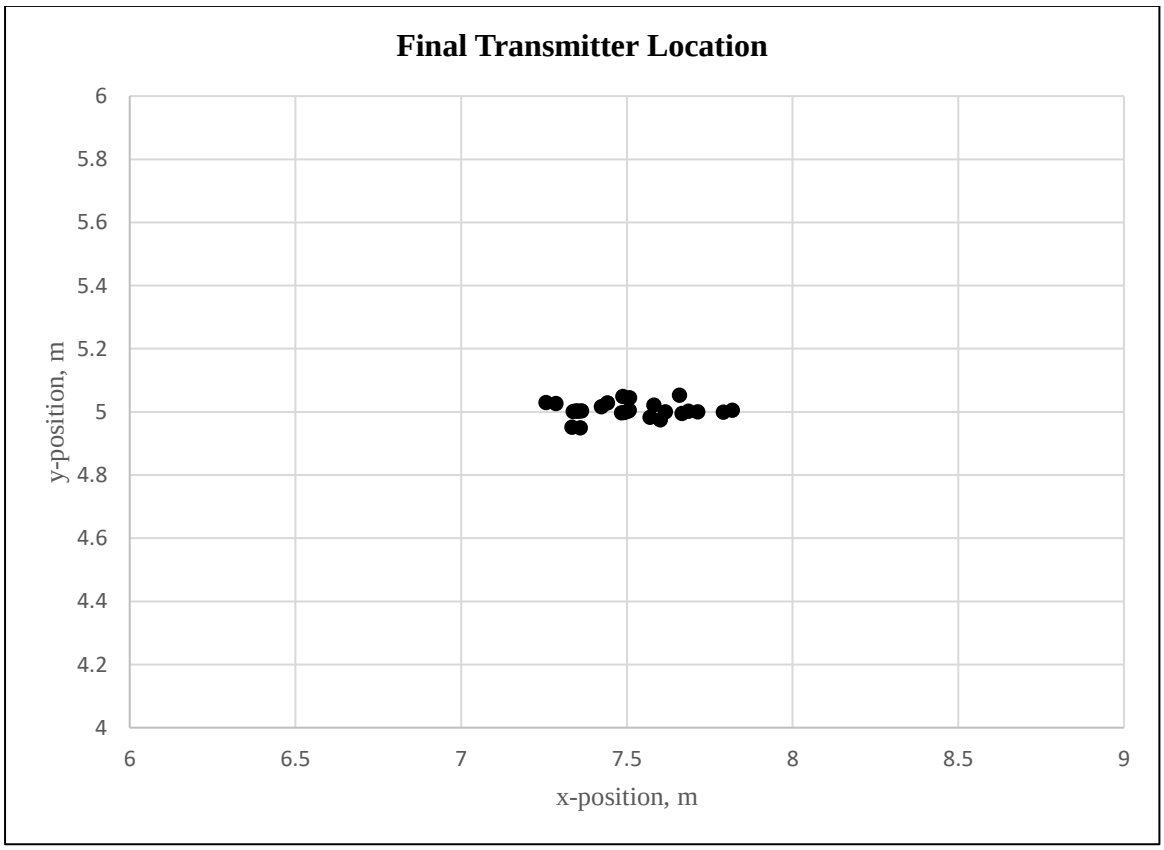

Figure 5.7. Scatter plot of gbest over 25 runs

The second case indicates how swarming is affected with interior walls added to the validation space. Figure 5.8 shows an interior wall from the location (12, 0) to location (12, 10) with a wall loss of 5 dB. The fitness of each transmitter location is shown in figure 5.9 with the point of greatest fitness located at (9.4, 5). This is moved closer to the wall (compared to the layout with no wall) from the geometric centre to compensate for wall losses.

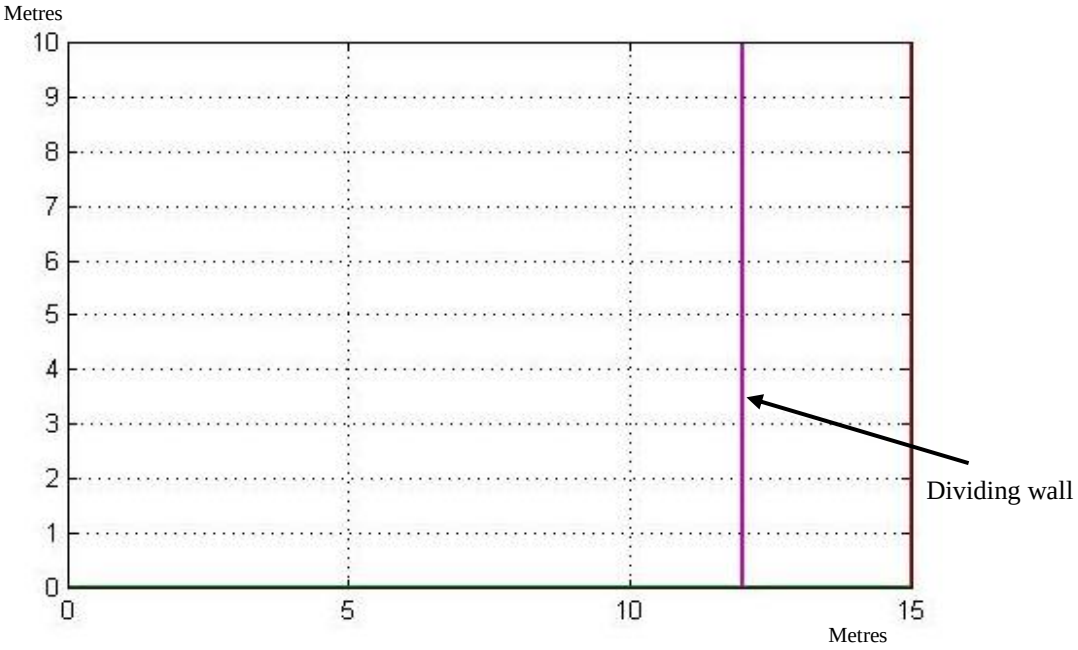

Figure 5.8. Low complexity layout with 1 wall

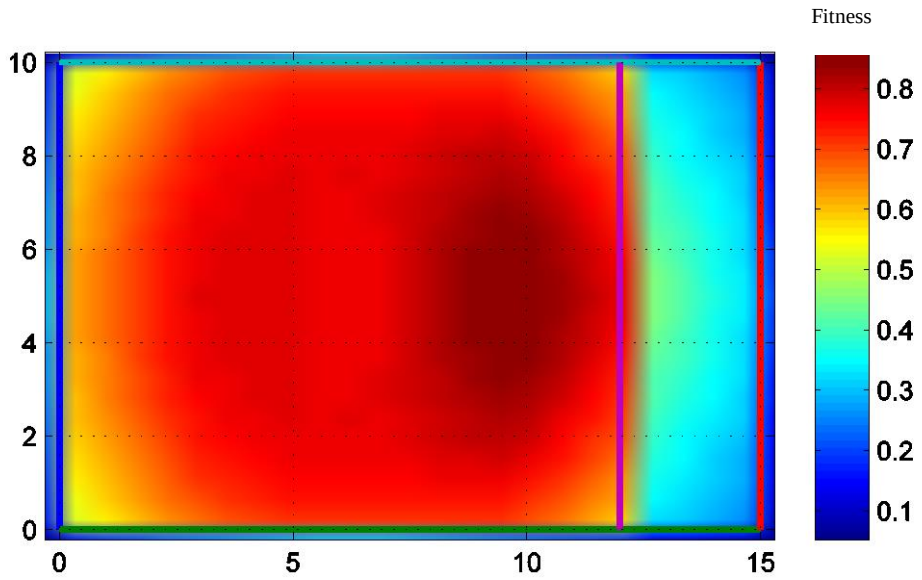

Figure 5.9. Low complexity layout with 1 wall

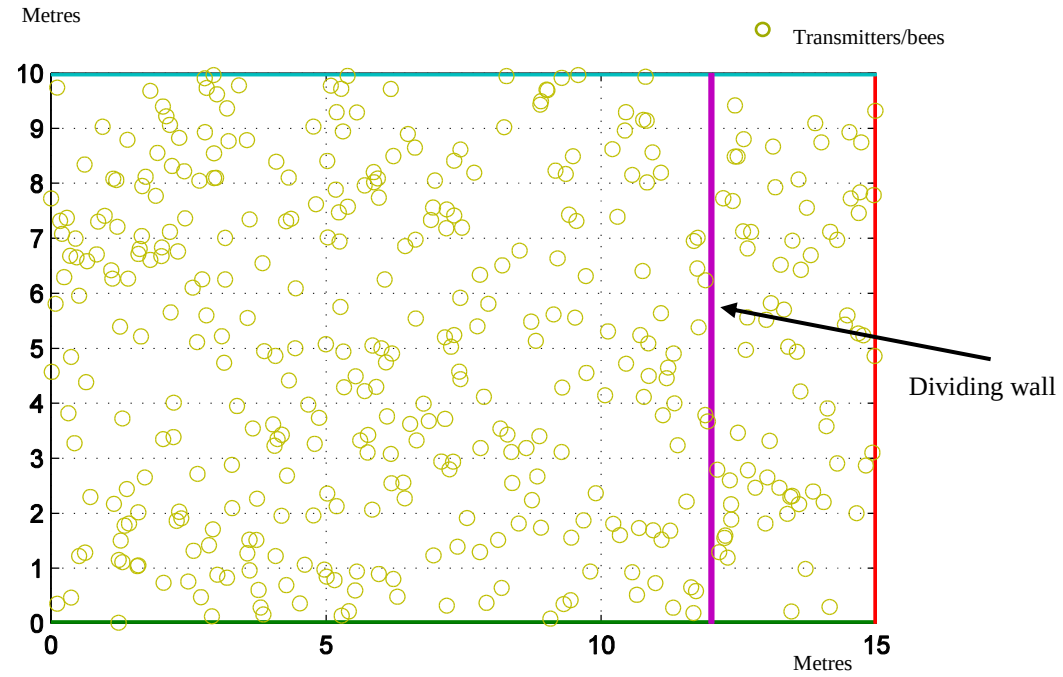

Figure 5.10. Initial transmitter location with 1 wall added to test layout

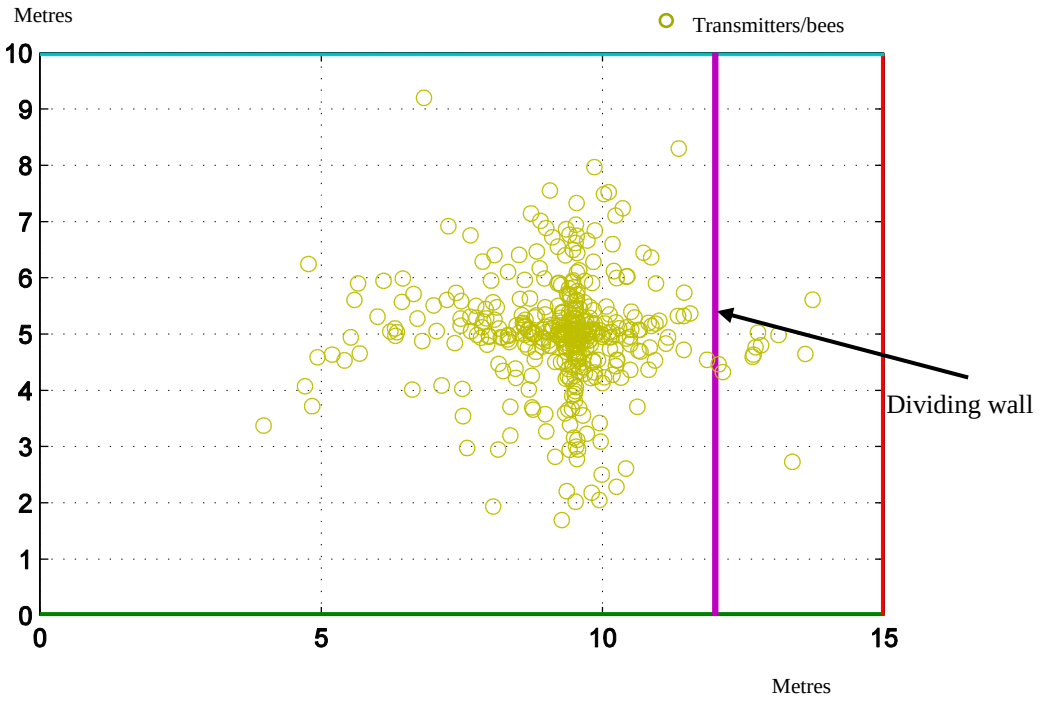

Figure 5.11 Swarming after 3 iterations (1 wall in low complexity layout)

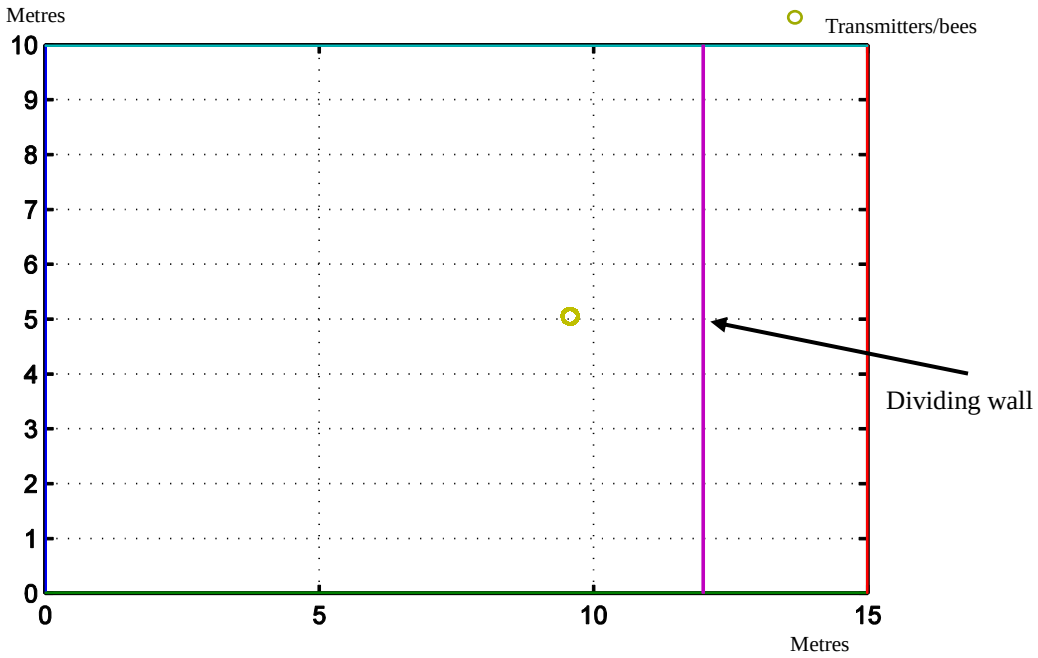

Figure 5.12 Final transmitter location after convergence after 30 iterations

Figure 5.12 shows a final location for *gbest(x,y)*=(9.5069, 4.997). With a single transmitter at this location, the transmit power required to meet the coverage requirements was 3 dBm. This is an increase in transmitter power compared to the first test when there were no partition walls. The received signal at different locations is plotted as indicated in figure 5.13. Shown here also is the effect that interior wall has on the received levels beyond the wall, with the levels being reduced due to the wall attenuation.

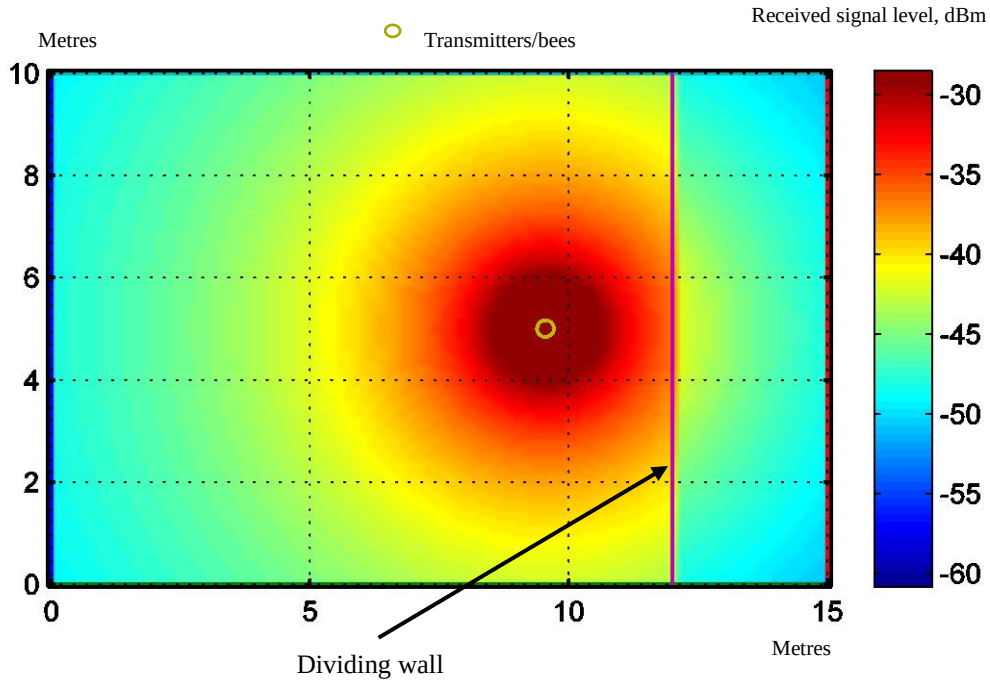

Figure 5.13. Received levels with an interior wall.

5.3 System Validation in Medium Complexity Layouts

In this research, a medium complexity layout is defined as one with an area greater than 500 m^2 and less than 4000 m^2 with more than three dividing walls. This area may require more than one transmitter or one transmitter transmitting at high power to meet the standard coverage requirements [6] of -85 dBm at 900 MHz and 95% of the area covered. The validation in the medium complexity layouts considers the following cases;

i. Long corridor with *n* rooms either side.

ii. Long corridor with *n* rooms either side and one no-go area

The ability of the system to deal with multiple partition walls, to swarm avoiding the no-go location and the power ramping process can be evaluated in the medium complexity layouts.

The validation parameters indicated in table 5.2, and figure 5.14 show a typical medium complexity layout.

Parameters	Validation Values
Swarm size	500
ω	0.01
C_1	2
C_2	1
α_1	1
α_2	1
Percentage coverage	95%
L_0	31.5
rxthreshold	-60 dBm
nb_points	100

Table 5.2. Validation parameters for medium complexity layout.

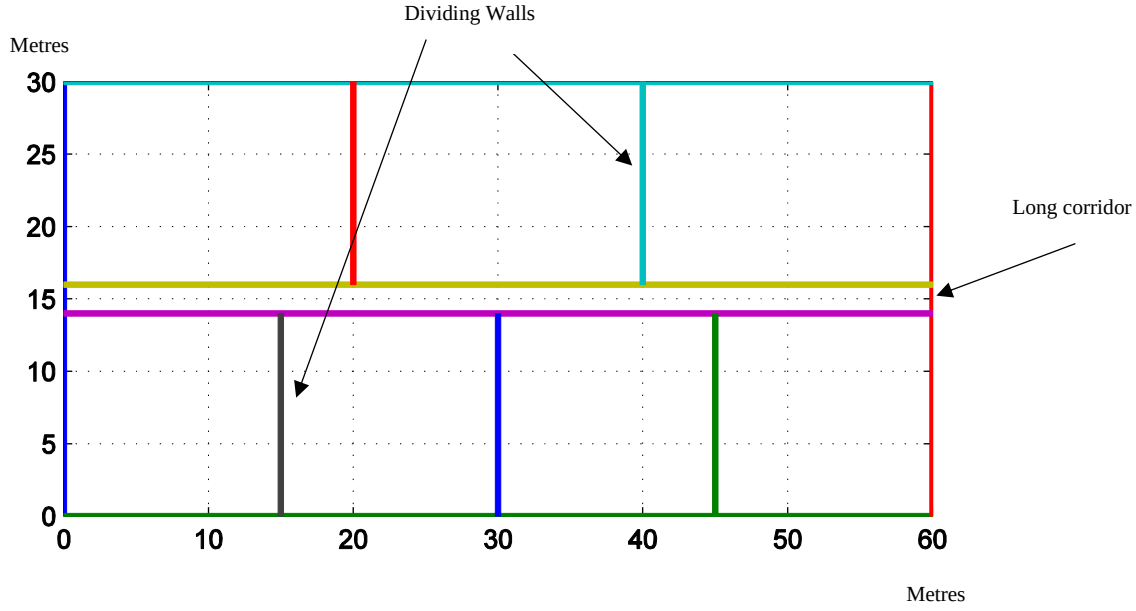

Figure 5.14. Typical medium complexity layout.

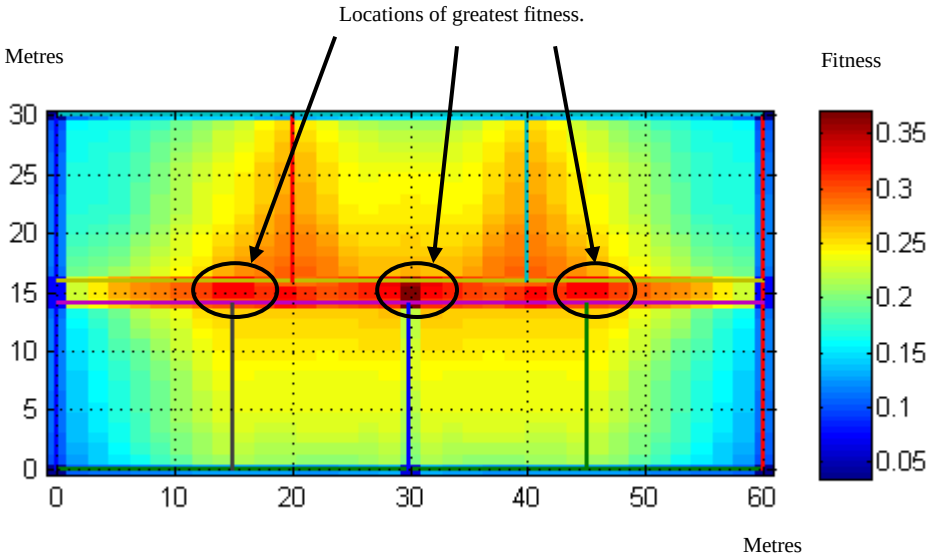

Figure 5.15. Transmitter locations fitness, medium complexity layout.

Figure 5.15 shows the fitness of the transmitter locations. This is calculated given P_{Tx} = 0 dBm with 1225 transmitter grids, 10000 receiver grids and a receiver signal threshold of -60 dBm. The point of greatest fitness was found at (30.00, 14.12).

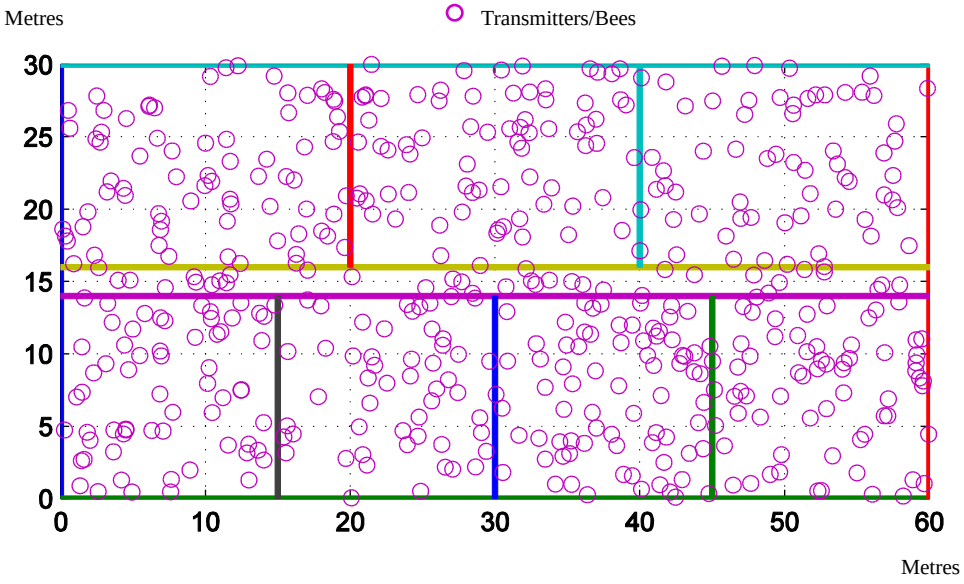

Figure 5.16. Initial random positions of the particles within the medium complexity layout.

Figure 5.16 shows the initial random positions of all (500) the transmitters in the swarm. The large swarm size is used to illustrate the random initial placement of each transmitter in the

swarm. High values are also chosen for the percentage coverage and the *rxthreshold* (refer to table 5.2) to reduce the number of solutions and create only one optimum solution. Figure 5.17 show the transmitters moving towards *gbest* (swarmed location) after three iterations.

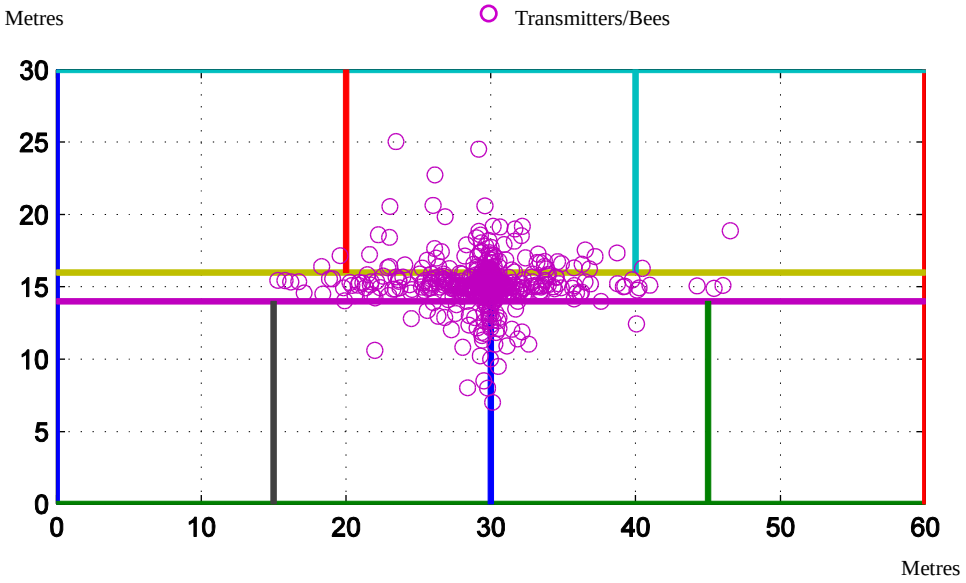

Figure 5.17. Swarming after 3 iterations (Medium complexity layout)

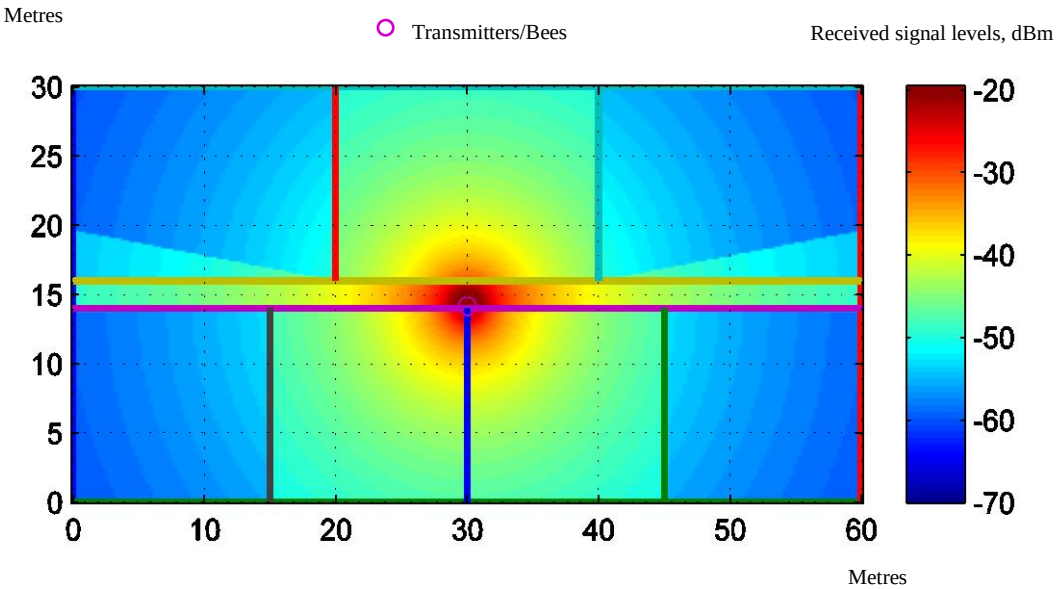

Figure 5.18. Received signal levels with the transmitter at the final location (after 30 iterations), medium complexity layout.

Figure 5.18. shows the plot of signal levels throughout the building with the transmitter at the final swarmed location. The mean for *gbest(x,y)*=(30.0002, 14.1709). This is in good agreement with the expected results as indicated in figure 5.15. The final location is in the *y*-direction is not in the geometrical centre. This is because there are more walls in the lower section of the layout. This means that the transmitter would have to be placed closer to the lower section to compensate for the greater signal losses (due to more walls) in this area.

The avoidance of no-go areas is also tested in the medium complexity layout. Figure 5.19 shows the medium complexity layout with a no-go location added. The initial transmitter location is illustrated in figure 5.20. It can be seen, that during the initial random placement of the transmitters, the no-go locations are avoided. Additionally, the transmitters avoid the no-go locations in the swarming phase. This is demonstrated in figure 5.21.

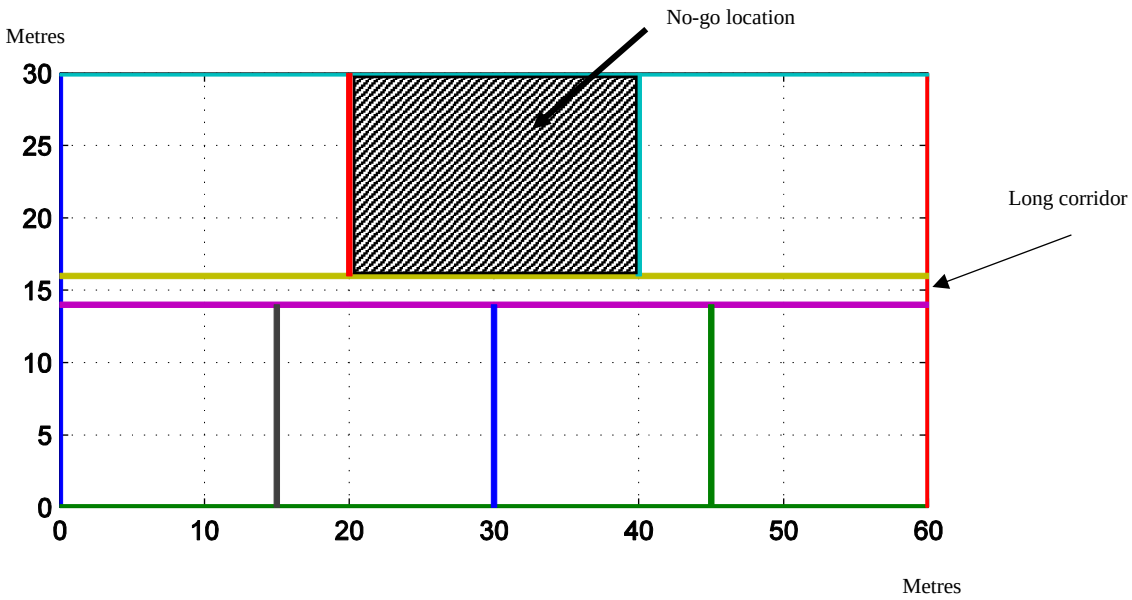

Figure 5.19. Medium complexity layout with no-go location.

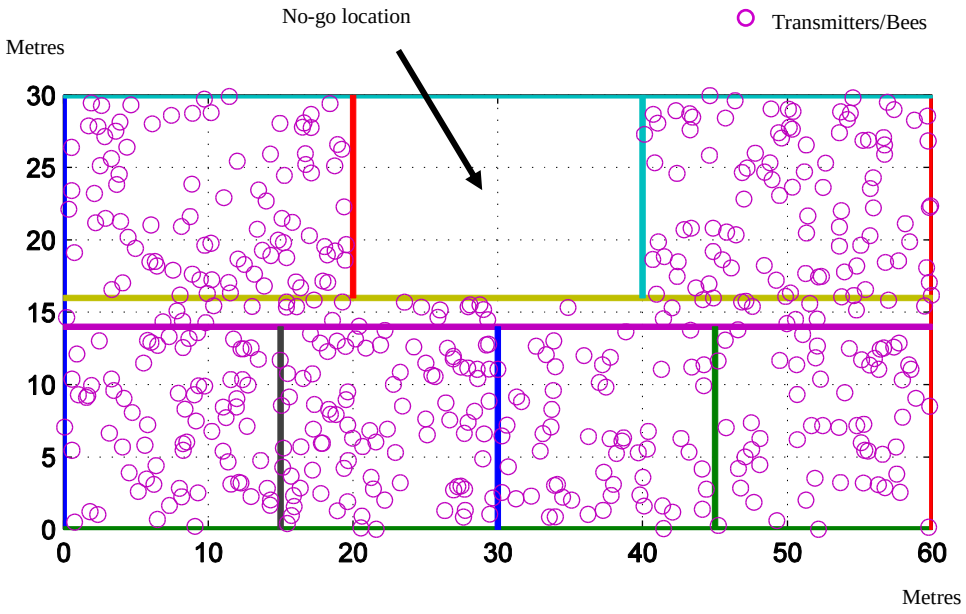

Figure 5.20. Initial random transmitter locations avoiding no-go locations

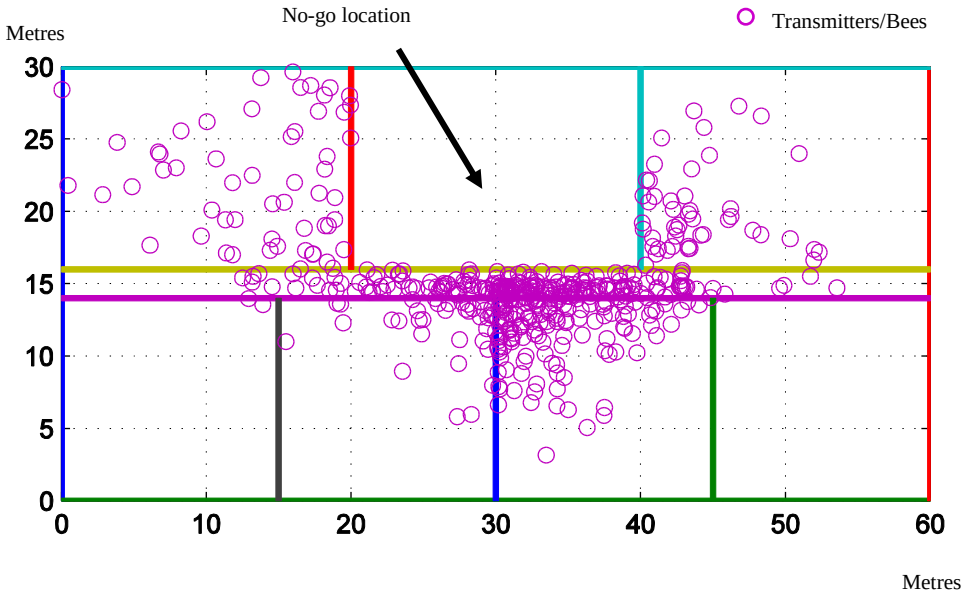

Figure 5.21. Swarming after 3 iterations (no-go locations avoided)

5.4 System Validation in High Complexity Layouts

In this research, a high complexity layout is defined as one with an area greater than 4000 m^2 with more than three dividing walls and possible no-go areas. This area may require more than one transmitter to meet the standard coverage requirements [6] of -85dBm at 900 MHz and

95% of the area covered. The floors WU and W2 of the Sir David Davies building at Loughborough University are specific examples for the high complexity layout. The validation considers the floor WU. The ability of the system to deal with multiple partition walls, to swarm avoiding the no-go location, power ramping and the geometric partitioning process can be evaluated in the high complexity layouts.

With the validation parameters indicated in table 5.3. Figure 5.22 shows a typical example of a high complexity layout. Figure 5.23 shows the transmitter locations fitness. This is calculated given P_{Tx} = 21 dBm with 500 transmitter grids, 10000 receiver grids and a receiver signal threshold of -75 dBm. At maximum power the coverage requirements are not met hence in this scenario, geometric partitioning is required. Figure 5.24 shows the initial transmitter locations and figure 5.25 shows the swarming process.

Parameters	**Validation Values**
Swarm size	400
ω	0.01
C_1	2
C_2	1
α_1	1
α_2	1
Percentage coverage	95%
L_0	31.5
rxthreshold	-75 dBm
nb_points	100

Table 5.3. Validation parameters for high complexity layouts.

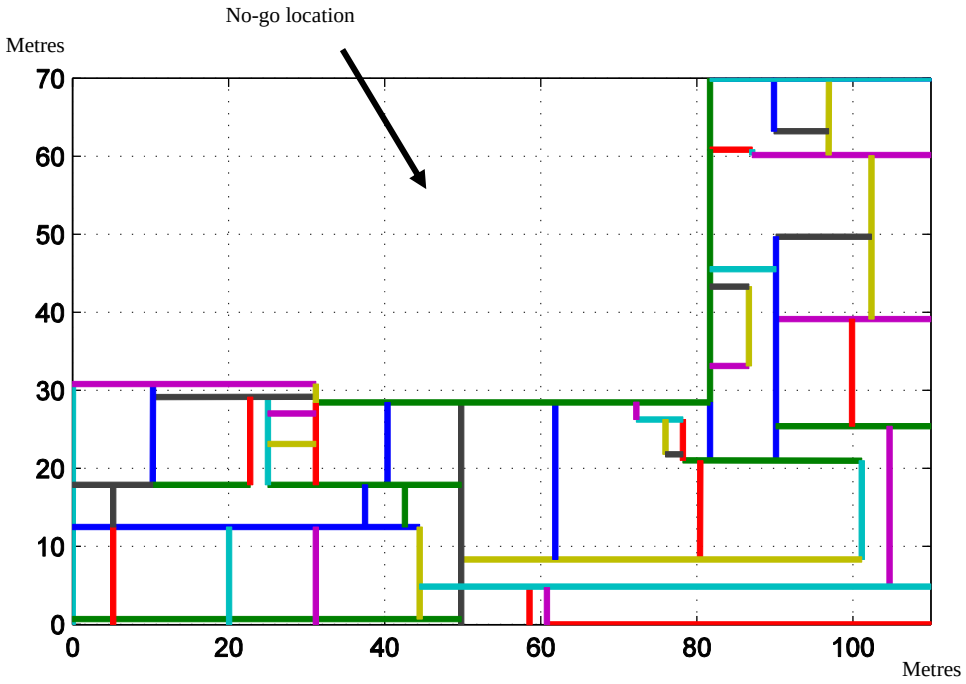

Figure 5.22. High complexity layout. (Floor WU of the Sir David Davis Building at Loughborough University)

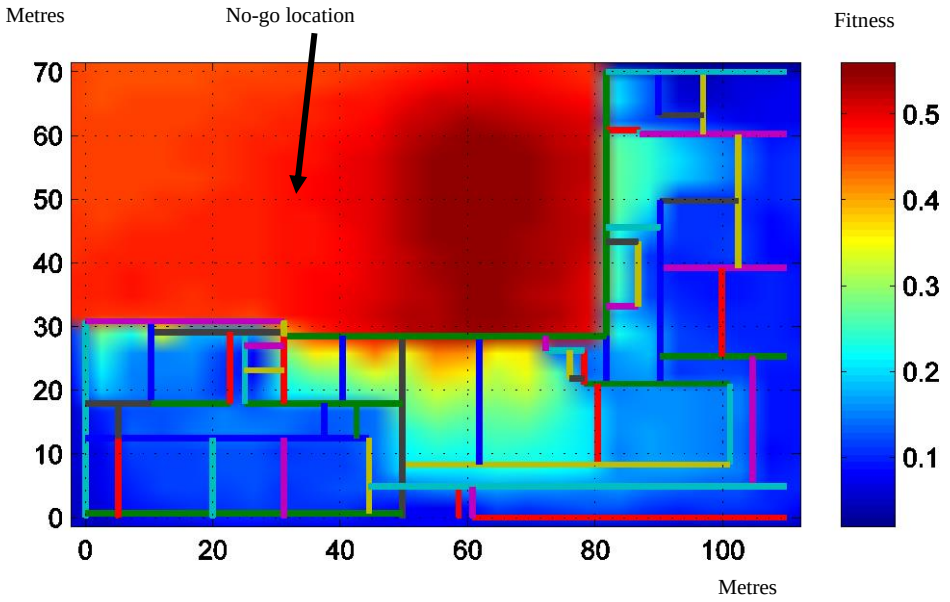

Figure 5.23. Transmitter fitness locations. High complexity layout. (Floor WU of the Sir David Davis Building at Loughborough University)

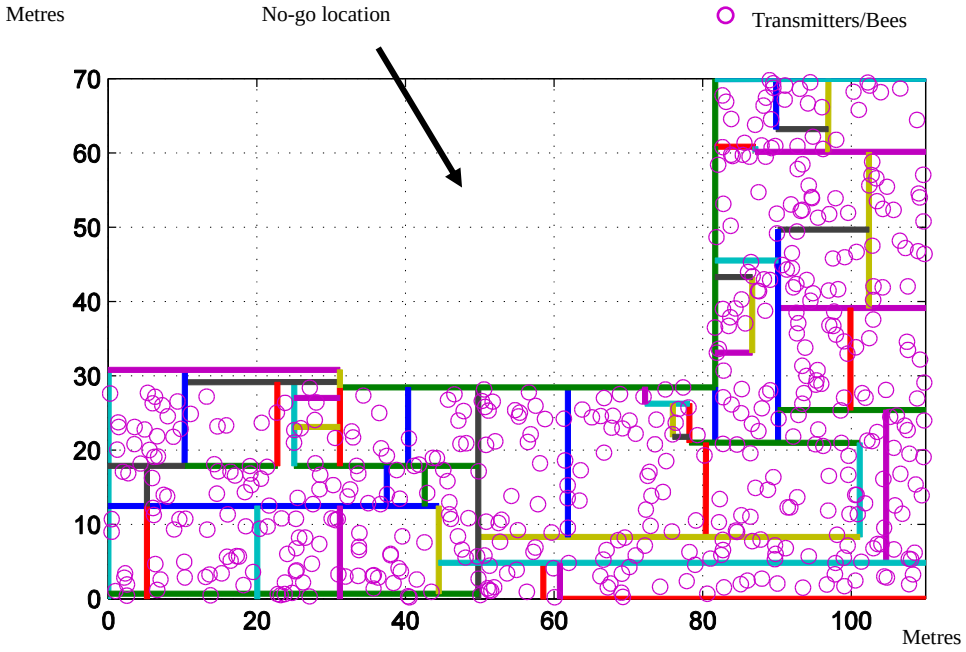

Figure 5.24. High complexity layout. Initial transmitter locations (500 transmitters)

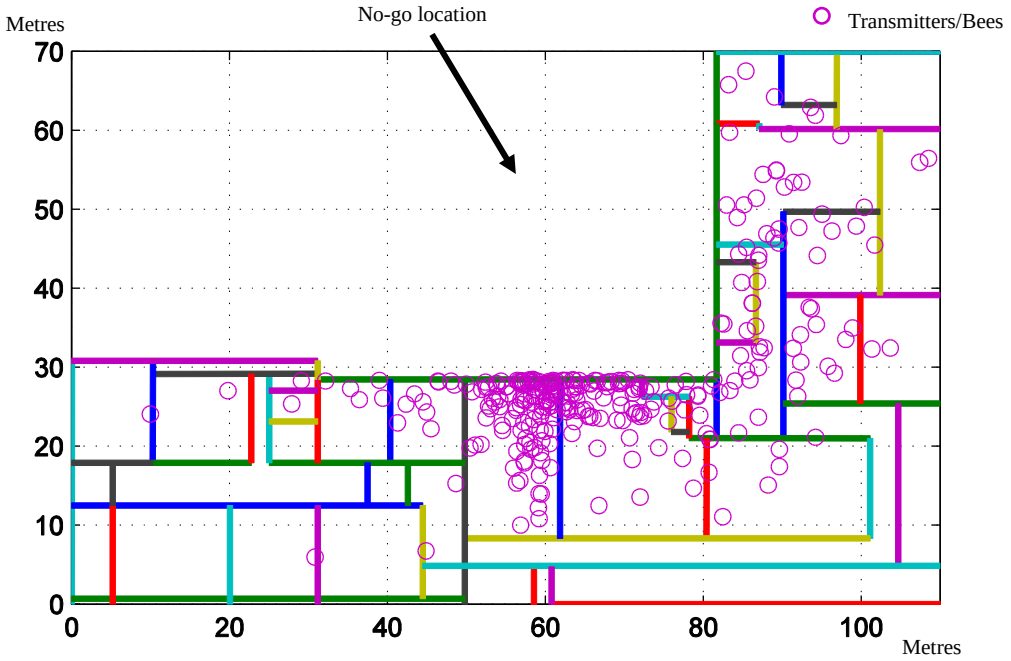

Figure 5.25. High complexity layout. Swarming after 3 iterations

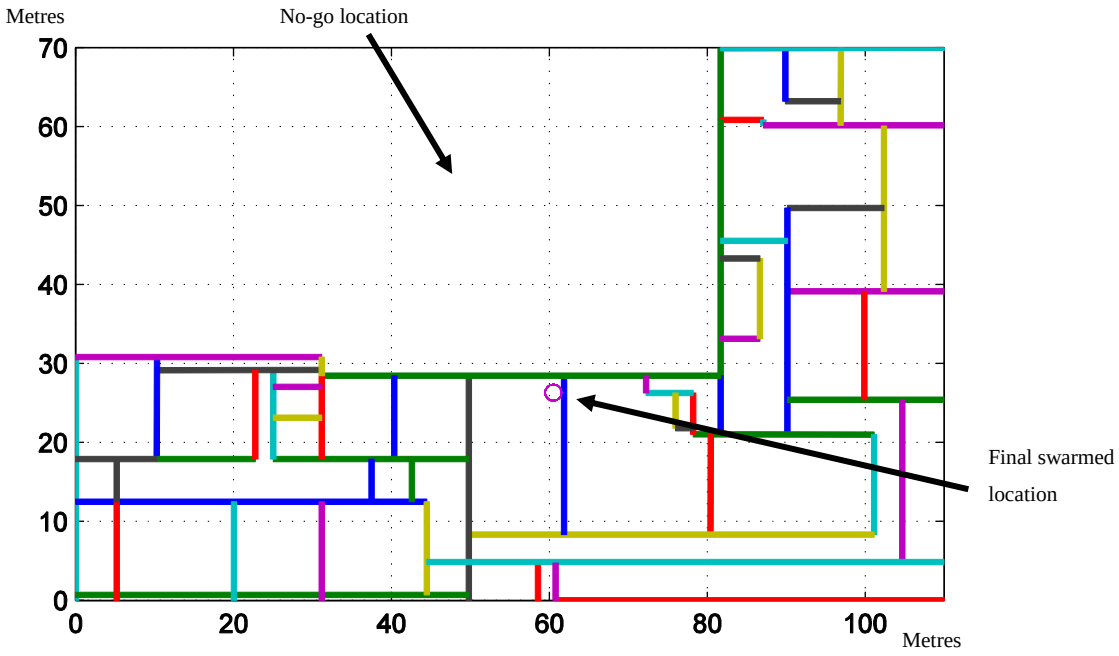

Figure 5.26. High complexity layout. Final swarmed location

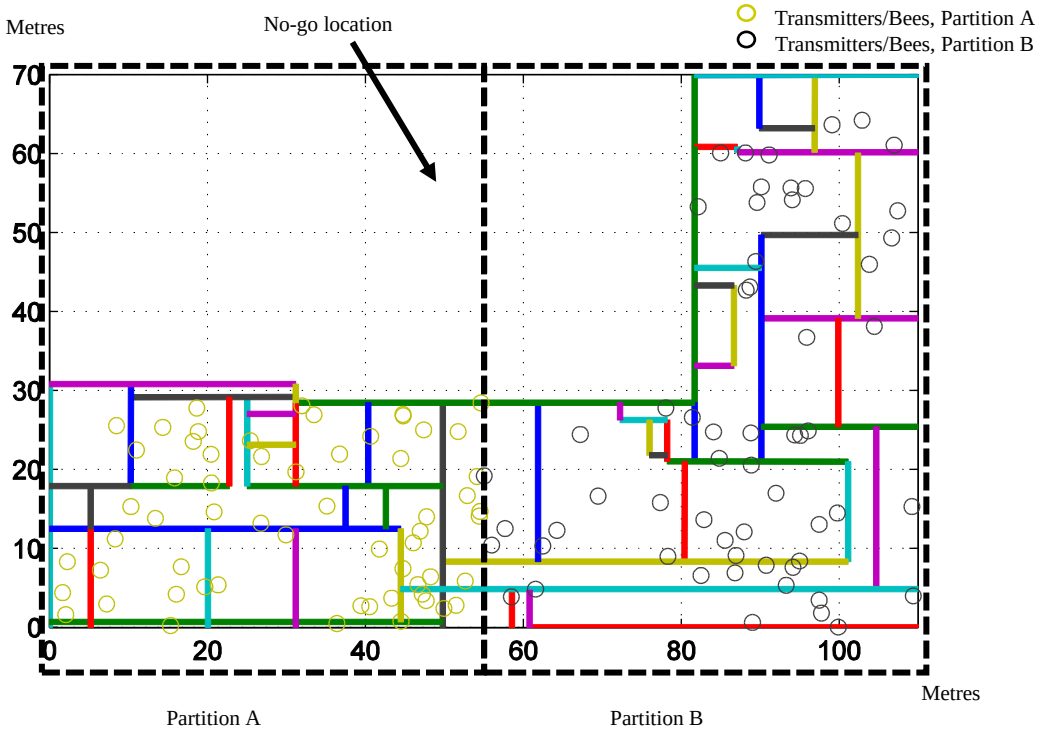

Figure 5.27. Initial random particle positions after geometric partitioning.

Figure 5.26 shows the final swarmed position for the high complexity layout. This is *gbest_x*=60.5763, *gbest_y* =28.2704.

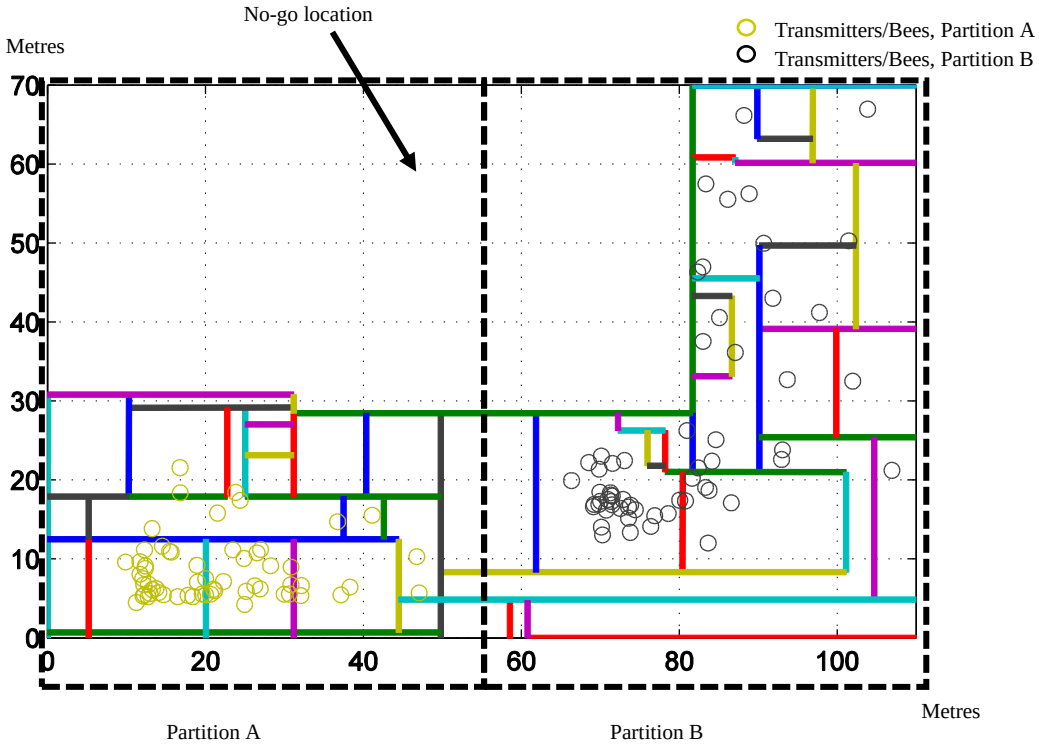

Figure 5.28. Swarming after geometric partitioning after 5 iterations.

The process of geometric partitioning is illustrated in figure 5.27 and 5.28. The entire optimisation space is divided in two parts and the swarming process is independently initiated in each part.

5.5 Discussion

5.5.1 Choosing Initial Parameters

Section 4.3 describes the list of most of the parameters used when creating the program. The parameters used in the swarming part of the program are very important in determining the effectiveness of the PSO algorithm [57]. These are the size of the swarm, and the constants ω, C_1, C_2, α_1, and α_2. Suggested values for these parameters are indicated in [58] and [61]. The validation process dictates the best sets of values for these parameters to apply to the test building. In this research, the suggested [58], [61] values for the constants ω, C_1, C_2, α_1, and α_2, are used. Throughout the entire validation process, extreme values for Rx-threshold and percentages coverage are chosen for the different complexity layouts to illustrate the performance of all phases of the program.

For a set number of bees, there exists a direct relationship between the speed of swarming of the program and number of receiver points. As indicated in section 4.5, the fitness of each bee/transmitter location is calculated by comparing the receiver level at each receiver location (for each transmitter location) to the receive threshold.

$$Fitness = \frac{number\ of\ receiver\ locations\ above\ threshold}{number\ of\ receiver\ locations} \tag{5.3}$$

Number of receiver locations per/m^2	**AVG Swarm time (seconds)**	**Swarm Precision, Sigma, m**	**Max Power Output (dBm)**
0.06	1.54	11.106	21
0.22	1.65	4.470	21
0.50	1.78	6.749	21
0.89	1.96	10.586	21
1.39	2.17	4.480	18
2.00	2.45	0.016	12
2.72	2.79	0.012	12
3.56	3.18	0.006	12
4.50	3.59	0.006	12
5.56	4.10	0.004	12
6.72	4.48	0.006	12
8.00	5.12	0.008	12
9.39	5.80	0.008	12
10.89	6.56	0.002	12
12.50	7.38	0.004	12
14.22	8.16	0.002	12
16.06	9.20	0.005	12
18.00	9.92	0.007	12
20.06	11.00	0.003	12
22.22	11.98	0.003	12

Table 5.4. Number of points vs execution time

The optimum number of receiver location per square metre compared to the swarming precision for the medium complexity layout is illustrated in table 5.4. The full table is available in Appendix A. This is for a swarm size of 30 bees. It can be seen, that there is no useful improvement in sigma values with the number of receiver locations greater than 3.56 per m^2. The execution time increases with more points and the output power remains at a minimum.

It has been shown [64]that a swarm size of 30 was enough for an accurate convergence of the PSO. Figure 5.29 (table available in Appendix-A) shows the effect of swarm size versus run time in the medium complexity layout. The convergence time is measured as the time it takes for all the transmitters to be in the same location with an accuracy of 0.01 m. The processing is with an Intel Core i7-5600U (speed 2.6 GHz) processer with Windows 10 64-bit operating systems with 12GB RAM. The sigma values are the standard deviation for five different executions for a specific swarm size.

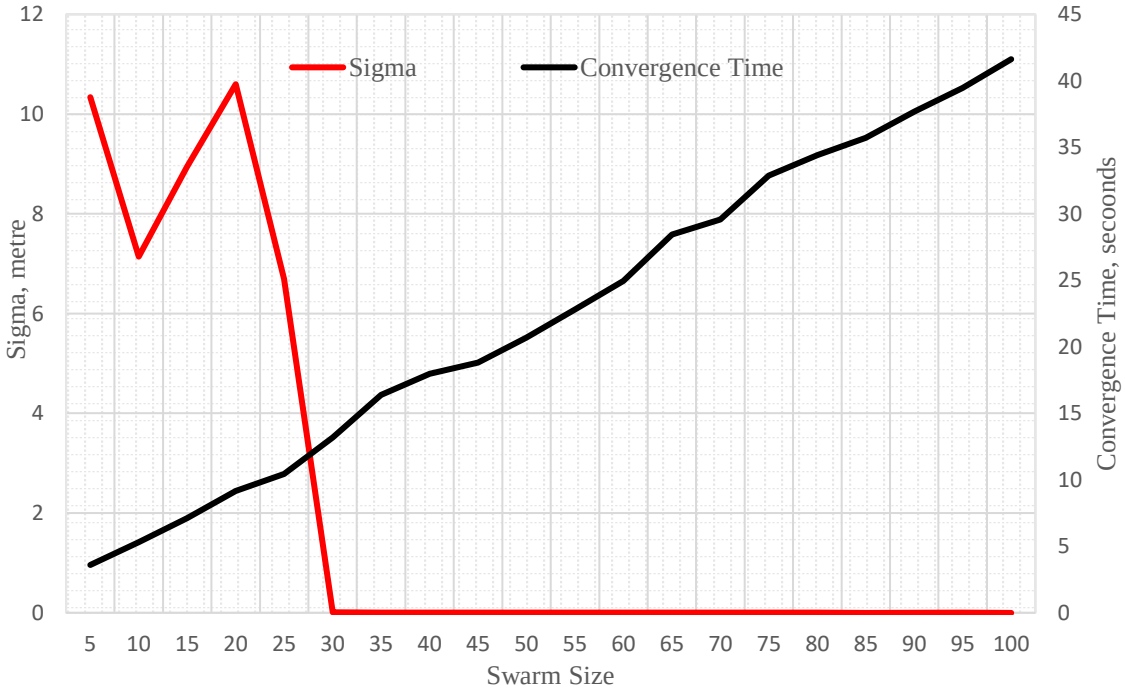

Figure 5.29. Swarm size versus run time.

The value for swarm size agrees with Yassin et. al. [64], as with a swarm size greater than 30 there is no significant improvement in the standard deviation for *gbest_x* values even though there is an increase in convergence time.

Table 5.5 shows the final set of values chosen parameters for the test building (floor W2 of the Sir David Davies building at Loughborough University). These are obtained by the noting the performance in the different validations cases as indicated above. These forms the set of values to be used in the test case and the case comparing the actual planning via the in-building design company [15].

Parameters	Validation Values
Swarm size/number of transmitters	30
ω	0.01
C_1	2
C_2	1
α_1	1
α_2	1
Percentage coverage	95%
L_0	31.5
rxthreshold	-85 dBm
nb_points[2]	100

Table 5.5. Parameters used in test building.

5.5.2 Exit conditions

Theoretically, the PSO algorithm may be considered to have converged to a useful solution when the all the particles have the same location. Depending computational resources this may take a long time and it may not be practical or efficient to have all the particles in the same positions. In this research, the number of movements/iteration of each particle is noted and compared against the standard deviation from *gbest* for each iteration. The standard deviation, σ (sigma) is calculated as:

$$\sigma = \sqrt{\frac{\sum_{Nt=1}^{bees}(pbest(Nt) - gbest)^2}{bees}} \tag{5.4}$$

[2] The number of points indicates the average number of receiver locations per square metre

Where *bees* is the size of the swarm, *Nt* is the number of transmitters in the swarm, *pbest* is the current position of the particle and *gbest* is the optimum position of all the particles.

At convergence, it is expected that the standard deviation for all the particles approaches zero. Figure 5.30 and figure 5.31 (table available in appendix A) show how the standard deviation changes compared to the number of iteration over an average of 10 run with 30 transmitters during the swarming phase for all three types of layouts. This is done for the *x*-coordinates only. A similar performance can be seen for the *y*-coordinates. In this research, acceptable convergence is considered when sigma is less than or equal to 0.001 metres. This convergence increases as with respect to the level of complexity of the layout. In the high complexity layout, the convergence occurs after a largest number of iterations compared with the other layout types.

There are no no-go locations within the low complexity layouts, hence, the convergence curve is much smoother than it is in the other layout types. In medium and high complexity layouts, a transmitter's position will be randomly repositioned if it falls within a no-go area during swarming. This is like the process described in [74] that will allow additional exploration of the optimisations for that transmitter. This may affect the smoothness of the convergence as it now introduces the ability to "jump" from local optimums and improves the overall solution.

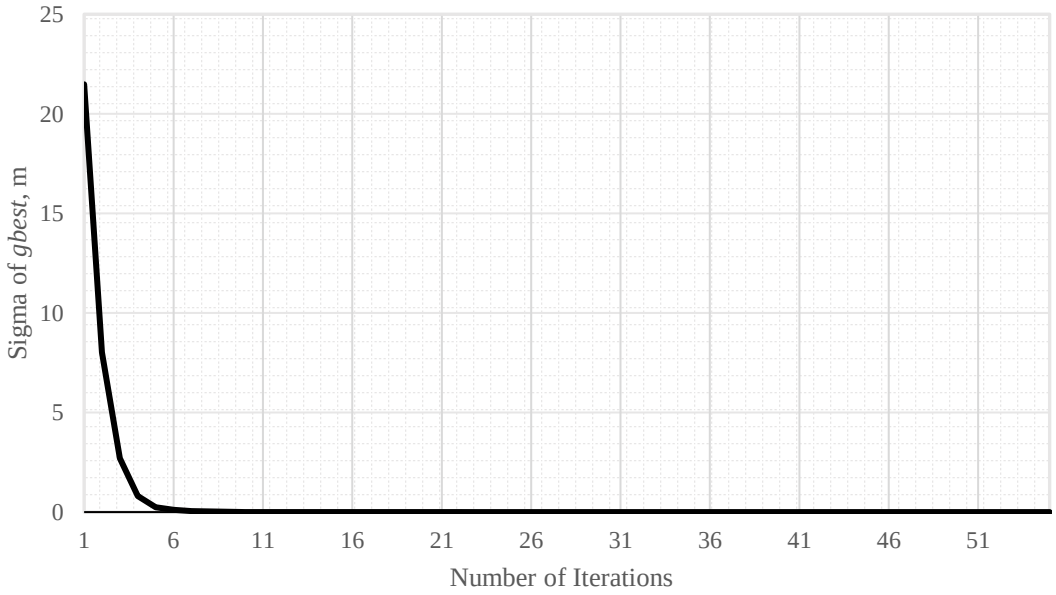

Figure 5.30. Sigma vs number of iterations in low complexity layout table A-5

Based on the convergence results in figure 5.30 and figure 5.31 a quicker exit point can be used to speed up the optimisation process. This can be set at 50 iterations. The overall solution now uses two swarming exit points; one is when sigma equal 0.001 metres the other when 50 iterations are reached. Exit occurs if either of these conditions is met. Practically, the latter condition is will be met first.

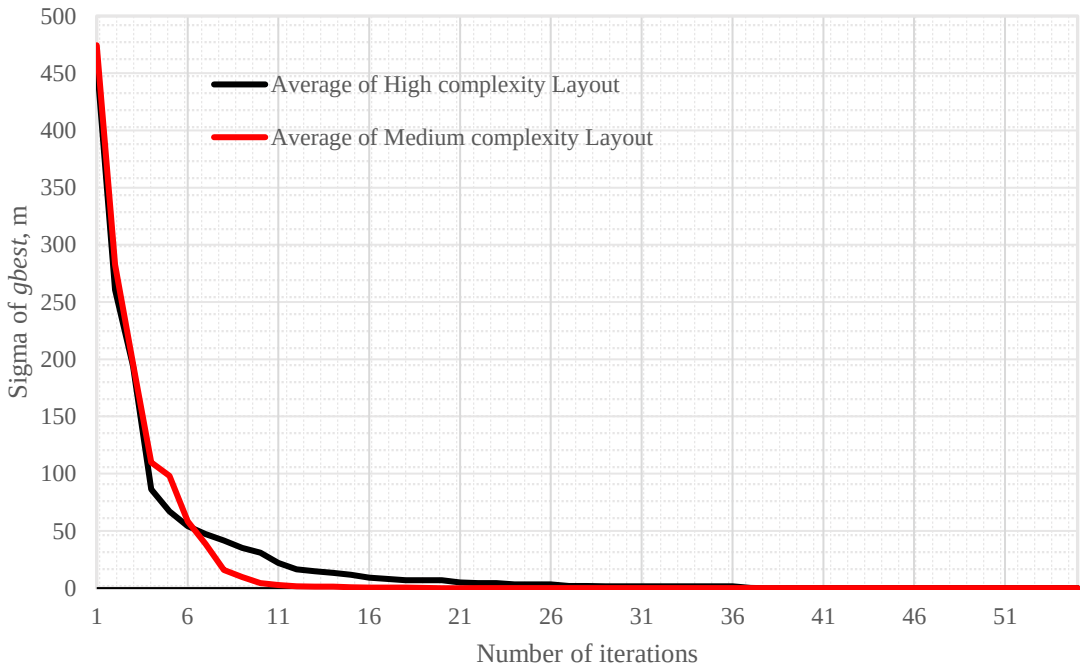

Figure 5.31. Sigma vs number of iterations in medium and high complexity layouts from table A-5

5.5.3 Power Ramping

The power ramping stage is demonstrated in the medium complexity layout and high complexity layouts. If the fitness at the final swarmed position does not meet the coverage requirement (percentage coverage) the transmitter power is increased in steps of 3 dB and the fitness recalculated. The output from the power ramping phase is shown in the medium complexity layout in table 5.6 and in the high complexity layout in table 5.7

Power (dBm)	AVG Percentage Coverage
0	37.84
3	46.56
6	55.02
9	75.93
12	98.61

Table 5.6. Power ramping in medium complexity building

In table 5.6 the percentage coverage is given at 95% with a receiver threshold of -60 dBm. After the final swarmed location, the fitness was calculated to be 37.84 %. Because this is less than the percentage coverage required the power is increased to 12 dBm where the fitness was calculated to be 98.61%. Here the coverage requirements are met and a solution is found with 1 transmitter.

Power, dBm	AVG Percentage Coverage, %
0	58.57
3	61.05
6	65.88
9	68.65
12	71.46
15	75.79
18	78.39
21	83.01

Table 5.7. Power ramping in high complexity layout

5.5.4 Geometric Partitioning

The process of partitioning is validated in the high complexity layout. After power ramping, if the maximum power is reached and the percentage coverage have not been attained then, the geometric partitioning phase is initiated. This has been described in detail in section 3.4.

The power ramping process is illustrated in table 5.7 for the high complexity layout. The power is increased from 0 dBm to 21 dBm. At 21 dBm the percentage coverage is still below the

required levels of 95%, hence the optimisation space is divided and the swarming is independently initiated in the in each partition with separate swarms. This is shown in figure 5.21 and 5.22.

5.6 Planning Using Conventional Methods

The effectiveness of the solution is compared with the normal planning methods described in [1]. The top floor (W2) of the Sir David Davies building at Loughborough University has been planned using "normal" planning methods. This will later be compared to the proposed method (implemented via the MATLAB code).

With the normal planning method, the main consideration is the "worst case" areas in the building. These receiver locations should be at the least be equal to the minimum receiver level. For the test building, the required coverage level is -85 dBm.

The Rx level at the worst-case locations (Rx_{min}) is calculated for each antenna. The Rx_{min} location is defined as the physical receiver location inside the building where the received signal strength is at a minimum. After choosing the initial transmitter locations, the first estimation for finding Rx_{min} locations is by examining the building layout drawings and identifying the receiver locations where the distance to the transmitter is the greatest and the number of traversing walls is the greatest. It may be found that more than one single location exists, all these locations must be considered. The receive signal level is calculated using the following equation:

$$L_{total} = L_0 + 20log_{10}d + \sum k_i Lw_i \tag{5.5}$$

Where: L_{total} is the total path loss from the transmitter to receiver, dB; L_0 is the loss at 1m given as 31.5 dB at 900 MHz; d = transmitter-receiver distance, m; k_i= the number of types i separating walls; Lw_i= the penetration loss in type i walls, dB.

The received signal strength any point is given as follows:

$$RxLev = P_{Tx} - L_{total} \tag{5.6}$$

Where: *RxLev* = received signal strength, dBm; P_{Tx}= total transmitted power, dBm,
The transmitters are moved around or more transmitters added to the optimisation space until the all estimated Rx_{min} at is greater than the $RxLev_{min}$.

5.6.1 Worst Case Locations (Conventional Planning)

The manual method has no means of calculating percentage coverage during the initial antenna location phase (nominal planning phase), instead, the worst-case locations are analysed. Four Transmitters are chosen and placed in the locations shown in figure 5.32. Table 5.8 list the actual positions (*x*-*y* coordinates) based on the references system used in the MATLAB program. Table 5.9 list the worst-case locations and the contributing antennas. The P_{Tx} of each antenna is 0 dBm and worst-case points are at A, B, C, D, E and F. The received levels at each worst-case location are calculated as below:

At point A: The maximum Rx levels will be due to antenna 1. d = 17.5 m, k = 8, L_w= 5 dB

$Rx_{min} = P_{Tx} - (L_0 + 20log_{10}d + k_w L_w)$

Rx_{min} = 0 - (31.5 + 20log(17.5) + 8 x 5)

Rx_{min} = - 96.36 dBm

At point B: Maximum Rx level will be due to antenna 2. d = 12.5 m, k = 6, L_w= 5 dB.

$Rx_{min} = P_{Tx} - (L_0 + 20log_{10}d + k_w L_w)$

Rx_{min} = 0 – (31.5 +20log(12.5) + 6 x 5)

Rx_{min} = - 83.44 dBm

At point C: Maximum Rx level will be due to antenna 3. d = 23.75 m, k = 5, L_w= 5 dB.

$Rx_{min} = P_{Tx} - (L_0 + 20log_{10}d + k_w L_w)$

Rx_{min} = 0- (31.5 + 20log(23.52) + 5 x 5)

Rx_{min} = - 84.04 dBm

At point D: Maximm Rx level will be due to antenna 3. d = 23 m, k = 7, L_w= 5 dB.

$Rx_{min} = P_{Tx} - (L_0 + 20log_{10}d + k_w L_w)$

Rx_{min} = 0 – (31.5 + 20log(23) + 7 x 5)

Rx_{min} = - 93.74 d Bm

At point E: Maximum Rx level will be due to antenna 4. d = 20 m, k = 6, L_w= 5 dB.

$Rx_{min} = P_{Tx} - (L_0 + 20log_{10}d + k_w L_w)$

Rx_{min} = 3 – (31.5 + 20log(20) + 6 x 5)

Rxmin = - 84 dBm

At point F: Maximum Rx level will be due to antenna 4. d = 15 m, k = 4, L_w= 5 dB.

$Rx_{min} = P_{Tx} - (L_0 + 20log_{10}d + k_w L_w)$

Rx_{min} = 0 – (31.5 + 20log(15) + 4 x 5)

Rx_{min} = - 82.02 dBm

Transmitter Location	Position *x*, (m)	Position *y*, (m)	Transmit Power. dBm
1	62.80	132.4	0
2	17.29	132.4	0
3	46.53	96.11	0
4	70.31	33.02	3

Table 5.8. Manual planning transmitter locations and transmit power

Receiver Location	Position *x*, (m)	Position *y*, (m)	Estimated Receiver Power. dBm	Contributing Transmitter
A	95.05	141.6	-96.36	1
B	34.52	141.6	-83.44	2
C	9.34	87.33	-84.04	3
D	58.40	87.33	-93.74	3
E	68.78	68.12	-84.00	4
F	74.29	11.82	-85.02	4

Table 5.9 Worst case receiver locations and the contributing antennas

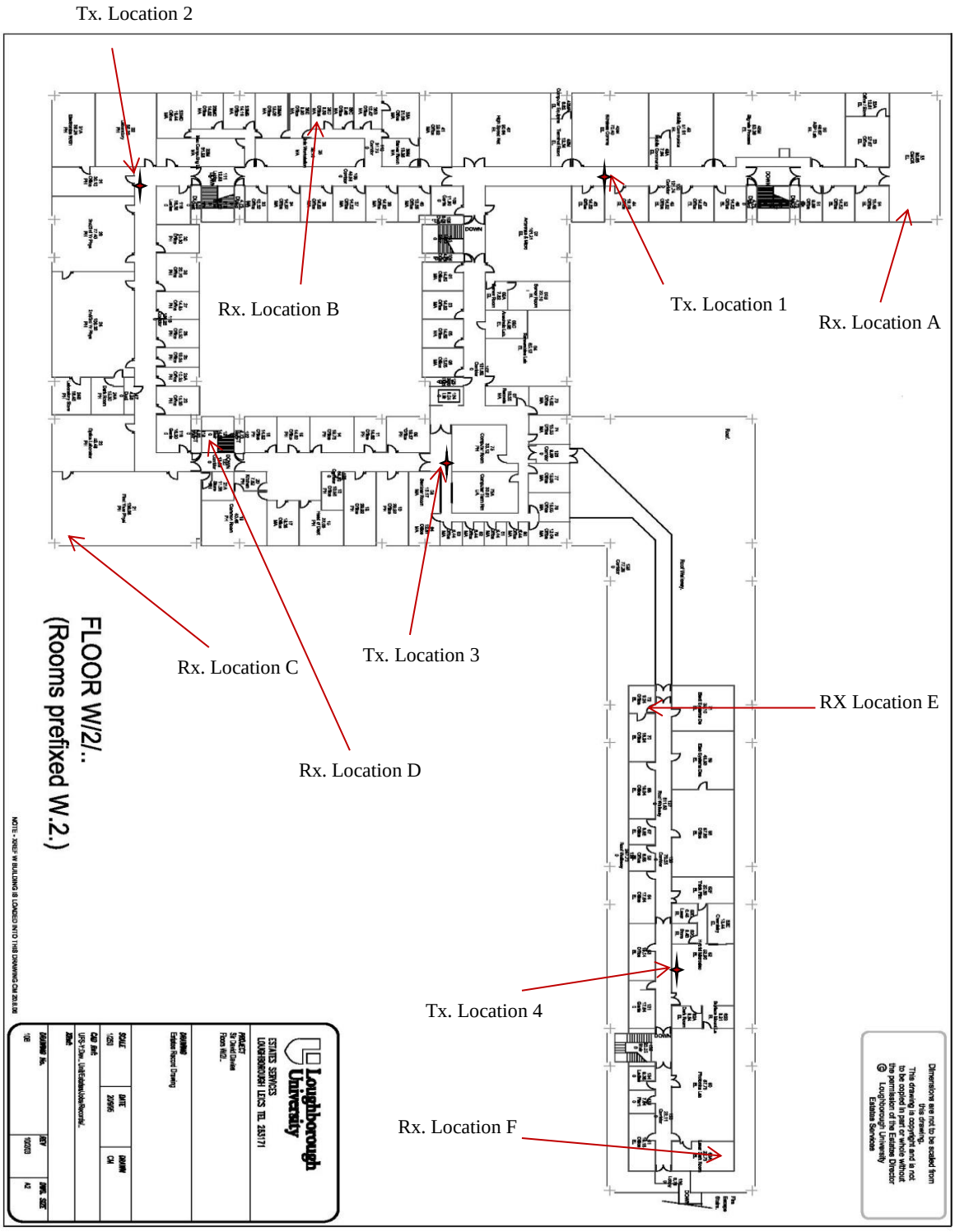

Figure 5.32. Building layout showing transmitter and receiver locations.

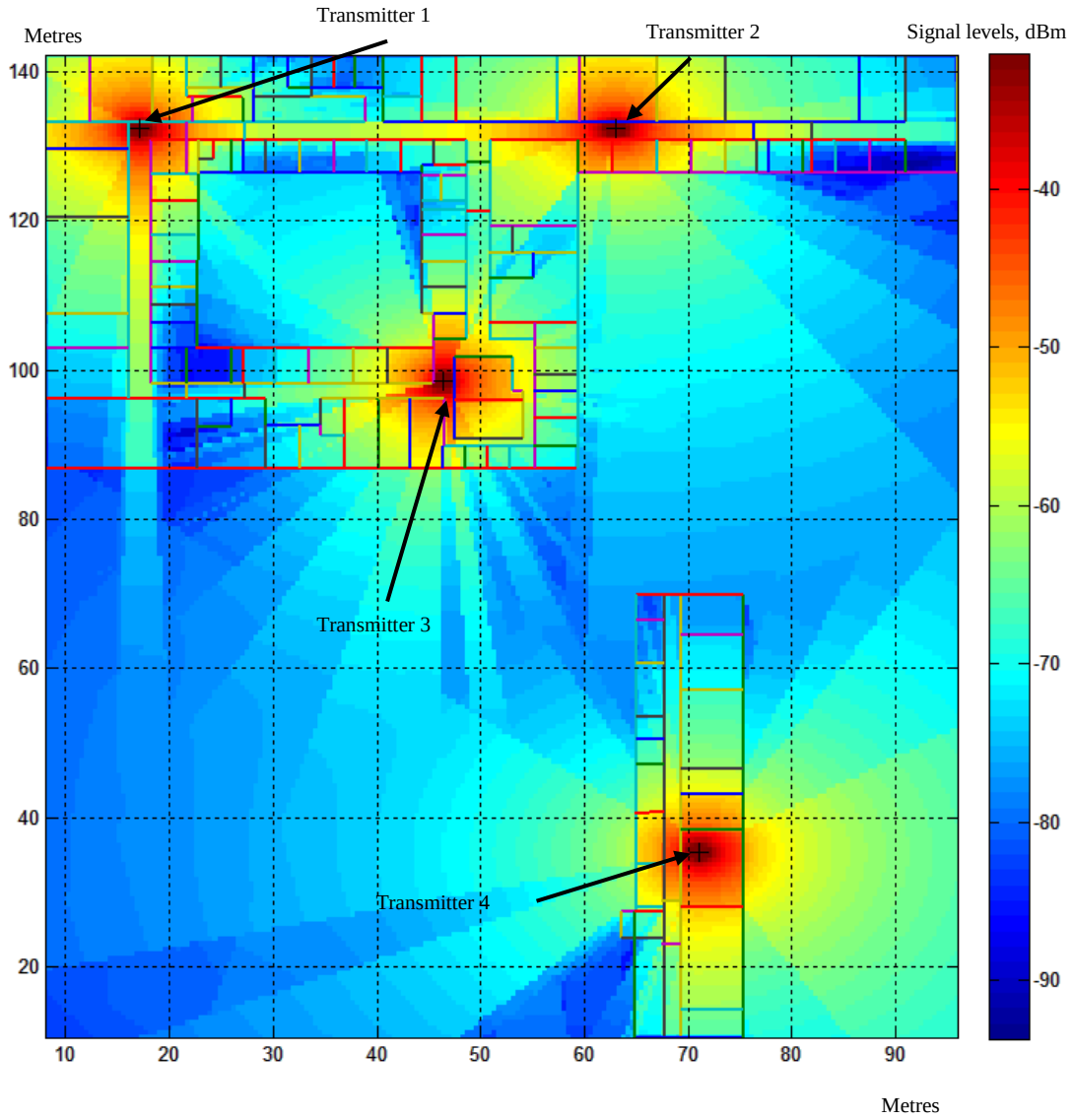

Figure 5.33. Building layout showing transmitter and receiver locations.

Figure 5.33 show the receive signal levels with the transmitters at the locations chosen via the manual methods. This plot is obtained using the MATLAB simulation.

5.7 Planning with Proposed System

The proposed solution is now applied in the test building (the top floor (W2) of the Sir David Davies building at Loughborough University) with the parameters listed in table 5.5. Additionally, the number of swarming iterations was set to 50. The final solution produced three transmitters at the locations indicated in figure 5.34 along with a display of the received

signal levels throughout the building. Table 5.10 shows the final transmitter positions and the out power.

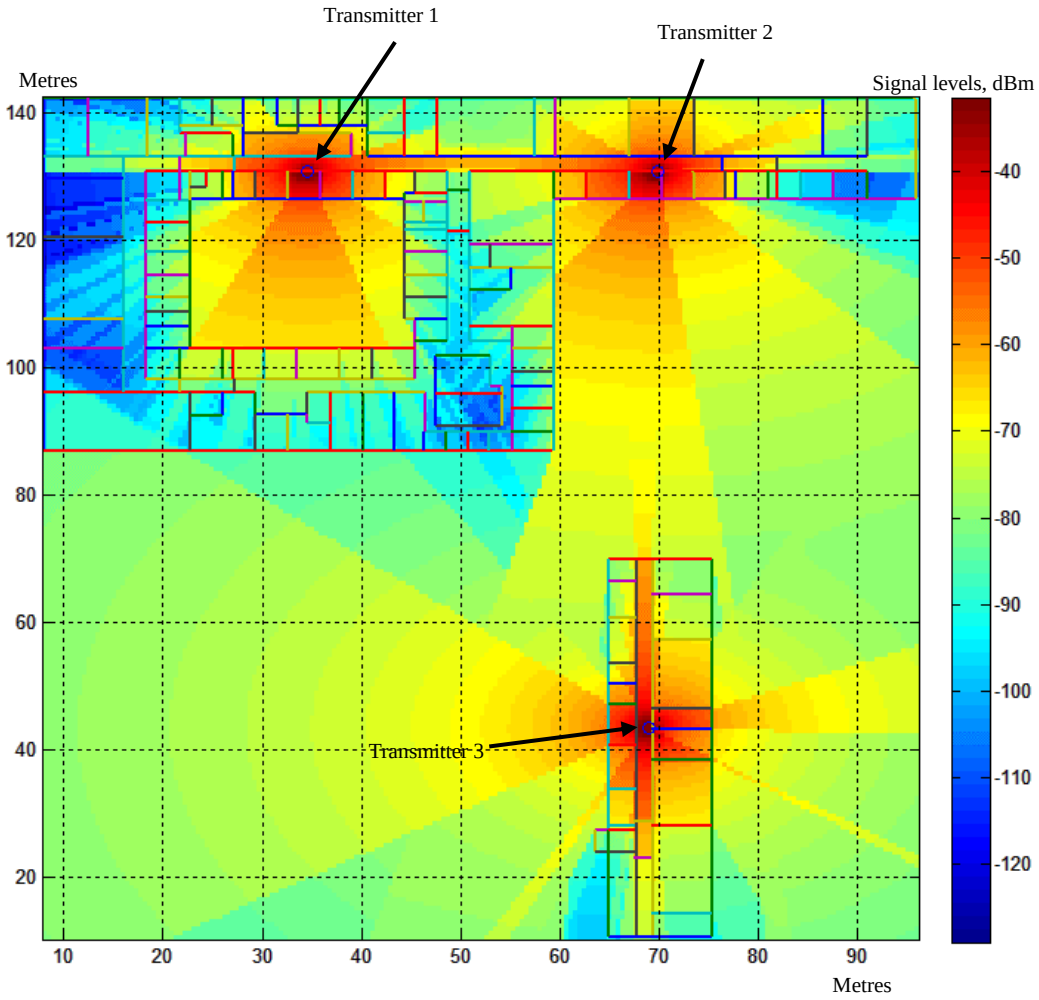

Figure 5.34. Simulation results using the developed MATLAB code

Transmitter	Position *x*, (m)	Position *y*, (m)	Transmit Power, dBm
1	34.52	130.8	12
2	69.82	130.83	12
3	69.01	43.37	12

Table 5.10. Final transmitter positions and out power based on MATLAB program

5.7.1 Worst Case Locations (Proposed System)

In the conventional planning system described in section 5.6, the transmitter placement is structured around the worst-case locations. In the proposed system, the worst-case location is automatically calculated and is the composite coverage of the entire transmitter system. This was found to be (8.06, 142.3) with a signal level of -128.05 dBm.

5.8 Comparing Both Systems

The outputs of both methods are similar. The conventional planning methods results in 4 transmitters with power output between 0 dBm and 3 dBm while the results from the proposed systems are 3 transmitters with higher transmitter power. The choice of best results is dependent on the building layout. Generally, the aim is to produce the smallest numbers of transmitters as possible as the cost for installations would be greater than increasing base station transmit power. For this reason, the solution proposed by the PSO system is more practical.

The proposed method also provides the ability to estimate the percentage coverage and shows how this will be affected by a change in transmit power. Via the traditional planning method, the coverage percentage can only be estimated via a walk test after the initial transmitter locations have been selected. This makes the proposed system more flexible and can be more cost effective.

5.9 Measurements

The aim of the measurements campaign is the following:

1. Verify the transmit locations specified by the MATLAB simulation gives expected coverage.
2. Evaluate the accuracy of the propagation model used in the simulation
3. Improve the estimation of the wall attenuation losses.

5.9.1 Measurement Setup

The block diagram of the setup is shown in figure 5.35. It consists of a transmitter and receiver system. The transmitter system is a Spectrum Analyser with tracking Generator set to single frequency mode on 880 MHz connected to a Bi-conical Antenna (VUBA-9117). The antenna

specifications are included in Appendix B. The spectrum analyser is used to generate a signal at 880 MHz and transmit it via the bi-conical antenna. A similar setup is implemented for the receiver system with the receiver antenna gain of 3 dBi. Figure 5.36 shows photographs of the measurement setup. Table 5.11 shows the general transmit specification for the measurement setup.

	Frequency(MHz)	**Antenna Gain (dBi)**	**Power (dBm)**	**EIRP (dB)**
Transmitter	880	-3	-10	-13

Table 5.11. Transmitter specifications

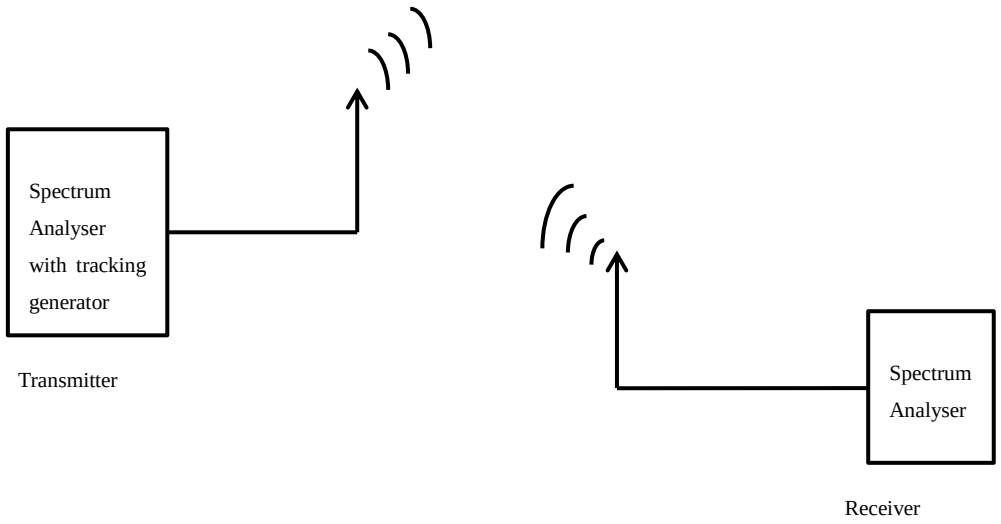

Figure 5.35. Measurement setup

5.9.2 Measurement Procedure.

The transmitter is placed at the Tx location 2 as indicated in figure 5.37. The receiver is then used to measure the receive levels at specified test locations. The complete set of measurement locations are outlined in figure 5.37

Figure 5.36. Photographs of receiver system placed at different locations throughout the building.

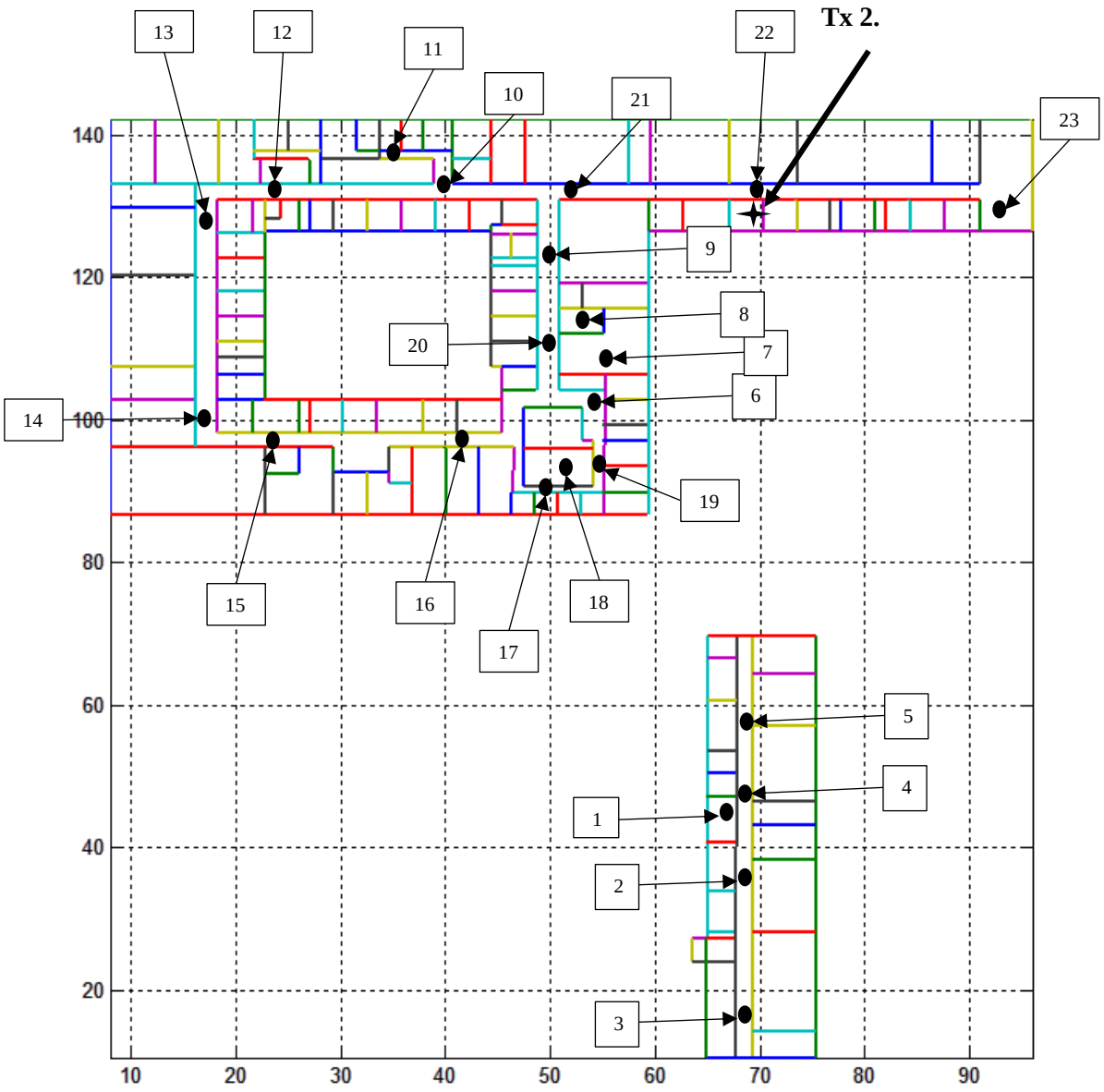

Figure 5.37. Measurement locations.

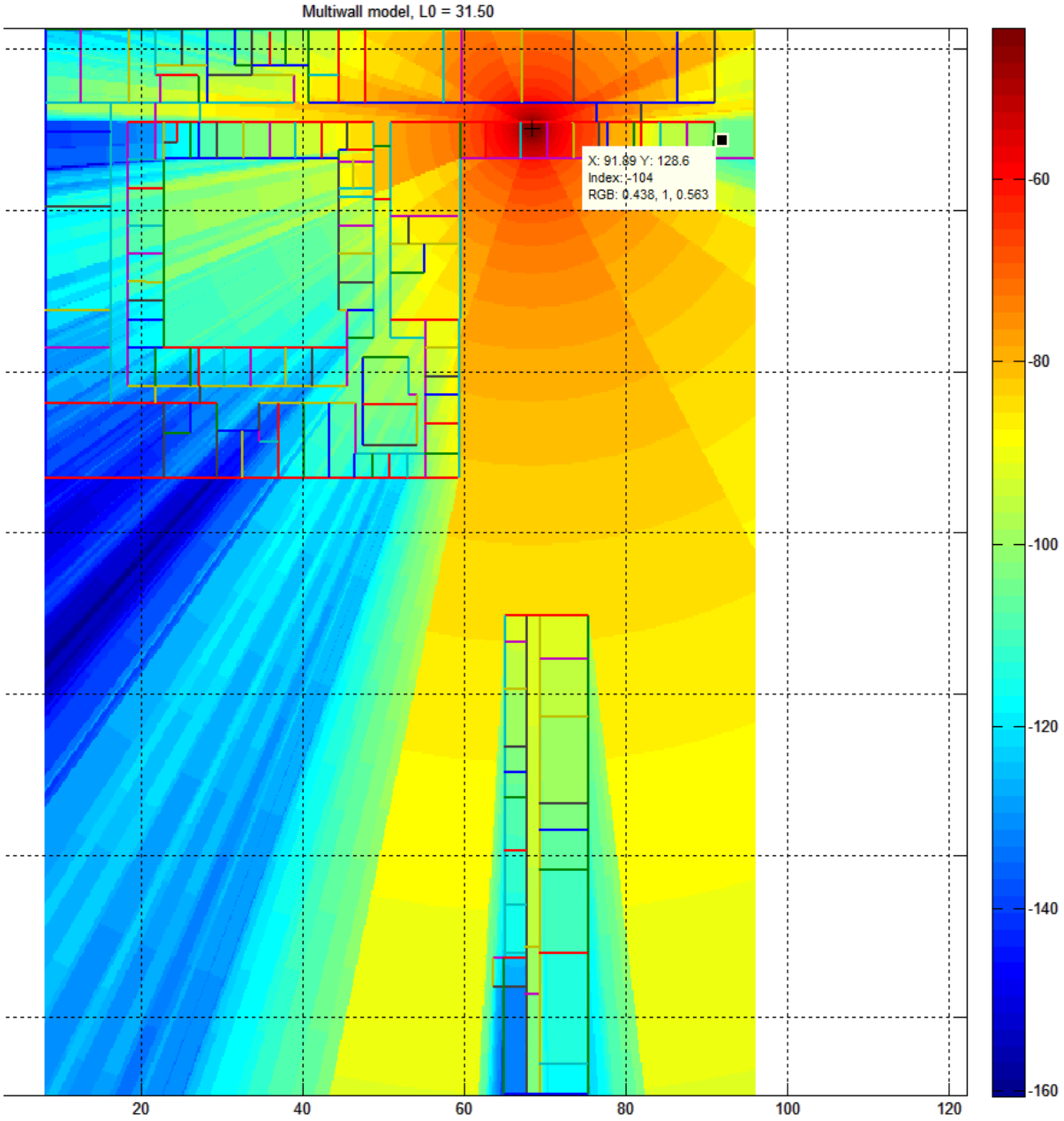

Figure 5.38. Receive level Simulation from Tx2.

5.9.3 Measurement Results

Figure 5.38 shows the simulation levels with a transmitter at transmitter location 2 with the transmitter EIRP indicated in table 5.11. This simulation is done using elements of the proposed system. Table 5.12 and figure 5.39 show the Rx level measured and simulated at these locations.

Generally, there is a good agreement between measured and simulated received levels, this indicates the propagation model was providing acceptable results. The mean error was 0.66 dB and the greatest error was 17 dB. The greatest errors occur at locations 13, 14 and 15. At these locations the measured values are at the noise floor and simulated are way below the noise floor. Here it is difficult to resolve the transmitted signal compared to the noise levels and the measurement becomes limited by the noise levels.

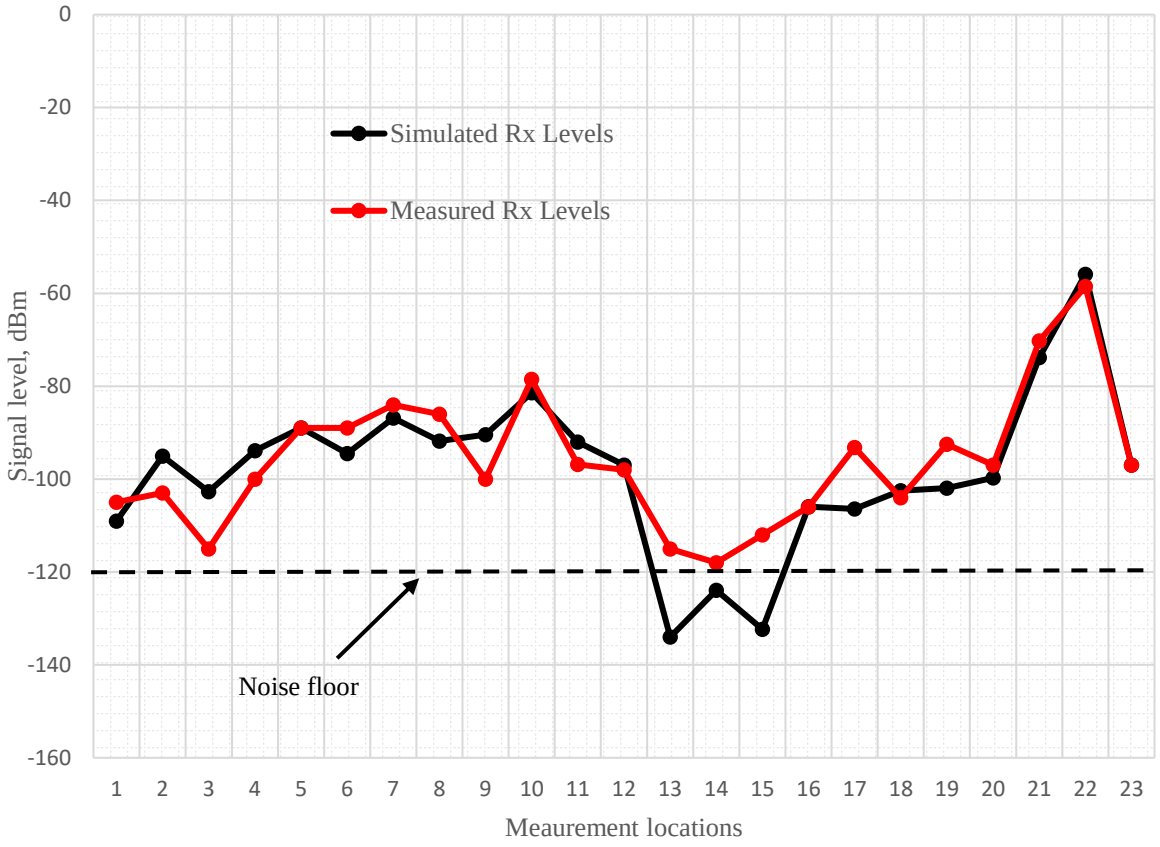

Figure 5.39. Plot of measured and simulated

Rx location	Measured Rx Level(dBm)	Simulated (dBm)	Error (dB)
1	-105	-107	2
2	-103	-93.16	-9.84
3	-115	-100.7	-14.3
4	-100	-91.8	-8.2
5	-89	-89	0
6	-89	-89.27	0.27
7	-84	-85.11	1.11
8	-86	-89.75	3.75
9	-100	-89.06	-10.94
10	-78.5	-79.8	1.3
11	-96.8	-96.35	-0.45
12	-98	-89.66	-8.34
13	-115	-132.8	17.8
14	-118	-122	4
15	-112	-127.3	15.3
16	-106	-116	10
17	-93.2	-101.5	8.3
18	-104	-103.9	-0.1
19	-92.5	-97.2	4.7
20	-97	-97.45	0.45
21	-70.2	-72.38	2.18
22	-58.5	-54.62	-3.88
23	-97	-97	0

Table 5.12. Measurement results

5.10 Re-calculating Wall losses

Table 4.1 shows the estimated values for wall losses. This was estimated from the measurements taken at location 5 and location 23. These locations were carefully pre-selected to estimate the wall losses due to the different types of walls found in the building construction. At location 5 there are only external walls (type 2) between transmitter and receiver while there are only internal walls (type 1) between transmitter and receiver at location 23. At these

locations, there is a direct ray path (perpendicular to the walls) between transmitter and receiver. These transmit-receive areas in the building provides a means of approximating the non-free space losses between transmitter and receiver. These losses are mainly due the intercepting walls as the Motley-Keenan model disregards the effects of multipath and other signal interferences and considers the direct ray only. Given the transmit power, the measured receiver signal and the distance between transmitter and receiver at these locations, the path loss equation (equation 2.19) can be re-arranged to calculate the average wall losses. Given as:

$$\sum k_i Lw_i = Rx_{lev} - P_{Tx} + 31.5 - 20\log_{10} d \tag{5.7}$$

5.11 Blind Test on Real Building

Figure 5.40 shows the layout of the Xerox office in Montego Bay, Jamaica. The in-building systems for this building have been designed by a local in-building design company, Aramos Telecommunications and Engineering Consultants (Aratel). With no prior knowledge of the actual inbuilding plan (implemented by Aratel), the proposed system is used to design the antenna plan for this building.

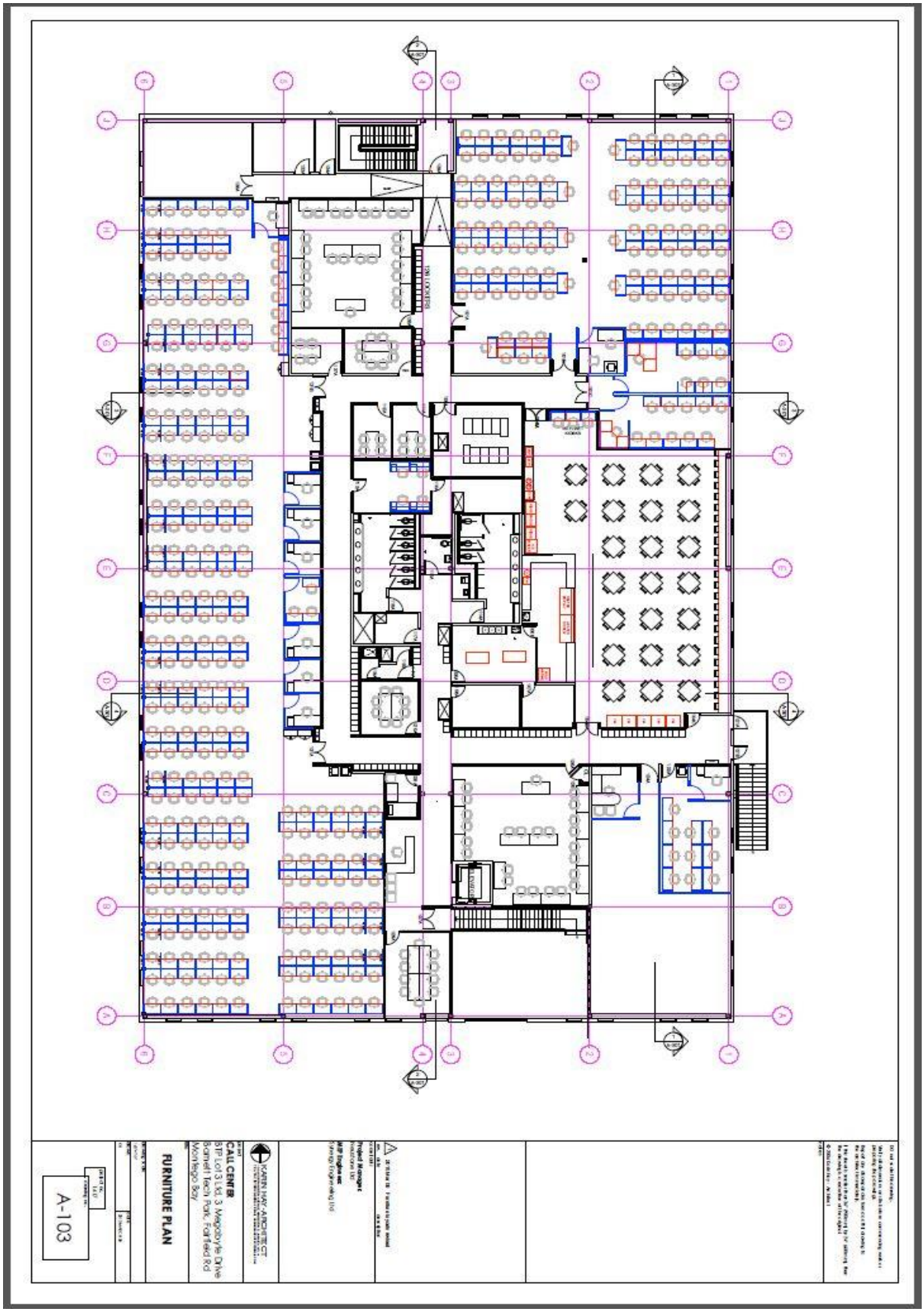

Figure 5.40. Xerox office building in Montego Bay, Jamaica

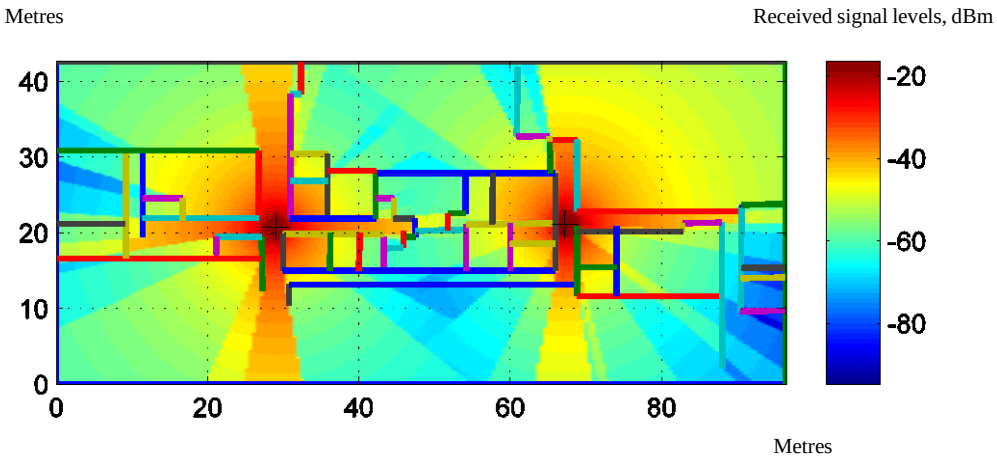

Figure 5.41. Xerox office building in Montego Bay, Jamaica

Figure 5.41 shows the layout when imported into the MATLAB program. The existing antenna locations are also shown along with the simulated receiver coverage (via the MATLAB program) at with these antenna locations.

The proposed planning method is then used to plan the antenna locations with the parameters in table 5.5. Figure 5.42 shows the initial random placement of the swarm.

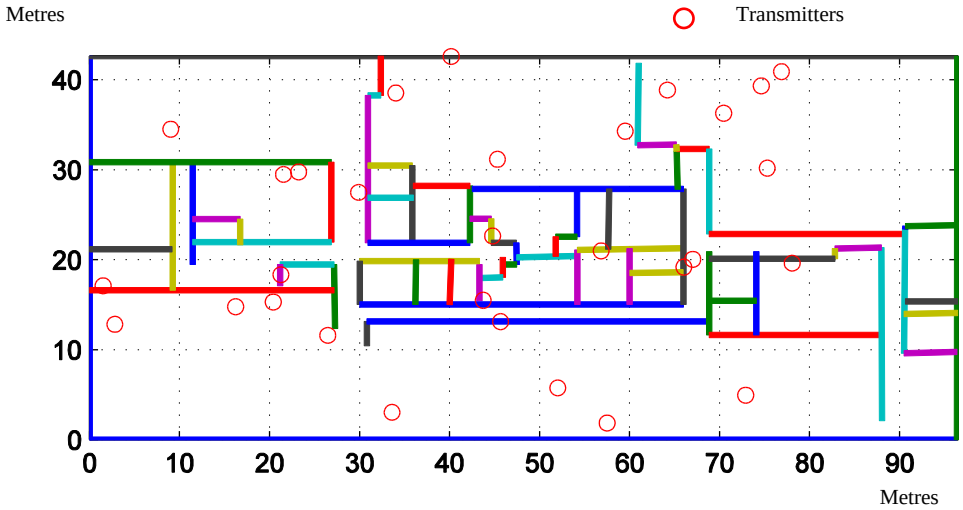

Figure 5.42. Initial swarm position, Xerox office building in Montego Bay, Jamaica

Figure 5.43 illustrates the initial swarming after 5 iterations. At the final swarmed location (figure 5.44), with the transmitter at maximum power the coverage requirements are not

reached hence the geometric partitioning is initiated with the random initial swarmed positions shown in figure 5.45.

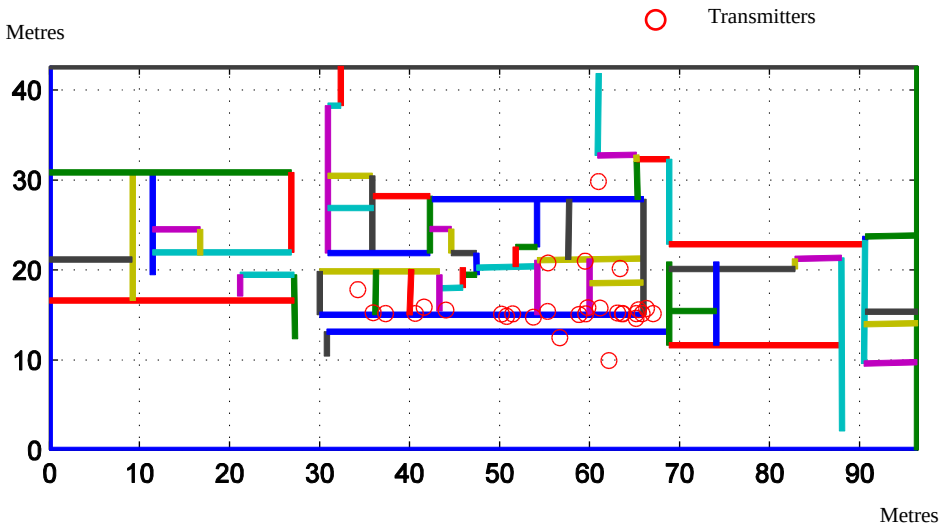

Figure 5.43. Swarming after 5 iterations, Xerox office building in Montego Bay, Jamaica

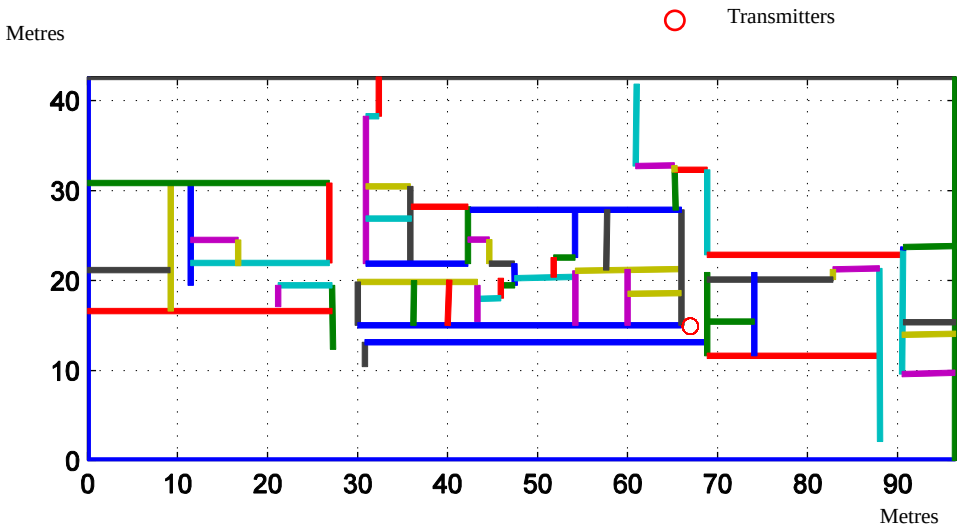

Figure 5.44. Final initial swarmed location, Xerox office building in Montego Bay, Jamaica

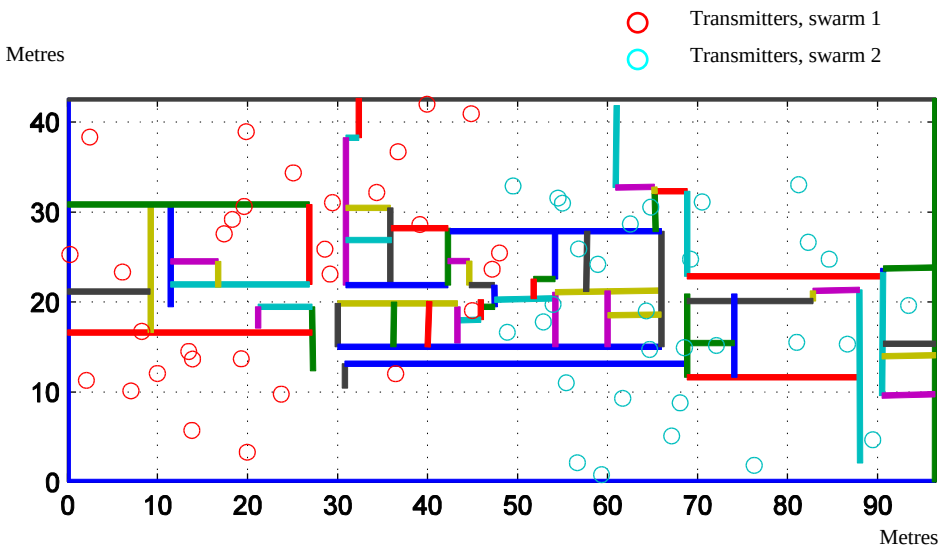

Figure 5.45. Initial random locations after geometric partitioning, Xerox office building in Montego Bay, Jamaica

Figure 5.46 show the swarming process after the swarm splitting and the final solution is displayed in figure 5.47 along with the receiver level plots.

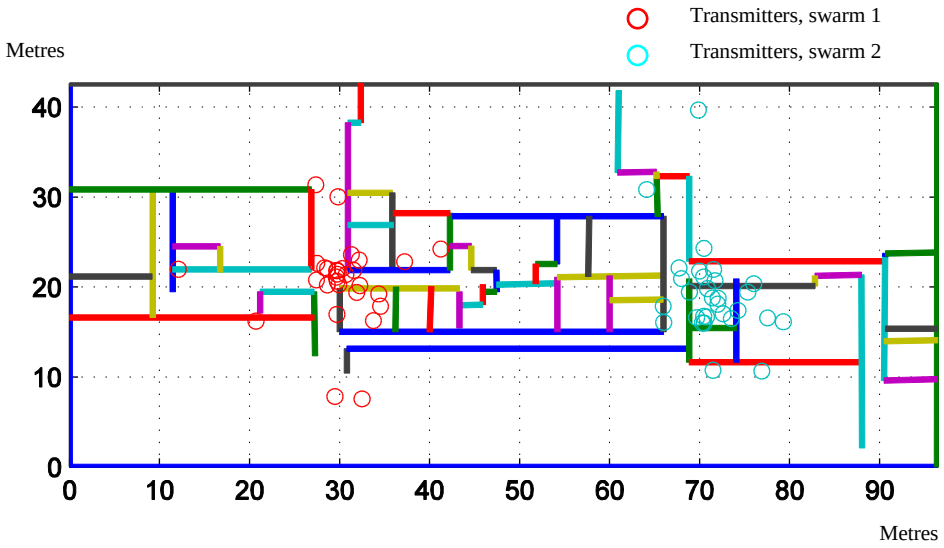

Figure 5.46. Swarming (5 iterations) after partitioning, Xerox office building in Montego Bay, Jamaica

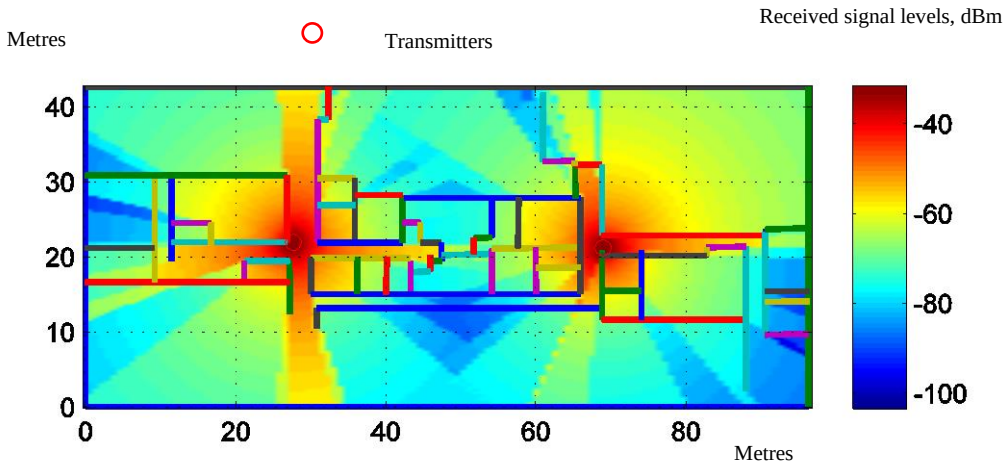

Figure 5.47. Final solution Xerox office building in Montego Bay, Jamaica

The solution via the proposed system is compared with Aratel solution. Table 5.13 shows the general solutions and table 5.14 shows the solutions for the antennas. Both solutions are similar, with the same number of antennas and very similar antenna locations. The EiRP was calculated to be 0 dBm, whereas the existing EiRP was 15 dBm. Aratel has noted the difference and indicated that their analysis also indicates that the power output of the system can be reduced.

	Aratel Planning	**Proposed System**
Percentage Coverage (%)	100% (estimated)	96.73
Number of Transmitters	2	2
Minimum Coverage (dBm)	-93.6	-103.88
Location of Minimum Coverage *(x, y)*	98, 9	96.5, 6.81

Table 5.13. Design comparison for Xerox building, Montego Bay, Jamaica

	Aratel Planning		**Proposed system**	
	Location *(x,y)*	**EiRP, dBm**	**Location *(x,y)***	**EiRP, dBm**
Antenna 1	30, 21	15	27.70, 21.95	0
Antenna 2	65, 21	15	69.00, 21.21	0

Table 5.14. Antenna solution, Xerox building, Montego Bay, Jamaica

5.12 Conclusion

The main goal of this research was to devise a system to automatically plan an in-building an antenna system. This system should be similar to the conventional planning method discussed in [1]. In section 5.6 and 5.7 the output of the manual system and the proposed system is presented. It can be seen, that the output of both systems is very similar. The conventional planning methods result in 4 transmitters with power out between 0 dBm and 3 dBm while the results from the proposed systems are 3 transmitters with higher transmitter power.

In the "blind" design of the in-building system at the Xerox building in Montego Bay, Jamaica, the proposed system compares very well with the existing solution implemented by Aratel. It also indicated the possibility of reducing the transmit power and still meet the required coverage thresholds.

The measurement results show that the propagation model used is very effective. There is a good agreement between measured and simulated results with the differences due to receiver sensitivity. The values for the wall losses were further refined with the measurement results.

Chapter 6 : Conclusions

The aim of this research was to find a means of solving the antenna location problem within an indoor environment. This has been met via the use of Particle Swarm Optimisation. This chapter outlines the contributions of this research and suggests areas of improvements.

6.1 Contribution of this thesis

In this thesis, a solution to the antenna location problem within an indoor environment has been proposed. This solution replaces the normal in-building planning methods suggested in [1] by automating the search process. The same propagation models and receiver signal level calculations have been employed as in the normal planning methods but the method of determining the number of tranmitters, their location within the building and their output power has been automated and improved upon.

This novel approach uses Particle Swarm Optimisation combined with geometric partitioning. The PSO algorithm uses swarm intelligence to determine the optimal transmitter location within the building layout. It uses an established propagation model and the PSO to determine the fitness of a location. If a transmitter placed at that optimum location, transmitting a maximum power is not enough to meet the coverage requirements of the entire layout, then the optimisation space is geometrically partitioned and the PSO initiated again independently in each partition.

This overall algorithm has been implemented via a MATLAB code and applied to the top floor (W2) of the Sir David Davies building at Loughborough University. The result is a more efficient antenna layout design when compared to the design obtained by the use of the more traditional design methods. This system also simulates and plots the receive signals levels throughout the building and gives the percentage of areas meeting the coverage threshold. Traditional planning methods [1] usually plan at 100% percent coverage with a crude estimation to find the areas not meeting the coverage threshold. With these methods, transmitters are usually setup in the initially planned transmitter locations and a walk test is usually done to collect receive signal measurements at different transmitter power. This may

then be used to estimate percentage coverage or to optimise the transmitter location and output power. This proposed method provides the flexibility to make initial design changes, such as receiver threshold levels and transmit power and then evaluate how these changes will affect the overall design layout and coverage requirements without having to perform walk tests.

6.2 Suggestions for further research

The proposed method is can be divided into two main areas, these are the propagation and the optimisation areas. Improvements to the overall process can be seen by looking at the functionality of these different areas. The following are possible ways in which the proposed method may be improved.

6.2.1 Propagation Improvements.

The measurement results in chapter 5 shows a good agreement between actual and simulated results. This indicates a good choice of propagation model, however, there are possible aspects of the signal modelling that can be improved.

Generally, the walls are considered to be solid exterior walls or interior portioned walls, this is usually acceptable for practical purposes as described in [1]. No consideration is made for the windows and doors materials. Also, there was no consideration for the cases where there are glass partitions to the exteriors. Further studies could look at incorporating each of these specific types of wall losses in the propagation model considerations for the test building to see the general effect on the final solution.

6.2.2 Optimisation Improvements

General Improvements

Within the optimisation space, there are dividing walls and no-go areas. Walls locations are not considered when finding the initial location of the transmitters as described in section 4.4.1. This means that the transmitters can have initial locations in the middle of walls. The program can be modified to ignore these locations similarly to how the avoidance of no go locations was initiated. Also in the swarming phase, the walls are treated as invisible [65], this means that the final swarmed location can be in the middle of a wall. Again, considering the walls as no-go locations will resolve this.

In the current program implementation, the overall boundaries are defined to be rectangular shaped. Depending on the building shape there may be areas within this rectangular shape that are not a part of the building layout and are therefore treated as no-go areas. These are no-go areas for the transmitters only but are considered receiver areas. These areas are currently included in the fitness and overall percentage coverage calculations. This can have a negative effect on the efficiency of the overall solution as considerations are given to these receiver areas that are not physically a part of the building layout. The algorithm can be improved to ignore these areas for both transmitters and receivers.

Geometric Partitioning

The assumed rectangular defined optimisation layout also affects the accuracy of the geometric partitioning. This implementation makes it easy to divide the optimisation space during the geometric partitioning phase but in reality the actual building may not be rectangular and hence the division may include a lot of empty space. In the test building, the second partitioning process creates a space that does not contain any of the actual building layouts. This is shown in figure 6.1 as Partition C. No particles are allowed to swarm in this area so this partition did not progress toward a better solution. This is a case where the final number of transmitters is less than the number of partitions created.

By improving how the optimisation space is defined, the general performance of the overall system can be improved. A method would be needed to define the optimisation boundaries to be close as possible to the actual building layout.

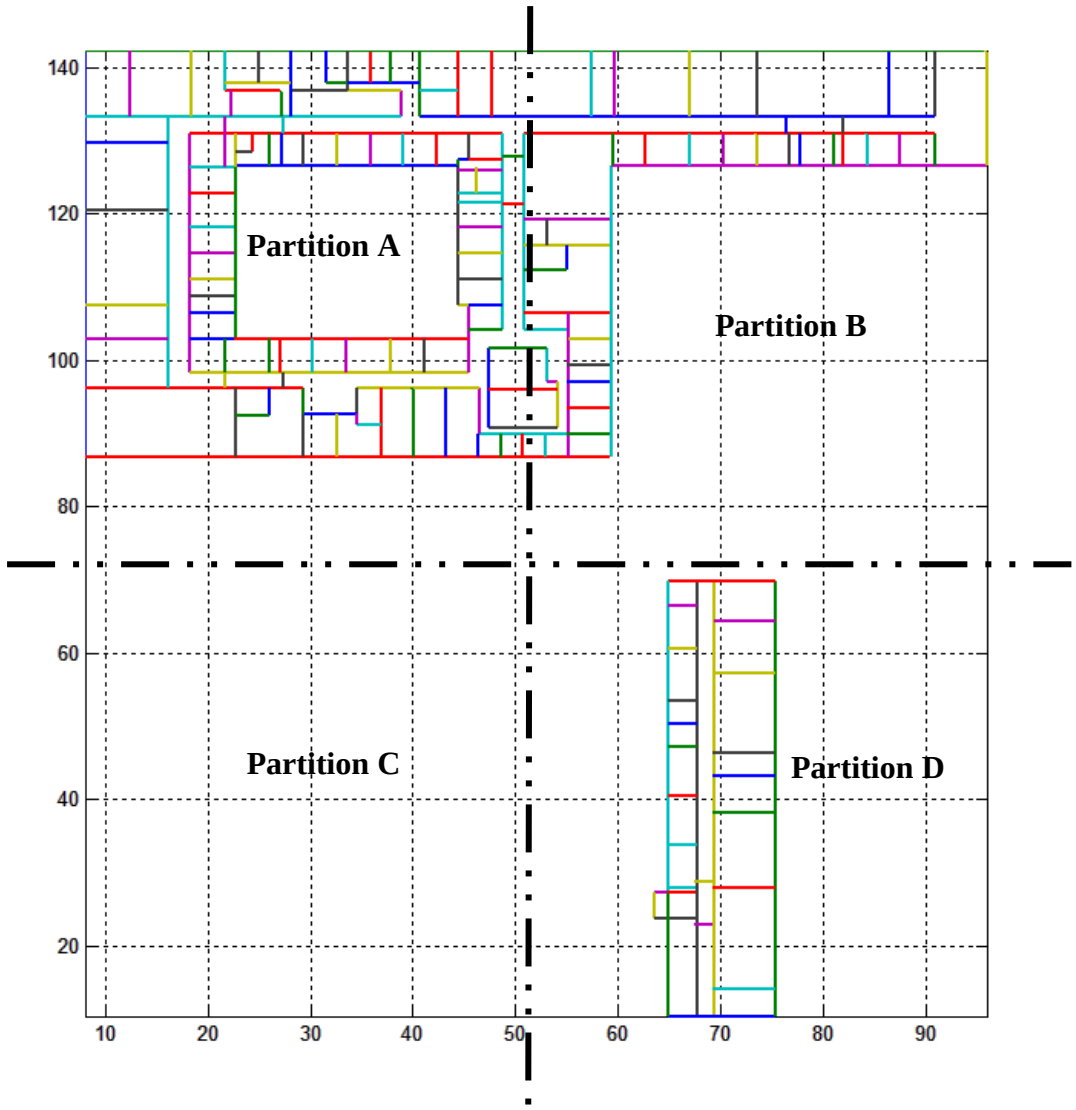

Figure 6.1. Partition that contains an empty optimisation space.

Power Ramping

After the PSO have converged, the power ramping stage will increase the power by 3dB steps from 0 dBm to 21 dBm. Currently, this power ramping involves only a power increase. Further improvement to the power optimisation phase could employ a means of also decreasing the power if the coverage requirements are met after convergence.

6.2.3 General Programming Concerns

The main focus of this research has been the optimisation method rather than its execution via MATLAB program. While the MATLAB program does the basics in implementing the optimisation strategy and output simulation, to an expert programmer its implementation may seem crude and there may be a few things that can be done to improve its efficiency.

Firstly, defining the optimisation space is a manual process which involves transcribing the layout drawing into a Cartesian coordinate system. An improvement here will see this process be done automatically where the layout drawing can be loaded and re-defined directly by the program.

There could also be further improvement in the structure and the implementation of the program. The current program flow is sequential, restructuring the program in a modular style may be more efficient. Additionally, creating the program via C++ may improve the speed of execution. Currently with a laptop employing 12G B of memory and a CPU speed of 2.6 G Hz on MATLAB version R2011a, it takes on average 7 minutes to implement the algorithm with 30 transmitters within the test building. This may be decreased with C++.

6.3 Overall Summary

The proposed in-building planning system can be a good substitute for the manual planning system described in [1]. Both systems employ the same propagation model but the proposed system produces a more efficient antenna design when employed in the same test building.

The proposed system uses Particle Swarm Optimisation combined with a method of geometrically dividing the optimisation space to find a solution to the indoor antenna placement problem. With a MATLAB code, this solution was implemented in the top floor (W2) of the Sir David Davies building at Loughborough University. The output gives the optimal number of transmitters, there optimum location and the optimum transmit power of each to ensure that the entire building is covered to a minimum signal level. Additionally, a simulation of the receiver levels throughout the building is also produced

The system also produced more efficient results when used in the “blind-test” at the Xerox building in Montego Bay, Jamaica. It proposed a reduction in the transmitter power while still maintaining the planned coverage requirements.

Chapter 7 : References

[1] Ericsson Radio Systems AB, GSM inbuilding solutions, Ericsson Radio Systems, EN/LZT 123 7136, R1C, 2002.

[2] T. K. Sarkar, Z. Ji, K. Kim, A. Medouri and M. Salazar-Palma, "A survey of various propagation models for mobile communications," *IEEE Antennas and Propagation Magazine,* vol. 45, no. 3, pp. 51-82, June 2003.

[3] R. Ezzine, A. Al-Fuqaha, R. Braham and A. Belghith, "A new generic model for signal propagation in Wi-Fi and WiMax environments," *Wireless Days,* pp. 1-5, Nov 2008.

[4] A. J. Motley and J. M. P. Keenan, "Personal communication radio coverage in buildings at 900 MHz and 1700 MHz," *Electronics Letters,* vol. 24, no. 12, pp. 763-764, June 1988.

[5] Digital mobile radio towards future generation systems,, COST 231 Final report, 1999.

[6] Ericsson Radio Systems AB, GSM cell planning principles, Ericsson Radio Systems, EN/LZT 123 3314, R4A, 2000.

[7] IBwave Solutions Inc, "http://www.ibwave.com/en/ibwave-design," iBwave Solutions Inc, [Online]. Available: http://www.ibwave.com/en/ibwave-design. [Accessed 12 March 2017].

[8] "Ran plan radio planning software," [Online]. Available: www.ranplan.co.uk. [Accessed 16 May 2011].

[9] F. J. Berenguer Ciscar and M. Montero del Pino, "A method for the automatic selection of the radiated power and location of radio transmitters in indoor environments," in *The 14th IEEE 2003 International Symposium on Personal, Indoor and Mobile Radio Communication Proceedings*, 2003.

[10] J. He, A. Verstak, L. Watson, C. Stinson, N. Ramakrishnan, C. Shafer, T. Rappaport, C. Anderson, K. Bae, J. Jiang and W. H. Tranter, "Globally optimal transmitter placement for indoor wireless communication system," *IEEE Transactions on Wireless Communications,* vol. 3, no. 6, pp. 1906-1911, November 2004.

[11] H. Sherali, C. Pendyala and T. Rappaport, "Optimal location of transmitters for micro-cellular radio communication system design," *IEEE Journal on Selected Areas in Communications,* vol. 14, no. 4, pp. 662-673, May 1996.

[12] M. H. Wright, “Optimization methods for base station placement in wireless environments,” in *48th IEEE Vehicular Technology Conference*, 1998.

[13] D. Stamatelos and A. Ephremides, “Spectral efficiency and optimal base station placement for indoor wireless networks,” *IEEE Journal on Selected Areas in Communications,* vol. 14, no. 4, pp. 651-661, May 1996.

[14] Y. Xu, M. Zhou and L. Ma, “Optimization of WLAN indoor location network based on signal coverage requirement,” in *1st International Conference on Pervasive Computing, Signal Processing and Applications*, 2010.

[15] S. Newman, *Xerox Montego Bay inbuilding plan,* Montego Bay: Aratel Limited, 2015.

[16] M. F. Iskander and Z. Yun, “Propagation prediction models for wireless communication systems,” *IEEE Transactions on Microwave Theory and Techniques,* vol. 50, no. 3, pp. 662-673, March 2002.

[17] T. T. Ha, Theory and design of digital communication systems, Cambridge: Cambridge University Press, 2011.

[18] F. E. Mahmood, Mobile radio propagation prediction for two different districts in mosul-city, 2012.

[19] J. Walfisch and H. Bertoni, “A theoretical model of UHF propagation in urban environments,” *IEEE Transactions on Antennas and Propagation,* vol. 36, no. 12, p. 1788 – 1796, 1988.

[20] C. B. Andrade and R. P. F. Hoefel, “IEEE 802.11 WLANS: A comparison of indoor coverage models,” in *23rd Canadian Conference on Electrical and Computer Engineering (CCECE)*, 2010.

[21] A. A. Tahat and Y. A. Alqudah, “Analysis of propagation models at 2.1GHz for simulation of a live 3G cellular network,” *Wireless Advanced,* pp. 164-169, 2011.

[22] M. F. Iskander and Z. Yun, “Propagation prediction models for wireless communication systems,” *IEEE Transactions On Microwave Theory And Techniques,* vol. 50, no. 3, pp. 662 - 673, 2002.

[23] R. Wahl and G. Wölfle, “Combined urban and indoor network planning using the dominant path propagation model,” in *EuCAP Proceedings on Antennas and Propagation*, 2006.

[24] Y. Okumura, E. OHMORI, T. Kawanao and Fukuda.K, “Field stength and its variability in VHS and UHF land mobile radio service,” *Rev. Elec. Comm. Lab,* vol. 16, pp. 825-73, 1968.

[25] M. Hata, “Empirical formula for propagation loss in land mobile radio services,” *IEEE Transactions on vehicular technology,* vol. 29, no. 3, pp. 317-325, 1980.

[26] S. R. Saunders, “Outdoor mobile propagation,” in *Propagation of Radio Waves,* London, The Institution of Engineering and Technology, 2003, pp. 185-219.

[27] F. Ikegami, T. Takeuchi and S. Yoshida, “Theoretical prediction of mean field strength for urban mobile radio,” *IEEE Transaction on antenna and propagation,* vol. 39, no. 3, pp. 299-302, March 1991.

[28] F. Ikegami, S. Yoshida, T. Takeuchi and M. Umehira, “Propagation factors controlling mean field strength on urban streets,” *IEEE Transactions on Antennas and Propagations,* vol. 32, no. 8, pp. 822-828, August 1984.

[29] E. O. Rozal and E. G. Pelaes, “Statistical adjustements of walfisch-ikegami model based in urban propagation measurements,” in *BMO/IEEE MTT-S International Microwave & Optoelectronics Conference*, 2007.

[30] Z. Ji, B.-H. Li, H.-X. Wang, H.-Y. Chen and T. K. Sarkar, “Efficient ray tracing methods for propagation prediction for indoor wireless communications,” *IEEE Antennas and propagation magazine,* vol. 43, no. 2, pp. 41-49, 2001.

[31] J. Roh, S. Kong, N. Im and C. Ahn, “Adaptive in-building propagation simulator using ray tracing in WCDMA networks,” in *2008 IEEE Region 10 Conference*, 2008.

[32] C. C. Constantinou, “Numerically intensive propagation prediction methods,” in *Propagation of Radio Waves*, London, UK, Institution of Electrical Engineers, 2003, pp. 179-183.

[33] A. E. Shaikh, F. Majeed, M. Zeeshan, T. Rabbani and I. Sheikh, “Efficient Implementation of deterministic 3-D ray tracing model to predict propagation losses in indoor environments,” in *The 13th IEEE International Symposium on Personal Indoor and Mobile Radio Communications*, 2002.

[34] C.-F. Yang, B.-C. Wu and C.-J. Ko, “A ray tracing method for modelling indoor wave propagation and penetration,” *IEEE Transctions on Antennas and Propagation,* vol. 46, no. 6, pp. 907-919, JUNE 1998.

[35] Y. S. Seidel and T. S. Rappaport, “Path loss prediction in multi-floored buildings at 914 MHz,” *Electronics Letters,* vol. 27, no. 15, pp. 1384-1387, July 1991.

[36] M. J. Feuerstein, K. L. Blackard, T. S. Rappaport, S. Y. Seidel and H. H. Xia, "Path loss, delay spread, and outage models as functions of antenna height for microcellular system design," *IEEE Transaction on Vehicular Technology*, vol. 43, no. 3, pp. 487-498, August 1994.

[37] "Indoor path loss," http://ftp1.digi.com/support/images/XST-AN005a-IndoorPathLoss.pdf. Accessed on 20/11/2015@11am, June 2012.

[38] T. G. Kolda, R. M. Lewis and T. Virginia, "Optimization by direct search: new perspective on some classcal and modern mehtods," *Society for Industrial and Applied Mathematics*, vol. 45, no. 3, pp. 385-342, 2003.

[39] J. Nelder and R. Mead, "A simplex method for function minimization," *The Computer Journal*, vol. 7, no. 4, pp. 303-307, 1965.

[40] D. M. Olsson and L. S. Nelson, "The nelder-mead simplex procedure for function minimization," *Technometrics*, vol. 17, no. 1, pp. 45-51, 1975.

[41] F. Aguado-Agelet, A. M. Martinez Varela, L. J. Alvarez-Vaquez, J. M. Hernando and A. Formella, "Optimization method for optimal transmitter locations in a mobile wireless system," *IEEE Transaction on Vehicular Technology*, vol. 51, no. 6, pp. 1316-1321, 2002.

[42] R. Saljo, "Masters thesis implementation of a bundle algorithm," [Online]. Available: http://www.math.chalmers.se/Math/Research/Optimization/reports/masters/Reine_exjobb.pdf. [Accessed 7 December 2015].

[43] F. Aguado Agelet, A. Martinez, J. Hernado, I. F and D. Mosteiro, "Bundle method for optimal transmitter location in indoor wireless system," *Electronics Letters*, vol. 36, no. 6, pp. 573-574, March 2000.

[44] L. Armijo, "Minimization of function having Lipchitz continuous first partial derivatives," *Pacific Journal of Mathematics*, vol. 16, no. 1, pp. 1-3, 1966.

[45] "What is genetic algorithms," [Online]. Available: http://www.doc.ic.ac.uk/~nd/surprise_96/journal/vol1/hmw/article1.html. [Accessed 13 December 2015].

[46] P. Byoung-Seong, Y. Jong-Gwan and P. Han-Kyu, "The determination of base station placement and transmit power in an inhomogeneous traffic distribution for radio network planning," in *2002 IEEE 56th Vehicular Technology Conference Proceedings*, 2002.

[47] M. A. Mangoud, "Optimization of channel capacity for indoor mimo systems using genetic algorithm," *Progress in Electromagnetics Research C,*, vol. 7, pp. 137-150, 2009.

[48] A. Abdi, J. A. Barger and M. Kaveh, “A parametric model for the distribution of the angle of arrival and the associated correlation function and power spectrum at the mobile station,” *IEEE Transaction on Vehicular Technology* , vol. 51, no. 3, pp. 425-434, May 2002.

[49] L. Jacobson, “Simulated annealing for beginers,” 11 April 2013. [Online]. Available: http://www.theprojectspot.com/tutorial-post/simulated-annealing-algorithm-for-beginners/6. [Accessed 10 January 2016].

[50] S. Luke, “Essentials of metaheuristics,” Lulu, 2009. [Online]. Available: http://cs.gmu.edu/~sean/book/metaheuristics/. [Accessed 9 December 2015].

[51] S. H. Chargas, J. B. Martins and L. L. de Oliveira, “Genetic algorithms and simulated annealing optimisation methods in wireless sensors neywork localization using artificial neural networks,” in *IEEE 55th International Midwest Symposium on Circuits and Systems (MWSCAS), 2012* , Boise, ID, 2012.

[52] A. Prugel-Bennett, “When a genetic algorithm outperforms hill-climbing,” *Theoretical Computer Science,* vol. 320, no. 1, pp. 135-153, 2004.

[53] L. Graham, J. Borbone and G. Parker, “Comparison of a greedy selection operator to tournament selection and hill-climber,” in *IEEE Congress on Evolutionary Computation (CEC), 2011* , New Orleans, 2011.

[54] R. Atawia, M. Ashour, T. El Shabrawy and H. Hammad, “Optimized transmitted antenna power indoor planning using distributed antenna systems,” in *Wireless Communications and Mobile Computing Conference*, 2013.

[55] I. Kocsis, L. Farkas and L. Nagy, “3G base station positioning using simulated annealing,” in *The 13th IEEE International Symposium on Personal, Indoor and Mobile Radio Communications, 2002.* , 2002.

[56] J. Kennedy and R. Eberhart, “Particle swarm optimization,” in *Proceeding of the 1995 IEEE Intrnational Conference on Neural Networks*, 1995.

[57] Y. Zhang, S. Wang and G. Ji, “A comprehensive survey of particle swarm optimisation algorithm and its applications,” *Matematical Problems in Engineering,* vol. 2015, pp. 1-38, 2015.

[58] J. Robinson and Y. Rahmat-Samii, “Particle swarm optimisation in electromagnetics,” *IEEE Tranctions on Antennas and Propagation* , vol. 52, no. 2, pp. 397-407, February 2004.

[59] C. Chien-Hung, H. Min-Hui, C. Chien-Ching and L. Shu-Han, "PSO and APSO evolutionary computing in indoor wireless communication," in *Sixth International Conference on Genetic and Evolutionary Computing,* 2012.

[60] I. Vilovic, B. Niksa and I. Cendo, "Optimal location of transmitter for indoor wireless communications," in *53rd International Symposium ELMAR-2011,* Zadar, September 2011.

[61] R. C. Eberhart and Y. Shi, "Particle swarm optimisation: developments, applications and resources," in *Proceedings Congress on Evolutionary Computation 2001* , Seoul, 2001.

[62] A. Ratnaweera, S. Halgamuge and H. Watson, "Self-organizing hierarchical particle swarm optimizer with time-varying acceleration coefficients," *IEEE Transactions on Evolutionary Computation,* vol. 8, no. 3, pp. 240 - 255, 2004.

[63] M. Jiang, Y. Luo and S. Yang, "Stochastic convergence analysis and parameter selection of the standard particle swarm optimization algorithm," *Information Processing Letters,* vol. 102, no. 1, pp. 8-16, 2007.

[64] I. M. Yassin, M. N. Taib, R. Adnan, M. K. M. Salleh and M. K. Hamzah, "Effect of swarm size parameter on binary particle swarm optimisation-based NARX structure selection," in *2012 IEEE Symposium on Industrial Electronics and Applications (ISIEA2012),* Bandung, Indonesia, 2012.

[65] C. Jen-Shiun, H. Wei-Ming, C. Yu-Kai and L. Shu-Han, "PSO and APSO for optimal antenna locations in indoor environment," in *International Conference on Intelligent Green Building and Smart Grid (IGBSG), 2014* , 2014.

[66] M. Talau, E. C. G. Wille and H. S. Lopes, "Solving the base station placement problem by means of swarm intelligence," in *IEEE Symposium on Computational Intelligence for Communication Systems and Networks (CIComms),* 2013.

[67] Z. Talepour, S. Tavakoli and J. Ahmadi-Shokouh, "Transmitter antenna placement in indoor environments using particle swarm optimisation," *International Journal of Electronics,* vol. 100, no. 7, pp. 999-1009 , 2013.

[68] S. Grubisic, W. Carpes(Jr), J. Bastos and G. Santos, "Association of a PSO optimizer with a quasi-3D ray tracing propagation model for mono and multi-criterion antenna positioning in indoor environments," *IEEE Tranctions on Magnetics,* vol. 49, no. 5, pp. 1645-1648, 2013.

[69] R. Hassan, C. Babak, d. W. Oliver and V. Gerhard, "A comparison of particle swarm optimization and genetic algorithm," in *46th AIAA/ASME/ASCE/AHS/ASC Structures, Structural Dynamics & Materials Conference,* Austin, Texas, 2005.

[70] S. Ethni, B. Zahawi, D. Giaouris and P. Acarnley, "Comparison of particles warm and simulated annealing algorithms for induction motor fault identification," in *7th IEEE International Conference on Industrial Informatics,* 2009.

[71] C. Chien-Ching, Y.-T. Cheng and C.-W. Chang, "Comparison of article swarm optimization and genetic algorithm for path loss reduction in an urban area," *Journal of Applied Science and Engineering,* vol. 15, no. 4, pp. 371-380, 2012.

[72] T. Kong, D. M. Mount and M. Werman, "The decomposition of a square into rectangle of minimal perimeter," *Discreter Applied Mathematics,* vol. 16, no. 3, pp. 239-243, 1987.

[73] D. J. Kleitman, "Partitioning a recatangle into small perimeter rectangles," *Discrete Mathematics,* vol. 103, no. 2, pp. 111-119, 1992.

[74] Y. C. Lu, J. C. Jan, S. L. Hung and G. H. Hung, "Enhancing particle swarm optimization algorithm using two new strategies for optimizing design of truss structures," *Engineering Optimization,,* vol. 45, no. 10, pp. 1251-1271, 2012.

[75] S. Fedorov, "GetData graph digitizer, Version 2.25.0.2 [Software]," htttp://getdata-graph-digitizer.com, 2002-2012.

[76] D. De Luca, F. Mazzenga, C. Monti and M. Vari, "Performance evaluation of indoor localization techniques based on RF power measurements from active or passive devices," *EURASIP Journal on Applied Signal Processing,* vol. 2006, pp. 1-11, 2006.

[77] S. Paris, "Compute -2D multiwall model," 2008. [Online]. Available: https://uk.mathworks.com/matlabcentral/fileexchange/20209-2d-multiwall-model. [Accessed 24th September 2011].

[78] M. Gavrilova and J. Rokne, "Reliable line segment intersection testing," *Computer-Aided Design,* vol. 32, no. 12, pp. 737-745, 2000.

[79] Y. Zhu, J. Yong and Z. G.Q, "Line segment intersection testing," *Computing,* vol. 75, pp. 337-357, 2005.

[80] S. Walton, "Finding the intersection point of two line segments in R," [Online]. Available: http://www.cs.swan.ac.uk/~cssimon/line_intersection.html. [Accessed 19 Februay 2016].

[81] Y. Zhang, C. Ji, P. Yuan, M. Li, C. Wang and G. Wang, "Particle swarm optimization for base station placement in mobile communications," in *IEEE International Conference on Networking, Sensing and Control, 2004* , 2004.

List of Publications

M. G. Kelly, J. A. Flint, R. D. Seager, “PSO for multiple antenna placement indoors, “ in *Antennas and Propagation Conference (LAPC*), 2015 Loughborough

Appendix A

	***gbest* Values**	
Number of run	x-position	y-position
1	7.4836	4.997
2	7.659	5.0524
3	7.4232	5.0159
4	7.6168	4.9994
5	7.3599	4.9493
6	7.338	5.0004
7	7.2563	5.0292
8	7.3344	4.9508
9	7.3541	5.0018
10	7.4417	5.0277
11	7.7912	4.9991
12	7.5085	5.0448
13	7.3634	5.0026
14	7.8185	5.0052
15	7.6008	4.9744
16	7.6857	5.0021
17	7.5697	4.9829
18	7.714	4.9996
19	7.3473	5.0027
20	7.5811	5.0215
21	7.2863	5.0261
22	7.5036	5.002
23	7.4924	4.9976
24	7.4878	5.0486
25	7.6664	4.9944
Mean	7.507348	5.0051
Standard deviation	0.158752	0.02543

Table A.1. gbest locations over a series of 25 runs

Iteration	Sigma, run 1	Sigma, run 2	Sigma, run 3	Sigma, run 4	Sigma, run 5	Sigma, run 6	Sigma, run 7	Sigma, run 8	Sigma, run 9	Sigma, run 10	AVG
1	678.048959	577.509282	866.117978	1253.239726	661.269933	935.332146	511.110536	1194.113628	1101.747561	1347.421560	912.591131

2	985.3703	1264.453	1762.705	3204.605	642.7875	1454.400	431.3183	1317.969	940.5705	1079.417	1308.359
3	1311.603	1243.145	2449.060	3105.302	1478.050	1861.215	421.0163	1523.101	1229.670	1696.490	1631.865
4	1247.146	658.4296	4052.975	7289.371	1404.308	2358.886	334.5354	2244.463	2358.155	3440.882	2538.915
5	1146.390	643.1847	1035.039	7227.699	995.9081	2628.227	256.1583	5760.979	2930.568	5099.923	2772.407
6	605.5734	2112.060	3050.668	6600.118	1332.873	4810.820	179.3406	3652.160	2110.454	2657.810	2711.188
7	603.7251	2115.471	3573.004	6275.243	1068.487	1586.104	98.25125	1588.059	2070.293	4663.790	2364.243
8	252.0239	2087.264	3481.420	4372.627	1933.309	1576.981	57.20854	4060.430	4522.716	2932.207	2527.618
9	168.0949	2374.735	7562.480	1793.780	1233.775	1553.908	52.63998	3826.364	1116.230	192.4437	1987.445
10	162.0688	563.9729	977.4947	800.4446	2742.410	4086.092	45.46630	6922.496	975.0826	818.6352	1809.416
11	153.1503	550.5571	976.6605	3061.909	4505.338	1112.659	27.17815	3323.848	1331.473	4647.026	1968.980
12	330.3008	527.5609	599.2669	316.7410	2408.621	1111.895	26.18654	2885.687	3672.985	4624.854	1650.409
13	322.8658	1972.004	598.4611	306.6668	5066.669	354.5055	23.64796	474.7085	493.4538	6780.196	1639.317
14	42.33490	4419.417	313.9754	689.4032	1098.125	184.0784	18.00659	809.6482	792.8423	18261.06	2662.890
15	40.72283	1108.753	311.1609	678.7448	1097.469	184.1217	17.25762	2093.379	794.7489	12.29099	633.8650
16	0.283591	1108.769	310.7430	622.1679	382.8565	183.0634	14.49993	2081.891	417.4582	14.44604	513.6179
17	0.159193	1141.086	178.6993	502.0133	382.6000	481.5740	13.96784	667.0986	153.6530	14.25175	353.5103
18	0.110634	1133.278	149.8132	39.25411	1684.451	867.7036	12.04736	476.2754	124.4228	14.24397	450.1601
19	0.077499	1.414784	149.7075	26.12991	1630.037	1812.628	11.02002	1004.976	108.7676	12.05047	475.6810
20	0.007699	0.936564	149.6754	26.12176	1629.847	1812.632	10.49262	1399.532	106.6029	0.148844	513.5998
21	0.004562	0.278789	149.6670	25.83639	1629.741	1808.641	9.370301	1342.264	11.53516	0.137995	497.7476
22	0.001393	0.214670	149.6585	25.81676	1629.728	132.6992	9.342836	995.1473	0.585536	0.051707	294.3247
23	0.000325	0.109961	149.6581	25.81889	2898.901	0.246803	9.166018	1458.691	0.147813	0.049477	454.2790
24	0.000115	0.038296	149.6584	2.952536	781.9459	0.243671	8.319679	3350.311	0.111724	0.049224	429.3631
25	0.000110	0.022370	94.39202	2.417184	781.9044	0.101927	5.955991	929.3899	0.063429	0.011115	181.4258
26	0.000071	0.006919	0.273697	2.326069	781.9051	0.105728	5.945055	2289.492	0.002935	0.004176	308.0062
27	0.000062	0.002188	0.235288	2.325989	6.260853	0.020942	4.757287	1729.968	0.002097	0.000737	174.3573
28	0.000031	0.000850	0.201687	0.062717	6.259040	0.014169	4.757346	6065.471	0.001231	0.000506	607.6769
29	0.000016	0.000338	0.130051	0.015190	6.238509	0.009417	4.416945	3204.261	0.000376	0.000011	321.5071
30	0.000004	0.000173	0.003136	0.015478	6.233051	0.009418	4.416916	628.7232	0.000102	0.000000	63.94015
31	0.000001	0.000060	0.003137	0.001017	6.232681	0.006139	4.416896	234.4441	0.000011	0.000000	24.51040
32	0.000000	0.000018	0.000169	0.000201	6.232670	0.000326	4.416898	109.3636	0.000007	0.000000	12.00139
33	0.000000	0.000008	0.000001	0.000021	6.232678	0.000000	4.412037	109.3628	0.000004	0.000000	12.00075
34	0.000000	0.000003	0.000001	0.000020	6.232675	0.000000	2.387689	106.9221	0.000002	0.000000	11.55425
35	0.000000	0.000000	0.000001	0.000018	6.232683	0.000000	0.890673	106.9208	0.000000	0.000000	11.40436

36	0.000000	0.000000	0.000000	0.000000	6.232675	0.000000	0.589132	106.92008	0.000000	0.00000	11.374189
37	0.000000	0.000000	0.000000	0.000000	6.232675	0.000000	0.571769	17.04008	0.000000	0.00000	2.384453
38	0.000000	0.000000	0.000000	0.000000	6.232675	0.000000	0.561291	0.03980	0.000000	0.00000	0.683377
39	0.000000	0.000000	0.000000	0.000000	6.232675	0.000000	0.561172	0.03980	0.000000	0.00000	0.683365
40	0.000000	0.000000	0.000000	0.000000	6.232675	0.000000	0.271051	0.03980	0.000000	0.00000	0.654353
41	0.000000	0.000000	0.000000	0.000000	6.232675	0.000000	0.267636	0.00124	0.000000	0.00000	0.650155
42	0.000000	0.000000	0.000000	0.000000	6.232675	0.000000	0.267188	0.00014	0.000000	0.00000	0.650001
43	0.000000	0.000000	0.000000	0.000000	6.232675	0.000000	0.267189	0.00014	0.000000	0.00000	0.650001
44	0.000000	0.000000	0.000000	0.000000	6.232675	0.000000	0.024086	0.00010	0.000000	0.00000	0.625686
45	0.000000	0.000000	0.000000	0.000000	6.232675	0.000000	0.014233	0.00000	0.000000	0.00000	0.624691
46	0.000000	0.000000	0.000000	0.000000	6.232675	0.000000	0.014232	0.00000	0.000000	0.00000	0.624691
47	0.000000	0.000000	0.000000	0.000000	6.232675	0.000000	0.007726	0.00000	0.000000	0.00000	0.624040
48	0.000000	0.000000	0.000000	0.000000	6.232675	0.000000	0.005295	0.00000	0.000000	0.00000	0.623797
49	0.000000	0.000000	0.000000	0.000000	6.232675	0.000000	0.004761	0.00000	0.000000	0.00000	0.623744
50	0.000000	0.000000	0.000000	0.000000	0.000116	0.000000	0.004742	0.00000	0.000000	0.00000	0.000486
51	0.000000	0.000000	0.000000	0.000000	0.000287	0.000000	0.004358	0.00000	0.000000	0.00000	0.000465
52	0.000000	0.000000	0.000000	0.000000	0.000287	0.000000	0.004315	0.00000	0.000000	0.00000	0.000460
53	0.000000	0.000000	0.000000	0.000000	0.000075	0.000000	0.004268	0.00000	0.000000	0.00000	0.000434
54	0.000000	0.000000	0.000000	0.000000	0.000075	0.000000	0.004266	0.00000	0.000000	0.00000	0.000434
55	0.000000	0.000000	0.000000	0.000000	0.000029	0.000000	0.004257	0.00000	0.000000	0.00000	0.000429
56	0.000000	0.000000	0.000000	0.000000	0.000020	0.000000	0.004256	0.00000	0.000000	0.00000	0.000428
57	0.000000	0.000000	0.000000	0.000000	0.000020	0.000000	0.004256	0.00000	0.000000	0.00000	0.000428
58	0.000000	0.000000	0.000000	0.000000	0.000004	0.000000	0.004256	0.00000	0.000000	0.00000	0.000426
59	0.000000	0.000000	0.000000	0.000000	0.000004	0.000000	0.004256	0.00000	0.000000	0.00000	0.000426
60	0.000000	0.000000	0.000000	0.000000	0.000000	0.000000	0.004256	0.00000	0.000000	0.00000	0.000426
61	0.000000	0.000000	0.000000	0.000000	0.000000	0.000000	0.000064	0.00000	0.000000	0.00000	0.000006
62	0.000000	0.000000	0.000000	0.000000	0.000000	0.000000	0.000064	0.00000	0.000000	0.00000	0.000006
63	0.000000	0.000000	0.000000	0.000000	0.000000	0.000000	0.000064	0.00000	0.000000	0.00000	0.000006
64	0.000000	0.000000	0.000000	0.000000	0.000000	0.000000	0.000064	0.00000	0.000000	0.00000	0.000006
65	0.000000	0.000000	0.000000	0.000000	0.000000	0.000000	0.000064	0.00000	0.000000	0.00000	0.000006
66	0.000000	0.000000	0.000000	0.000000	0.000000	0.000000	0.000064	0.00000	0.000000	0.00000	0.000006
67	0.000000	0.000000	0.000000	0.000000	0.000000	0.000000	0.000064	0.00000	0.000000	0.00000	0.000006
68	0.000000	0.000000	0.000000	0.000000	0.000000	0.000000	0.000064	0.00000	0.000000	0.00000	0.000006
69	0.000000	0.000000	0.000000	0.000000	0.000000	0.000000	0.000064	0.00000	0.000000	0.00000	0.000006

70	0.000000	0.000000	0.000000	0.000000	0.000000	0.000000	0.000064	0.00000	0.000000	0.00000	0.000006
71	0.000000	0.000000	0.000000	0.000000	0.000000	0.000000	0.000064	0.00000	0.000000	0.00000	0.000006

Table A-2. Convergence of swarming process within test building

points per sq m	time					AVG time	gbest_x with 30 bees					Sigma	Power (dBm)				
0.056	1.528	1.548	1.575	1.479	1.566	1.539	19.882	15.030	14.835	14.779	40.488	11.106	21	21	21	21	21
0.222	1.694	1.620	1.699	1.660	1.599	1.654	30.047	30.001	29.916	29.994	39.984	4.470	18	18	18	18	21
0.500	1.807	1.736	1.873	1.741	1.729	1.777	30.000	29.982	45.068	29.950	29.977	6.749	18	18	21	18	18
0.889	1.962	2.005	1.903	1.914	2.001	1.957	15.017	30.005	30.022	30.005	44.958	10.586	21	18	18	18	21
1.389	2.198	2.198	2.188	2.117	2.131	2.166	30.024	30.006	30.023	30.001	40.031	4.480	15	15	15	15	18
2.000	2.406	2.506	2.386	2.493	2.464	2.451	30.019	29.991	30.002	29.991	29.975	0.016	12	12	12	12	12
2.722	2.888	2.721	2.785	2.809	2.739	2.788	30.000	30.004	30.013	29.980	29.995	0.012	12	12	12	12	12
3.556	3.124	3.129	3.277	3.159	3.192	3.176	30.003	29.992	29.990	29.986	29.989	0.006	12	12	12	12	12
4.500	3.562	3.522	3.538	3.707	3.619	3.590	29.995	30.000	30.007	29.999	29.992	0.006	12	12	12	12	12
5.556	4.104	4.095	4.058	4.097	4.146	4.100	30.000	30.006	29.999	30.007	30.006	0.004	12	12	12	12	12
6.722	4.509	4.503	4.505	4.430	4.430	4.475	29.996	30.001	30.010	29.998	30.007	0.006	12	12	12	12	12
8.000	5.089	5.135	5.156	5.118	5.111	5.122	29.988	30.008	30.002	30.001	29.992	0.008	12	12	12	12	12
9.389	6.001	5.707	5.672	5.679	5.943	5.800	30.002	30.001	29.998	29.988	30.010	0.008	12	12	12	12	12
10.889	6.522	6.640	6.568	6.484	6.570	6.557	29.998	29.999	30.000	30.002	30.000	0.002	12	12	12	12	12
12.500	7.284	7.481	7.407	7.350	7.392	7.383	30.003	29.997	30.000	30.000	29.991	0.004	12	12	12	12	12
14.222	8.227	8.138	8.248	8.103	8.091	8.161	30.000	30.002	29.997	30.000	30.000	0.002	12	12	12	12	12
16.056	9.613	9.124	8.872	9.016	9.368	9.199	30.000	29.994	30.006	29.993	29.998	0.005	12	12	12	12	12
18.000	10.155	9.924	9.878	9.837	9.814	9.922	30.009	30.008	29.995	29.993	30.005	0.007	12	12	12	12	12

20.056	11.399	10.901	10.891	10.911	10.889	10.998	30.000	30.006	30.002	30.000	30.003	0.003	12	12	12	12	12
22.222	12.180	11.763	11.988	12.019	11.944	11.979	30.000	29.993	30.000	30.001	29.997	0.003	12	12	12	12	12

Table A-3. Number of receiver points versus swarming precision.

bees	**time**					**AVG time**	**gbest_x**					**Sigma(gbest)**
5	3.445172	3.594095	3.71357	3.74809	3.482002	3.596586	19.9341	40.917	30.0148	19.7163	40.0691	10.3387604795
10	5.222149	5.197375	5.402623	5.479372	5.203235	5.300951	29.9954	27.802	29.9949	20.0082	40.018	7.1427560150
15	7.337378	7.234609	7.290029	7.086636	6.665268	7.122784	44.9966	29.9986	29.995	19.9837	29.9997	8.9481417751
20	10.26925	8.75006	9.653036	8.699971	8.445149	9.163493	29.9912	44.991	30.0081	29.9876	15.012	10.5991804094
25	10.53534	10.58599	10.43316	10.301	10.28226	10.42755	15.0071	29.9017	29.9996	30.0011	29.9973	6.6939484744
30	12.3068	13.55172	12.3236	13.67048	14.06111	13.18274	30.0022	30.0057	29.99	29.9999	29.9899	0.0072300069
35	15.69684	15.82485	16.61405	16.76806	17.01897	16.38455	29.9998	29.9947	30.0057	30	29.9977	0.0040319970
40	17.33323	16.63478	18.34796	18.46436	19.08153	17.97237	29.9992	29.9979	29.994	30.0024	30.0019	0.0033980877
45	18.83015	18.92507	18.72229	18.89351	18.64491	18.80319	30.0021	30.004	29.9995	30.0002	30.0005	0.0018036075
50	20.75852	20.77827	20.52724	20.67195	20.67302	20.6818	29.9977	29.9987	30.0004	29.9997	29.9976	0.0012275993
55	22.91007	22.98678	23.07892	22.40451	22.67605	22.81127	30.0003	30.0002	29.9977	29.9999	30.0003	0.0011189281
60	24.63989	24.56768	26.2001	24.76086	24.63334	24.96037	30.0001	30	29.9993	30.0017	30.0018	0.0011122050
65	26.9987	27.58895	27.77486	32.17688	27.65944	28.43977	30.0003	30.0002	29.9979	30.0002	30	0.0010232302
70	30.22164	30.95888	28.53799	29.22133	28.95374	29.57871	30.0004	30.0004	30.001	29.9971	30.0002	0.0015498387
75	35.21447	33.24821	31.46816	32.35506	32.11876	32.88093	30.0002	30	29.9994	30	30.0007	0.0004669047
80	36.05871	33.5993	35.12603	33.78674	33.52588	34.41933	29.9994	30.0004	29.9995	29.9996	29.9998	0.0003974921
85	35.80911	35.39643	35.65134	36.18764	35.50359	35.70962	30.0002	29.9998	29.9998	30.0002	30	0.0002000000
90	37.9946	37.56667	37.91118	37.61815	37.35035	37.68819	30	30.0001	29.9997	29.9997	29.9998	0.0001816590
95	39.86056	38.96486	39.65793	39.37116	39.45412	39.46172	29.9997	30.0002	29.9998	30	30.0014	0.0006870226
100	40.32945	41.00295	42.9818	41.50179	42.31783	41.62676	30.0002	30.0003	29.9997	29.9999	29.9999	0.0002449490

Table A-4. Swarm size versus run time.

	Average Sigma over 10 runs		
Number of iterations	**High complexity Layout**	**Medium complexity Layout**	**Low complexity Layout**
1	460.62348	474.44914	21.48036
2	260.65394	282.83843	8.02997
3	194.24403	196.17868	2.70368
4	86.33895	109.92293	0.80315
5	67.03259	98.04421	0.23688
6	54.04174	58.48275	0.12125
7	47.20814	38.53320	0.05474
8	41.64539	15.86514	0.03329
9	35.09844	9.54661	0.01477
10	31.05737	4.27375	0.00854
11	21.87665	2.64578	0.00372
12	16.43827	1.51963	0.00171
13	14.59982	1.30365	0.00095
14	13.25408	1.15966	0.00055
15	11.63380	0.83388	0.00040
16	9.08495	0.51618	0.00015
17	7.88880	0.38892	0.00028
18	6.99092	0.36670	0.00012
19	6.93859	0.02537	0.00007
20	6.80248	0.00027	0.00003
21	4.97340	0.00012	0.00001
22	4.32098	0.00002	0.00001
23	4.30282	0.00000	0.00000
24	3.31707	0.00000	0.00000
25	3.31159	0.00000	0.00000
26	3.29870	0.00000	0.00000
27	1.71998	0.00000	0.00000
28	1.71982	0.00000	0.00000
29	1.69061	0.00000	0.00000
30	1.61486	0.00000	0.00000
31	1.61483	0.00000	0.00000
32	1.59760	0.00000	0.00000
33	1.61700	0.00000	0.00000

34	1.60240	0.00000	0.00000
35	1.59745	0.00000	0.00000
36	1.59642	0.00000	0.00000
37	0.06067	0.00000	0.00000
38	0.00081	0.00000	0.00000
39	0.00002	0.00000	0.00000
40	0.00000	0.00000	0.00000
41	0.00000	0.00000	0.00000
42	0.00000	0.00000	0.00000
43	0.00000	0.00000	0.00000
44	0.00000	0.00000	0.00000
45	0.00000	0.00000	0.00000
46	0.00000	0.00000	0.00000
47	0.00000	0.00000	0.00000
48	0.00000	0.00000	0.00000
49	0.00000	0.00000	0.00000
50	0.00000	0.00000	0.00000
51	0.00000	0.00000	0.00000
52	0.00000	0.00000	0.00000
53	0.00000	0.00000	0.00000
54	0.00000	0.00000	0.00000
55	0.00000	0.00000	0.00000

Table A-5. Convergence in different layout types.

Appendix B

Antenna Specifications

SCHWARZBECK MESS - ELEKTRONIK

An der Klinge 29 D-69250 Schönau Tel.: 06228/1001 Fax.: (49)6228/1003

VUBA 9117 VHF-UHF Bikonus-Antenne
VUBA 9117 VHF-UHF Biconical Antenna

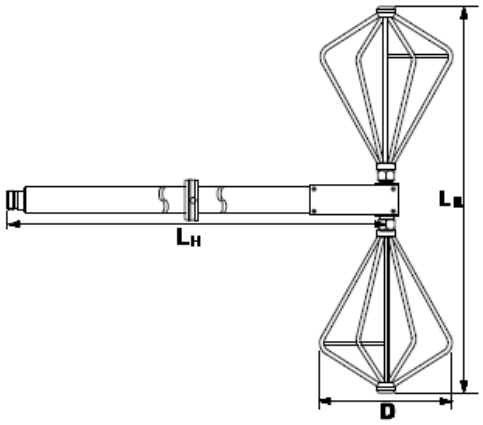

Technische Daten:		***Specifications:***
Frequenzbereich, nominell:	150 - 1000 MHz	*Frequency Range, nominal:*
Frequenzbereich, nutzbar mit externer Mantelstromsperre:	30 - 1000 MHz	*Frequency Range, usable with external ferrite braid choke:*
Impedanz (nominal):	50 Ω	*nominal Impedance:*
Antennenwandlungsmaß: (abhängig vom Elementtyp)	15 - 35 dB/m	*Antenna Factor: (depending on elem. type in use)*
Länge Halterung: LH=540 mm		*Length holder: LH=540 mm*
Balun:	1:1	*Balun:*
Breite LE:	440 mm	*Width LE:*
Antennenschaft (Halterungsrohr)	∅ 22 mm	*Antenna shaft (Tube):*
Gewicht der gesamten Antenne:	0.83 kg	*Total weight:*
HF-Leistung:	5 W	*Power (EMC TX):*
Koaxialanschluß:	N-Buchse / N - female	*Coaxial Connector:*

Die VHF-UHF-Breitbandantenne VUBA 9117 bietet im Frequenzbereich von 150-1000 MHz einen sehr gleichmäßigen Gewinnverlauf. Das Richtdiagramm in der H-Ebene ist rundstrahlend, in der E-Ebene "8"-förmig, ähnlich wie bei Dipolen. Die VUBA 9117 ist besonders zur schnellen und komfortablen Breitbandüberprüfung von Messgeländen geeignet.

The Biconical VHF-UHF Broadband Antenna VUBA 9117 offers a a flat gain characteristic in the frequency range 150-1000 MHz. The directional pattern is circular in the H-plane and "8"-shaped in the E-plane, similiar to dipole patterns. A typical application for the VUBA 9117 is the fast and convenient broadband evaluation of the actual site attenuation.

SCHWARZBECK MESS - ELEKTRONIK
An der Klinge 29 D-69250 Schönau Tel.: 06228/1001 Fax.: (49)6228/1003

Bikonus Breitbandantenne VUBA 9117
Biconical Broadband Antenna VUBA 9117

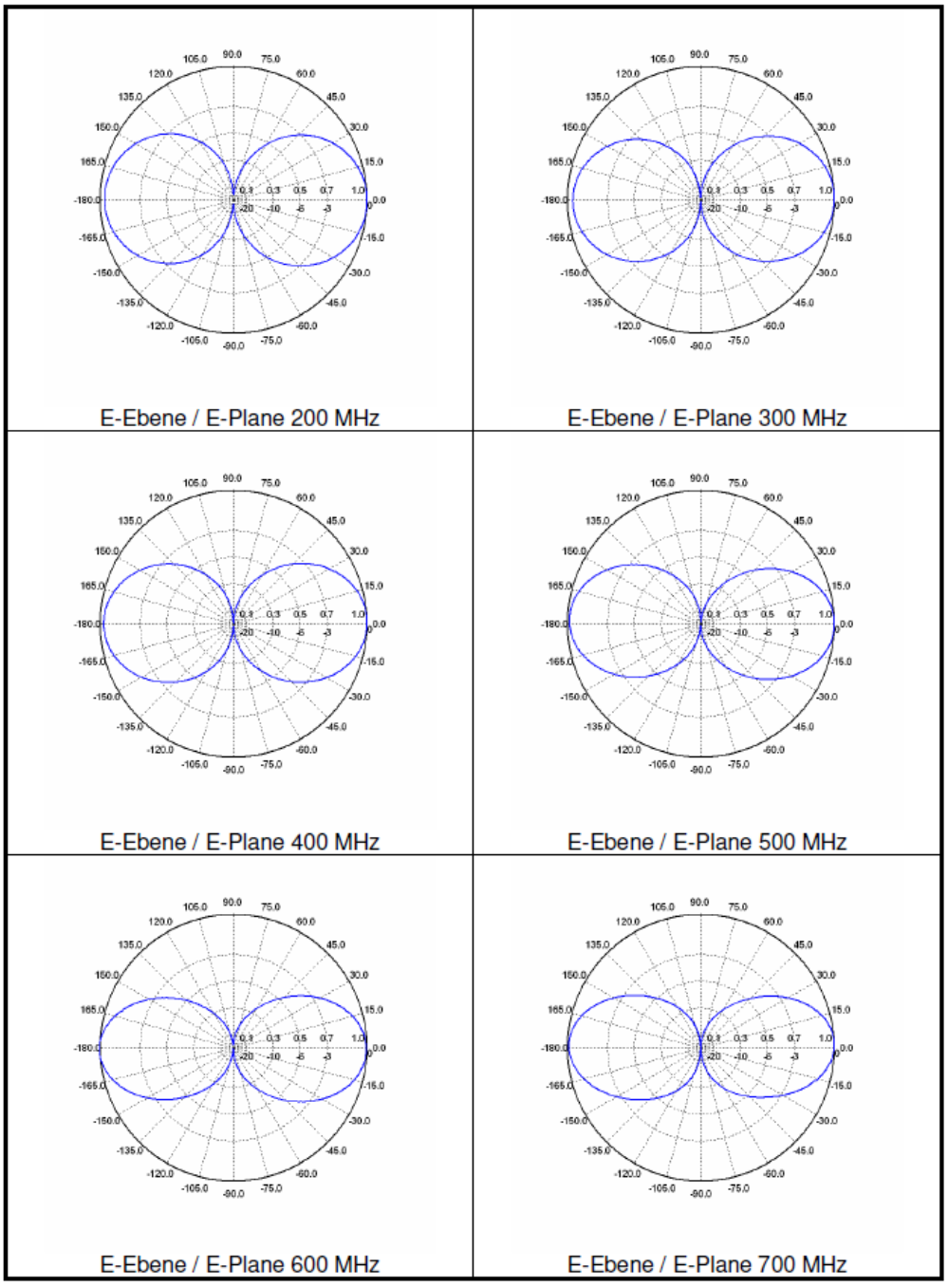

SCHWARZBECK MESS - ELEKTRONIK
An der Klinge 29 D-69250 Schönau Tel.: 06228/1001 Fax.: (49)6228/1003

Bikonus Breitbandantenne VUBA 9117
Biconical Broadband Antenna VUBA 9117

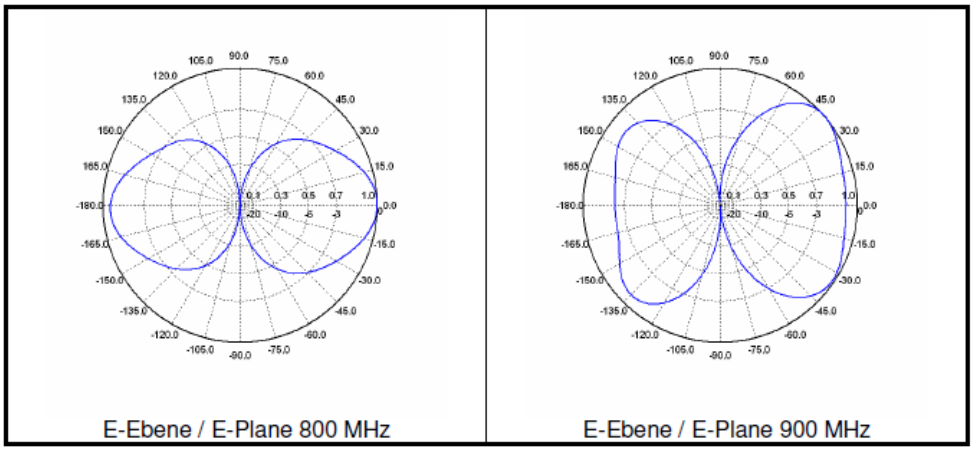

Frequenz *Frequency* [MHz]	Halbwertsbreite (- 3 dB) E-Ebene *Half-Power Beamwidth E-plane* [°]
200	87
300	81
400	77
500	71
600	66
700	64
800	69
900	126